EXPERIMENTAL AND THEORETICAL ASPECTS OF MEMBRANE BASED WATER COOLING SYSTEM

A THESIS SUBMITTED TO
THE GRADUATE SCHOOL OF NATURAL AND APPLIED SCIENCES
OF
MIDDLE EAST TECHNICAL UNIVERSITY

BY
HANDE KULAÇ

IN PARTIAL FULFILLMENT OF THE REQUIREMENTS
FOR
THE DEGREE OF MASTER OF SCIENCE
IN
CHEMICAL ENGINEERING

SEPTEMBER 2017

Approval of the thesis

EXPERIMENTAL AND THEORETICAL ASPECTS OF MEMBRANE BASED WATER COOLING SYSTEM

Submitted by **HANDE KULAÇ** in partial fulfillment of the requirements for the degree of **Master of Science in Chemical Engineering Department, Middle East Technical University** by,

Prof. Dr. Gülbin Dural Ünver
Dean, Graduate School of **Natural and Applied Sciences** _____

Prof. Dr. Halil Kalıpçılar
Head of Department, **Chemical Engineering** _____

Prof. Dr. Halil Kalıpçılar
Supervisor, **Chemical Engineering Dept., METU** _____

Prof. Dr. Yusuf Uludağ
Co-Supervisor, **Chemical Engineering Dept., METU** _____

Examining Committee Members:
Prof. Dr. Nihal Aydoğan
Chemical Engineering Dept., Hacettepe University _____

Prof. Dr. Halil Kalıpçılar
Chemical Engineering Dept., METU _____

Prof. Dr. Yusuf Uludağ
Chemical Engineering Dept., METU _____

Assoc. Prof. Dr. Çerağ Dilek Hacıhabiboğlu
Chemical Engineering Dept., METU _____

Asst. Prof. Dr. Harun Koku
Chemical Engineering Dept., METU _____

Date: 20.09.2017

I hereby declare that all information in this document has been obtained and presented in accordance with academic rules and ethical conduct. I also declare that, as required by these rules and conduct, I have fully cited and referenced all material and results that are not original to this work.

Name, Last name: Hande KULAÇ

Signature:

ABSTRACT

EXPERIMENTAL AND THEORETICAL ASPECTS OF MEMBRANE BASED WATER COOLING SYSTEM

Kulaç, Hande
M.S., Department of Chemical Engineering
Supervisor : Prof. Dr. Halil Kalıpçılar
Co-Supervisor: Prof. Dr. Yusuf Uludağ
September 2017, 131 pages

In the chemical industry, to cool the process water, cooling towers are installed. In towers, hot water directly contacts with air flow. With sensible and latent heat, mass transfer between two phases, water temperature is decreased. Water evaporates during the operation and a respectable amount of energy is transferred to the air stream. Although, the cooling tower is an efficient process to cool the water stream, water pools placed under the towers tend result in growth of bacteria and algae. This problem grows with time and contaminates parts of tower. For smaller capacity towers, the problem reveals itself immediately. Although antibacterial chemicals are used to clean the contaminated parts, a permanent solution is proposed by membranes. Membranes are developing technology spreading to different areas such as separation, treatment and dialysis. Membrane contactor is one of the usage type of membranes and it allows heat and mass transfer between two phases without mixing into each other. As membrane geometry, hollow fiber membranes provide large surface area per volume. In this study, polysulphone hollow fiber membranes are chosen since they are hydrophobic. Experimental and theoretical analysis of membrane based cooling system was conducted by seven independent variables which are water flow rate, air flow rate, transmembrane pressure, module length and number, inlet air and water temperature. Results shows that water cooling was achieved approximately between 4- 9°C and mathematical model matches with experimental results.

Keywords: Evaporative cooling, hollow fiber, polysulphone, water cooling

ÖZ

DENEYSEL VE TEORİK AÇIDAN MEMBRAN BAZLI SU SOĞUTMA SİSTEMİ

Kulaç, Hande
Yüksek Lisans, Kimya Mühendisliği Bölümü
Tez Yöneticisi : Prof. Dr. Halil Kalıpçılar
Ortak Tez Yöneticisi: Prof. Dr. Yusuf Uludağ
Eylül 2017, 131 sayfa

Kimya endüstrisinde, işlem suyunu soğutmak amacıyla soğutma kuleleri kullanılır. Bu kulelerde, sıcak işlem suyu havayla direkt temas ettirilir. Bu esnada, iki faz arasında hava ve kütle değişimi gerçekleşerek su sıcaklığı istenilen sıcaklığa düşürülür. Kuledeki işlem sırasında su buharlaşır ve önemli miktarda enerji havaya aktarılır. Soğutma kuleleri verimli çalışan sistemler olmasına rağmen, kule altında bulunan su havuzlar bakteri ve alg oluşumu için oldukça elverişlidir. Bu problem zamanla artar ve kulenin parçalarında kirliliğe sebep olur. Daha küçük kapasiteli kulelerde problemin ortaya çıkması daha kısa zaman alır. Kirlenen parçaları temizlemek amacıyla çeşitli antibakteriyel kimyasallar kullanılsa da membranlar kullanılarak daha kalıcı bir çözüm sunulabilir. Membranlar, kullanımı yaygınlaşan, gelişen bir teknoloji olup ayırma, iyileştirme, diyaliz gibi alanlarda kullanılır. Membran kontaktörler de membrane kullanım şekillerinden biri olup, iki fazın karışmadan ısı ve kütle transferi gerçekleştirmesine olanak sağlar. Membran geometrisi olarak ise kovuklu elyaflar hacmine oranla yüksek membran yüzeyi sağlarlar. Membran bazlı soğutma sisteminde polisülfon kovuklu elyaf membranları hidrofobiklik özellikleri nedeniyle seçilmiştir. Oluşturulan sistem için deneysel ve teorik analiz, yedi farklı parametre kullanılarak yapılmıştır. Bunlar su hızı, hava hızı, basınç, modül uzunluğu ve sayısı, giriş hava ve su sıcaklığıdır. Sonuçlara göre sistemde yaklaşık 4- 9 ˚C arasında soğuma gözlenmiştir.

Anahtar Kelimeler: Evaporatif soğuma, kovuklu elyaf, polisülfon, su soğuma

To My Family and Friends

ACKNOWLEDGMENTS

I want to thank you my supervisors Prof. Dr. Halil Kalıpçılar and Yusuf Uludağ for their guidance, suggestions and support in my study. I gained lots of experiences thanks to them. I express my gratitutes to my advisors. Also, I would like to thank you Assoc. Prof. Dr. Zeynep Çulfaz Emecen and her lab for their help throughout this study.

I would like to thank METU coordinator ship of scientific research projects (BAP) is financial support. For experimental set up, technicians in chemical engineering department wre very helpful and I want thank them.

I want to thank my parents, Nahide and Kemal KULAÇ. They are always be there for me in my good and bad times in my life. Nothing changes in my thesis study.
I want to express my love to my dearest sisters Ayça and Melike. They encourage and understand me in all my life. They are gifts to me since both of them are my best friends in my whole life.

Lastly, I would like to thank you my sisters that I choose, Kübra, Seren and Konçüy. Since the day we met, they always got my back, show patience, give support. In these years, we had good and bad times but we always take strength from each other. I want to express my endless gratitude and love to them.

TABLE OF CONTENTS

LIST OF TABLES

TABLES

LIST OF FIGURES

FIGURES

LIST OF SYMBOLS AND ABBREVIATIONS

D: Diameter

Di: Inlet diameter

T: Temperature

T_{wi}: Inner wall temperature

$T_{w,in}$: Inlet water temperature

T^{p}: Polymer temperature

h: Heat transfer coefficient

U: Overall heat transfer coefficient

P^{*}: Saturation vapor pressure

P_{∞}: Partial vapor pressure

k: Thermal conductivity

k_{p}: Mass transfer coefficient

Re: Reynold number

Nu: Nusselt number

Avr.: Average

Std. Standard deviation

Greek letters:

P: Permeance

ρ: density

CHAPTER 1

INTRODUCTION

Cooling towers are widely used in the chemical industry for cooling process fluid, mostly water. Temperature decrease of process water is important in a chemical plant since after the cooling of process water, it is recirculated in the plant or it is used in other operations such as heat exchangers. Recirculation of process water is significant because of economic concerns. Range of temperature decrease in process water depends on design and capacity of the cooling tower. Generally, the difference between inlet and outlet water temperature is 9-12 ˚C [1]. Towers are drafted by two ways, which are natural draft and mechanical draft. Natural draft cooling towers are mostly used in thermal power plants. Approximate tower height is 100 meters [2]. In natural draft towers, water temperature is decreased with both film flow and droplet flow [2]. On the other hand, in mechanical draft cooling towers, air flow is provided by fans and tower height varies between 2 to 12 meters [3].

The working principle of a cooling tower is evaporative cooling. Evaporative cooling is a very basic and common phenomenon. The energy needed for this operation is taken from the heat of vaporization of liquid (mostly water) [4]. In the packing side of the tower, with direct contact between air and hot process water, heat and mass transfer occur. Sensible and latent heat of water is transferred to the air. Air becomes humid during the process. If the latent heat of water evaporation were not high (2257 kJ/kg), much bigger tower will be needed to cool the water. At this point, heat of vaporization of water is the key point in energy transfer.

There are two terms that explain the effectiveness of evaporative cooling principle in cooling tower which are approach and range. Approach is the difference between wet bulb temperature and outlet cold water temperature [1]. Wet bulb temperature is measured by wetted tip. With the evaporation of water at the tip, air becomes humid. Air temperature cannot be decreased below wet bulb temperature [5]. Thus, wet bulb temperature is the limitation for driving force in evaporative cooling. On the other hand, range is basically the difference between inlet and outlet water temperatures.

Cooling tower capacity, approach and range change according to the design of the tower. According to ASHRAE green guide (2010) which follows American National Standards Institute, an example of cooling tower capacity and efficiency results are given as the following. A cooling tower with water flow rate of 3785 liter per minute cooling tower, design approach temperature and range are 15 and 10˚C, respectively [6].

In all cooling towers, there is a water collecting pool placed under the system. These pools are convenient to bacteria and algae growth. Especially, bacteria named Legionella pneuphila grows in places where water and air are in direct connect. Also, 20 - 45 °C of water temperature is most convenient condition for growth [7]. For this reason, this type of bacteria is commonly seen in cooling tower water collecting pods. With the increasing number of bacteria, respiratory sourced diseases arise. In addition to that, hygiene and sanitariness of the system decrease.

In the industry, anti-chemical agents are used as a temporary solution to this problem. However, in small capacity cooling tower system, bacteria growth will cause failure of the system performance. For this purpose, to prevent the bacteria growth and contamination in the system, a permanent solution can be proposed by

minimizing the contact of air and water. At this point, membranes can be the solution of this problem.

Since membranes can be used as barrier between air and water flows, bacteria growth will be minimized. On the other hand, with water evaporation from the membrane pores, water temperature can be decreased. Thus, membrane usage in water cooling system can be an efficient and sanitary solution for mentioned problem about cooling towers above.

Membranes are basically semi-permeable materials that are widely used in different industries for various purposes [8]. Mainly, ultrafiltration, microfiltration, electrodialysis and reverse osmosis are membrane based separation processes. Other than separation processes, membranes can be used for cooling processes as membrane contactor.

Membrane contactors are systems that provide mass transfer between two phases (gas-liquid or liquid-liquid) and these two phases are not dispersed in each other as in common membranes. Membrane contactor difference from membranes is they are not supposed to provide selectivity. They act as a tight porous barrier between two flows. Two phases can operate independently of each other with certain contact area of membrane surface.

Membrane contactors have advantages with respect to other conventional phase separators such as direct absorption or dew pointing by cooling [9]. Flooding does not occur in higher flow rates and interfacial area of the contactor is high [9]. With these advantages, membrane contactors are used in pharmaceuticals, VOC removal, waste-water treatment. On the other hand, contactors have the drawback that membrane is an additional resistance to mass transfer between two phases in the system. Resistance to mass transfer can be changed with membrane thickness. Resistance and membrane thickness are inversely proportional in each other.

Membrane geometries can differentiate according to the application. Geometries are mainly flat sheet, hollow fiber, spiral wound and tubular. Hollow fiber membranes are most commonly used geometry for membrane contactor applications since it provides much higher membrane surface area per volume. By this way, heat and mass transfer area will be increased.

A gas-liquid hollow fiber membrane contactor is shown schematically in Figure 1.1:

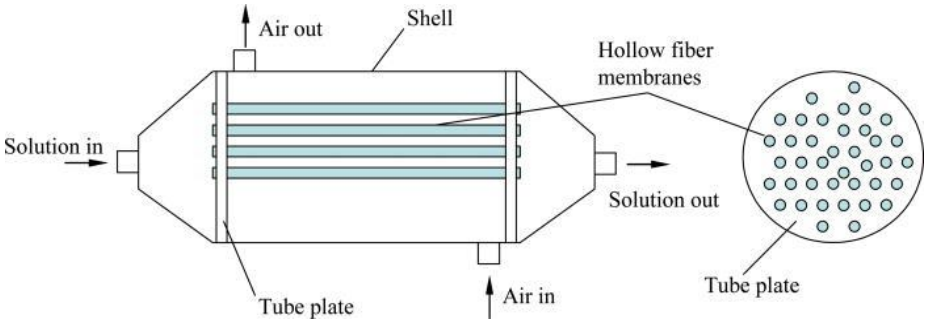

Figure 1.1: Gas-liquid hollow fiber contactor [10]

In Figure 1.1, cross flow of air through fiber bundles is shown. In the fiber bundle, solution is flowing through. Heat and mass transfer occur between air and solution into membrane pores. With penetration of solution vapor into the air, mass transfer exchange occurs, resulting in latent heat transfer to air flow. Also, sensible heat is exchanged because of the temperature difference between air and solution.

Membrane material can also change according to the application and desired results. Membrane material can be both organic and inorganic such as polymer, ceramic, metal.

Polymer based membranes are chosen since polymers can became bundles easily instead of one piece as in ceramic membranes and they have lower operational cost [11]. Nevertheless, there are evaporative cooling applications using ceramic pods. Aimiuwu (1992) used evaporative cooling principle to decrease temperature of water and achieved approximately 10˚C cooling. But, with the given advantageous features of polymeric membranes, for water cooling, polymeric hollow fiber membrane contactors are proposed. Polymers behave different in certain conditions. For this reason, polymer choice in the system plays important role. In industry, several polymers are used such as polyether sulfone, polyimide, PVDF, polysulphone in membrane based cooling applications. For instance, Loeb (2003) studied with polytetrafluoroethylene, polyurethane fluoroacrylate and polypropylene to cool water and achieve 10˚C temperature decrease of water.

For water cooling applications, polymer selection is important since it is directly related with the water cooling performance. Hydrophilic polymers should not be used since they cause water film on membrane surface. Since hydrophilic polymers have many active hydrogen bonds, adhesive force between polymer and water is high [12]. Thus, water molecules are attach to the polymer surface. Also, with hydrophilic polymers, direct contact of air and water increases which is an undesired situation because of bacteria growth. On the other hand, highly hydrophobic polymers are also undesired since they prevent the passage of water droplets. Thus, a polymer which is hydrophobic but also has hydrogen bonds would provide desired condition for water cooling system.

With the given information above, polysulphone is determined as membrane material in membrane based water cooling system. Polysulphone (PS, PSF, PSU) is thermoplastic polymer which can be molded into different shapes. In addition, it is a hydrophobic polymer. Also, it has high thermal stability. Since, in membrane based water cooling system, temperatures vary between 20-40˚C, thermal stability of the membrane polymer is not vital.

The chemical structure is shown below in Figure 1.2.

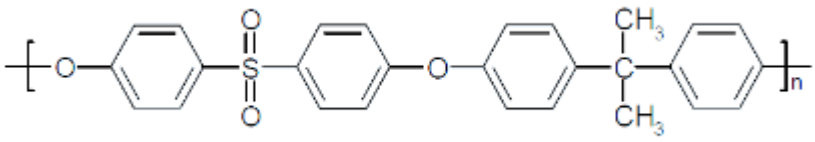

Figure 1.2: Structure of polysulfone [13]

In Figure 1.2, the structural formula of polysulphone is shown. As mentioned above, hydrophobicity of the polymer is important. To have hydrophilic structure, material should have active hydrogen bonds. With decrease of these bonds, polymer becomes hydrophobic. According polysulphone has a few active hydrogen bonds, it can be classified as hydrophobic. Also, ether groups make the structure of polymer flexible [13]. Polymer flexibility is an advantage during module preparation.

In the membrane based water cooling system, polysulphone hollow fiber membrane contactors are placed and evaporative cooling principle is applied to decrease the water temperature. During the process, outlet air would be more humidified than inlet.

In this study, commercial polysulphone hollow fiber membranes (10000 Da) are bundled with 4 membranes having lengths of 30 and 39 cm, outer diameter of 0.09 cm. Each pack having 4 fiber membranes, are placed cross to the air flow. Distilled water temperature is decreased by using the evaporative cooling principle. In the study, feed air temperature, feed water temperature, module length, water flow rate, air flow rate, transmembrane pressure and module number are the independent parameters. The effect of these parameters on the cooling performance was measured. In addition to that, for theoretical and experimental comparison, a mathematical representation of the system is provided.

Main motivation in the membrane based water cooling system is provide an environment to decrease water temperature as in cooling towers. On the other hand, by using membranes as barrier, system will be sanitary. Cooled water can be used to decrease process water temperature in a heat exchanger. The reason of not using process water in membrane based system is it causes fouling problems in membranes.

CHAPTER 2

LITERATURE RESEARCH

2.1 Evaporative cooling principle

The evaporative working principle that is used to chill the process water is a technique that cools the contacting surface with evaporation of water [14]. It is a low cost and simple way of reducing water temperature in a system [15].

In cooling towers, the working principle is evaporative cooling. In towers, if water cooling is only caused by sensible heat transfer, air flow would be much higher. With evaporation of water, latent heat of vaporization is transferred and water temperature is decreased. Since evaporative cooling is a simple and usable principle, it has been used widely in the past.

Evaporative cooling was experimentally studied by Aimiuwu (1992) and he decreased the water temperature about 9.4-15.0 ˚C by porous ceramic. Taha et al. (1994) indicated the temperature fall in evaporative cooling chamber between 10-13 ˚C. Cooling was provided by chamber coating with wet charcoal from outside. Also, evaporative cooling chambers were found to be beneficial in increasing shelf lives of food and Thakur et al. (2002), Mordi and Olorunda (2003) showed evaporating cooling principle works better than sensible heat exhange. Anyanwu (2004) observed the effect of relative humidity and temperature on cooling performance. According to study, temperature decrease is between 3-12 ˚C in dry climates. Giabaklau and Ballinger (1996) studied the effect of evaporative cooling on entering air temperature and humidity and predicted 9-12˚C decrease in air temperature.

Ibrahim et al. (2003) achieved 6-8˚C decrease in dry bulb temperature of air and increase 30% in relative humidity. As it is seen from the studies, evaporative cooling principle is efficient for both water and air cooling and commonly used for these purposes.

An evaporative cooling system can be divided into three groups with respect to contact between air and water. Accordingly, system can be direct, indirect or semi direct.

In direct evaporative cooling system, water and air streams are contacted directly [16]. The disadvantage of this method is bacteria growth which will be explained in following parts [16,17]. In indirect evaporative cooling system, water and air flow are divided with non- porous surface. Water is evaporated but not through the air stream. Thus, with the water evaporation, only heat is exchanged between two flows. With heat transfer, both air and water temperature can be decreased but the cooling performance is lower than direct evaporative cooling system. On the other hand, bacteria growth problem is not observed in indirect systems [16].

Semi direct evaporative cooling system carries features of both direct and indirect evaporative cooling system. In semi direct evaporative cooling system, both heat and mass transfer occur between air and water as in direct systems. On the other hand, in indirect system, there is non- porous wall between air and water which allows heat transfer only. The difference of semi direct system is porous wall standing air and water flows [16].

2.2 Bacteria growth (Legionella) in direct evaporative systems

As mentioned in 2.1, in direct evaporative systems main disadvantage is bacteria growth. It is a common problem in systems that air and water contacts directly [16]. It is an air borne bacteria and causes Legionnaires diseases. Disease is a kind of respiratory infection and cause to Pontiac Fever [17].

It is not harmful to living beings as long as it does not reach to respiratory system. On the other hand, bacteria growth contaminates the system parts. Suitable conditions for Legionella growth is 20-45˚C water temperature. That is why 40-60% of cooling towers suffer from this bacteria [18].

In a water cooling system, value of bacteria colony in certain amount of samples can be known. The treatment is necessary when resulted value of bacteria is above the target. Target values are given in Table 2.1:

Table 2.1: Target values of bacteria in cooling systems [18]

Parameter	**Petri film**
Bulk Water	<10000 CFU*/mL
Surface	<100000 CFU*/cm^2

*CFU : Colony forming units

To clean the cooling system from bacteria, there are different treatment procedures used. Halogens are applied periodically. To help the cleaning operation, bio-dispersant are added. Since cooling process is important in chemical industry, to minimize the bacteria growth, mechanical parts of the tower should be designed accordingly. For instance, water spray part and air inlet should be reduce aerosol droplet occurrence. Also, water should be recirculated continuously without dead spots [18]. To minimize the bacteria growth and contamination in a water cooling system (direct evaporation), design considerations and treatment procedures should be followed. Instead of these procedures, water can be cooled with a more sanitary method by porous membranes.

2.3 Membrane evaporative cooling and membrane contactors

Membrane is a selective barrier between two phases [19]. It is mostly used to separate species. Membrane porosity affects the cooling efficiency in evaporative cooling systems since evaporation from membrane surface is related with permeating water. In evaporative cooling system, membrane can be used as porous barrier as semi direct system to cool water. Since air and water semi-contact occurs in membrane pores, more hygienic conditions are provided with respect to direct contact systems. Thus, cleaning procedures does not needed in membrane applications [18].

Membrane evaporative cooling systems are beneficial compared to traditional coolers. Corrosiveness and dripping problems are not observed [19]. Porous wall barrier minimizes bacteria growth according to direct systems and increases efficiency with respect to indirect evaporative systems.

There are important concepts in evaporative cooling affecting the cooling performance and driving force. One of them is wet bulb temperature. Wet bulb temperature shows humidity in air. It is measured by wet cloth connected to thermometer. In addition to that, dry bulb temperature indicates ambient air. The difference between wet bulb and dry bulb temperature indicates the driving force for water cooling [20]. Although wet bulb temperature is the lowest air temperature that temperature can be decreased by evaporation, water temperature cannot achieve wet bulb temperature. The difference between water temperature and wet bulb temperature is called as approach [21]. In common cooling tower, approach is approximately 9°C.

Water permeates from membrane pores with driving force of pressure. The driving force for evaporative cooling is difference between partial pressure of water in air and vapor pressure of water. The equation for water evaporation is shown in Equation 2-1:

$$m_{evap} = k_p A(P^* - P_\infty) \qquad \text{Equation 2-1}$$

In the equation, partial pressure of water in air is directly related with the wet bulb temperature of air. Higher water vapor in air results in higher wet bulb temperature. Equation 2-1.

In Equation 2-1, evaporation of water depends on mass transfer coefficient between air and water, contacting area and difference between partial pressure of water in air and vapor pressure of water. That means, with the decrease in the amount of water vapor in air flow causes higher driving force for water evaporation. The permeance of water will be equal to the value from Equation 2-1, if only all permeated water evaporates.

Heat exchange between air and water streams and membrane is shown below in Figure 2.1:

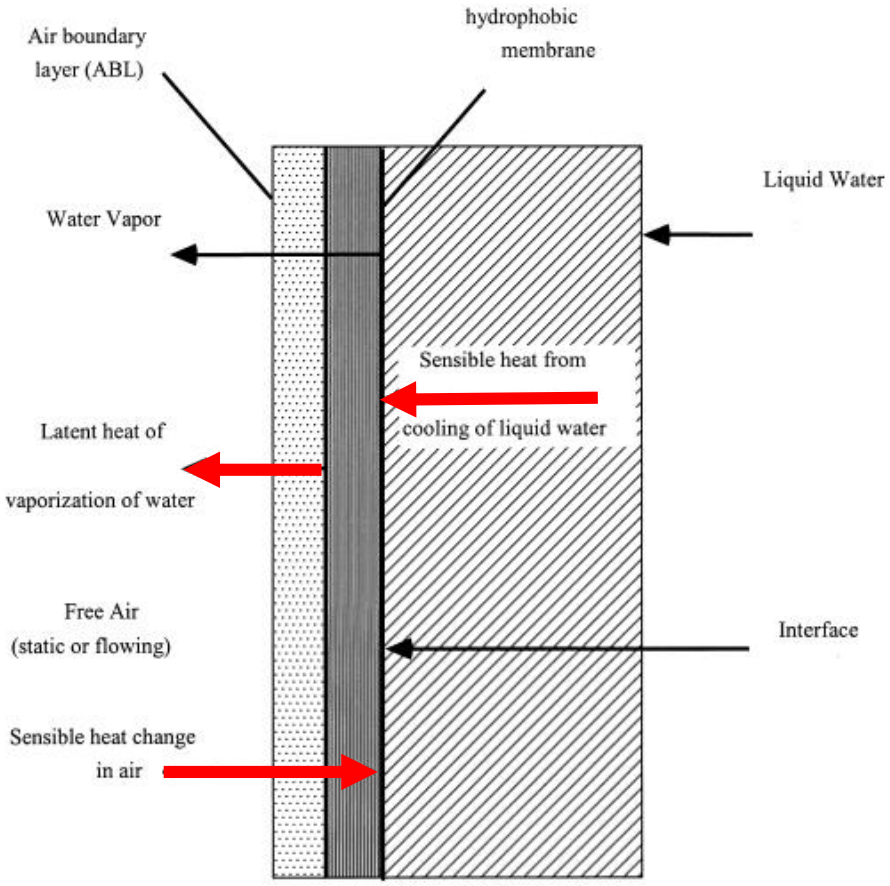

Figure 2.1: Heat transfer around membrane [19]

According to Figure 2.1, heat balance between water and air is given below in Equation 2-2:

$$Sensible\ heat\ of\ water + Latent\ heat\ of\ water = Sensible\ heat\ of\ air$$

Equation 2-2

In membrane based water cooling system, latent heat of vaporization is transported into air flow. Also, for both water and air streams, sensible heat exchange occurs.

At the interface of two phases is membrane and energy balance in this area is shown according to Figure 2.2, in Equation 2-3:

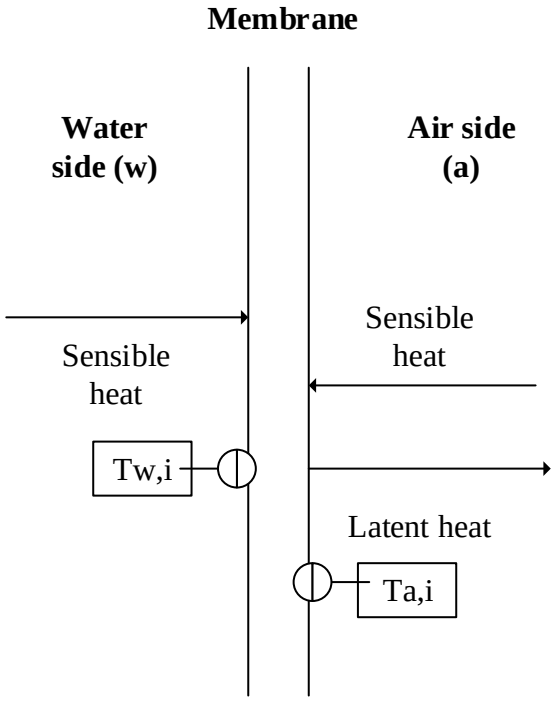

Figure 2.2: Interface of air and water streams

$$h_i A_i(T_w - T_{w,i}) + kA_m(T_{a,i} - T_{w,i}) = m_{evap}\Delta H^{vap} + h_a A_a(T_a - T_{a,i})$$

Equation 2-3

In Equation 2-3, energy transfer is shown between air and water side and interface point is membrane surface. In this equation, left hand side first term is convective heat transfer term from bulk liquid to interface. Here, h_i is inside heat transfer coefficient (water side) and A_i is inner contact area with interface. Same way, in right hand side, convective heat transfer term is placed for air side. Here, h_a shows air side heat transfer coefficient and A_a is contact area with interface. Second term in the left hand side is heat transfer through the membrane. In this term, k shows the thermal conductivity of membrane. Last, first term in right hand side is latent heat of vaporization with evaporated water amount. Here, ΔH^{vap} indicates the heat of vaporization and m is evaporated water amount.

In evaporative cooling system, membranes are not placed for separation but as barrier. Despite of traditional membrane processes, selectivity of a species is not the main purpose. This application is named as a membrane contactor. Membrane contactors prevent mixing of two phases but also allow heat and mass transfer due to membrane porosity [22].

The geometry of membrane contactors varies with the application but hollow fiber membrane geometry is most common [23]. Hollow fiber geometry provides some advantages over others. The most significant advantage is hollow fiber surface area per unit volume is high. With this way, heat and mass transfer area would be higher in small volumes. Surface area per unit volume is called as packing density and it varies between 2000 to 30000 m^2/m^3 [17]. Hollow fiber geometry reduces friction loss at surface.

Hollow fibers are assembled as bundles to place into system. To provide water circulation into fibers, epoxy resin is used. Epoxy is filler material for separation of permeate side from retantate side. Epoxy curing releases heat and heat affects the fiber when fiber number is high. It is not significant factor since modules are prepared in lab scale. During potting procedure, epoxy resin is filled at the ends of module without closing fiber tips. Curing procedure lasts 1 day [25].

In evaporative cooling applications, instead of hydrophilic polymers, hydrophobic polymers are chosen to maximize the water vaporization. In hydrophobic membranes, in pores, cohesive bonds works between air and water. According to mean pore radius and water surface tension, certain pressure is needed for water permeation through pores [26].

There are different hydrophobic polymers alternatives can be used in evaporative cooling applications. Water permeabilities of various polymers are given below in Table 2.2:

Table 2.2: Water permeabilities of different polymers [27]

Polymer	Water permeabilities (Barrer)
Polyethylene	12
Polypropylene	68
Polystyrene	970
Polysulphone	2000
Polyether sulfone	2620
Ethyl cellulose	20000
Polydimethyl siloxane	40000

According to water permeabilities shown above, polysulphone material can be chosen for membrane based evaporative cooling system because it is not highly hydrophobic or hydrophilic with respect to water permeability data in Table 2.2. That means water droplets permeating from the membrane pores do not form a film layer and facilitate the water vaporization from membrane surface. Since permeated water is evaporated from the membrane surface, permeation is a key to compare different polymers for membrane based water cooling system.

2.4 Experimental results of evaporative cooling applications

In studies, the systems working with evaporative cooling principle have the purpose of either air cooling or water cooling. For both purposes, hollow fiber modules with different polymers are used.

Johnson et al. (2003), have studied to find heat and mass transfer coefficients experimentally and the effect of operating parameters on cooling performance. For this purpose, polypropylene hollow fiber membranes with inside diameter of 200 micrometer were placed into system. Each hollow fiber bundle includes 96 fibers with the length of 0.53 m.

In this study, the aim was comparing heat and mass transfer coefficients found by experimentally and theoretically rather than cooling effectiveness. For this reason, although temperature of air was decreased approximately 0.5-1.0 ˚C and relative humidity of air is increased 1-2%, study was given as successful since heat and mass transfer coefficients match with literature values. Also, it was indicated that with higher fiber numbers and surface area, cooling will be improved. [24]

Loeb (2003), has worked with microporous hydrophobic hollow fiber membrane, to cool the water through evaporation. As polymer, polytetrafluoroethylene, polyurethane fluoroacrylate and polypropylene were placed into system. In the system, comparison of membrane and canvas material was conducted. Cooling results and overall heat transfer coefficients were compared among different materials.

According to water cooling results, by using membrane, temperature of water was decrease approximately 11˚C. On the other hand, by using porous canvas, cooling performance is higher. According to study, canvas was more cheap and efficient but this material has certain drawbacks. Most important disadvantage is presence of bacteria growth. Thus, microporous hydrophobic membranes were proposed to use in dry climates. [19]

Dohnal (2012), has worked with polypropylene hollow fiber membranes with outer and inner diameter of 0.49, 0.36 mm, respectively. By evaporative cooling principle, 600 fibers with the length of 0.69 m were placed to cool the air. The effects of water pressure and air flow were recorded. Air temperature is reduced approximately up to 5˚C. According to the results, air temperature decreases and outlet air relative humidity rises with the evaporative cooling effect. Relative humidity increase is about 50%. In the study, efficiency of membrane contactors are shown experimentally. Also, it is indicated that the fouling problem caused from water can be solved by bypass system. [23]

Mittal et al. (2006) studied on evaporative cooling of water by red clay pod. They observed that with lower relative humidity condition, cooling water performance would be high in the system with constant air temperature. Transient water temperature in clay pod is measured with time and approximately 5˚C fall is achieved. [14]

2.5 Theoretical approach for evaporative cooling systems

In evaporative cooling applications, theoretical approach or modelling is important to compare with experimental result and to foresee the effect of independent variables.

Halasz (1998), developed a general mathematical model for evaporative cooling devices. Process is assumed at steady state and evaporation process is non-adiabatic. For air and water side, heat and mass transfer equations are placed into model and transfer coefficients are found. For simplicity, partial differential equations were reduced to non-dimensional form. With this simplification, effect of parameters can be easily deduced from mathematical model.[28]

Mittal et al.(2006) experimental study was given in part 1.4. In addition to the experimental study, theoretical aspect of same system was investigated. Two different models were used for water temperature change with time and these were Van der Sman's model and simple model and. In Van der Sman's model, heat transfer is mono dimensional. Thermal properties of body were not effected from temperature. Also, body was assumed as completely wet. With these assumptions, heat and mass transfer equations were used to find relative humidity and temperature of surface. In simple model, body surface was assumed as pseudo equilibrium. In model, relative humidity varies and heat mass transfer coefficients were needed. With proper calculations, it was seen that, both models give satisfactory results with experiments. In experiments, air cooling effect was up to 7°C. In conclusion, these two models could be used in evaporative cooling applications contain hollow fiber membranes or ceramic pods.[14]

Zhang (2006), mathematical model of cross flow enthalpy exchanger was developed. Exhange mechanism is membrane based and flow is assumed laminar by conducting model. In this procedure, boundary conditions were included in thermal and momentum equations are real boundaries. With natural boundaries, air temperature, Nusselt and Sherwood number changes with flow direction is shown and fully developed Nusselt and Sherwood number are found very close to each other.[22]

Zhang (2012), developed a model including heat and mass transfer mechanism of hollow fiber membrane module for air humidification. Heat and mass transfer equalities are defined as dimensionless. Two variable partial differential equations are solved numerically. To compare the theoretical results of temperature and humidity, experiments are conducted. Results shows that model is satisfactory for low pressure drops. [29]

Johnson et al.(2003), has showed the theoretical approach for heat and mass transfer in evaporative cooling by using hollow fibers. By Chilton-Colburn correlations, heat and mass transfer coefficients for system were predicted and compared with experimental results. It seems that theoretical values were lower than the experimental results but similar to literature results. At this point, reason is explained by shield effect which is flowing air does not penetrate all fibers in the modules. [24]

Chiari (2000) studied evaporative cooling by 800 polypropylene capillaries with length of 45 cm. For decrease of air and water temperature, both experimental and theoretical analysis were contacted. While water was flowing into hydrophobic hollow fiber membrane, air was flowing cross through modules. In the system, water flow rate was changed to understand the effect on cooling performance. According to the results, decrease in temperature of water was high in low water flow rates.

For same evaporative cooling system, theoretical approach was developed. Air and water phases were assumed as perfectly mixed and flows were one dimensional. With these assumptions, mass and energy transfer equalities were developed for both air and water side. Humidification effectiveness for experimental and theoretical results were calculated for the system. According to the results, theoretical results match with the experimental data between +26% and -7%. [26].

CHAPTER 3

EXPERIMENTAL METHODOLOGY

3.1 Materials

Commercial polysulphone hollow fiber membranes was provided by Amicon (H10P10-20). In the cartridge, there are 1000 fibers with the length of 55 cm and outside diameter of 0.09 cm. The J type thermocouples (OM06-J130-10), universal data logger (UDL-100) and Dali programme, pressure gauge (Keller 0-20bar), temperature controller (SC441) and pressure indicator (PI440) were bought from Ordel Ankara. Peristaltic pump for water flow is provided by Masterflex.

3.2 Preparation of membrane modules

Hollow fiber bundles were prepared by using four pieces of membranes with a length of 38 cm each in a module. As potting material, epoxy was filled at both ends by using ¼'' diameter polyurethane tubing. During epoxy preparation, filler material and hardener were mixed in equal amounts. Prepared epoxy was filled the space between fiber and polyurethane tubing to provide water flow only through the fiber. Since each tubing has 4 cm length, active membrane length becomes 30 cm for each module. After filling procedure, membrane modules were left to dry in ambient conditions for three hours. After that, to ensure no leakage from the potted area, water was sent into the fibers with maximum pressure of 0.7 barg.

The scheme of one hollow fiber membrane module including four fibers is shown below in Figure 3.1:

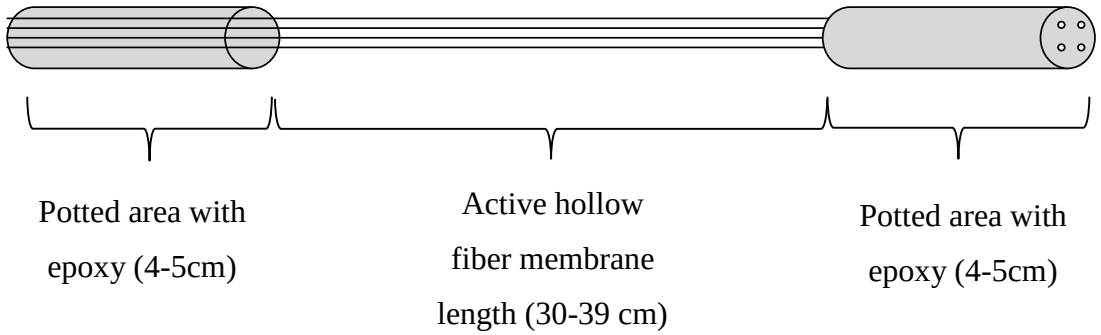

Figure 3.1: Scheme of 1 pack with 4 fibers

3.3 Water flux measurements to obtain permeate for a fiber

Polysulphone hollow fiber membrane modules were prepared for the water cooling system as mentioned in part 3.2. Since the system principle is based on evaporative cooling phenomenon, it is very important to know the water flux through the membrane at different pressures. The water flux was measured by the system is shown in Figure 3.2:

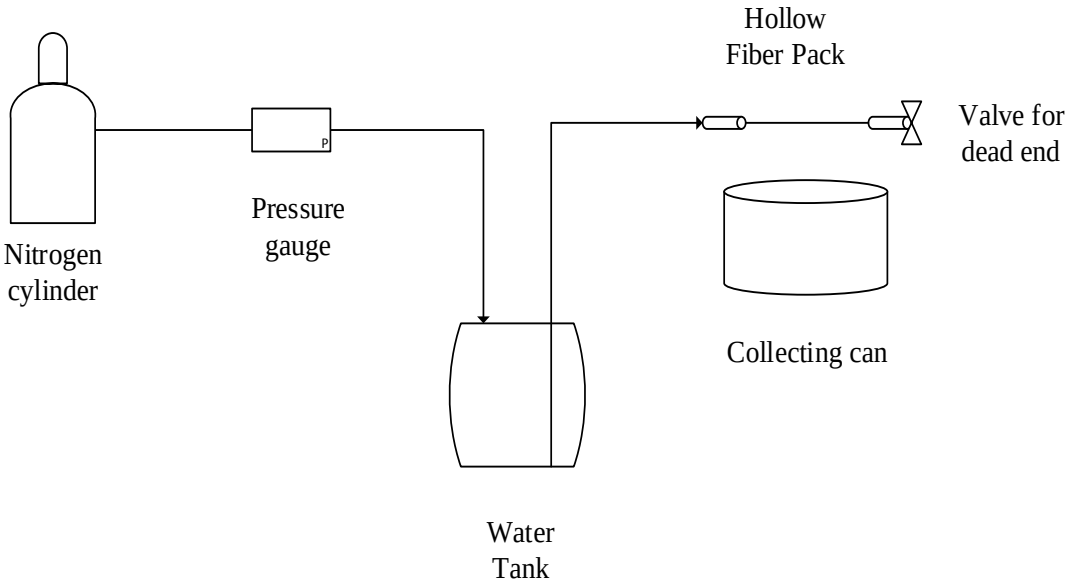

Figure 3.2: Scheme of water flux measurement system

For water permeation measurements, water tank with a capacity of 150 mL is used. It is connected to pressure gauge in the range of 0-5 bar. Also, it is connected to hollow fiber membrane module. Nitrogen (Linde 99% purity) is fed to the water tank at various pressures to increase permeated water amount from membrane surface. The end of the membrane module is connected to pneumatic valve (Aignep ¼''). It has closed water permeated through the membrane was accumulated with time to determine flux.

Since the maximum recommended operating pressure of the hollow fiber membranes is 0.8 bar, flux is measured between 0 and 0.7 barg. Water flux is measured in this system by using 10 different modules for each pressure. After that, average of the resulted data is taken for calculations.

3.4 Calibration of air flow rate

In the membrane based water cooling system, air is flowing from the bottom to the top by a suction fan (S&P TD1300-250). There is a flow rate arrangement switch from 1 to 10. With this switch flow can be changed according to the experiment.
Air velocity is measured by an anemometer at each level. According to five measurements at three different locations which are at the ends and middle portion of the membrane modules as shown in Figure 3.3 in the system from the front side, air velocity varies between 0.64 and 3.32 m/s. Since the air flow area of the system is 0.05 m^2, air flow rate becomes 115-597 m^3/hour.

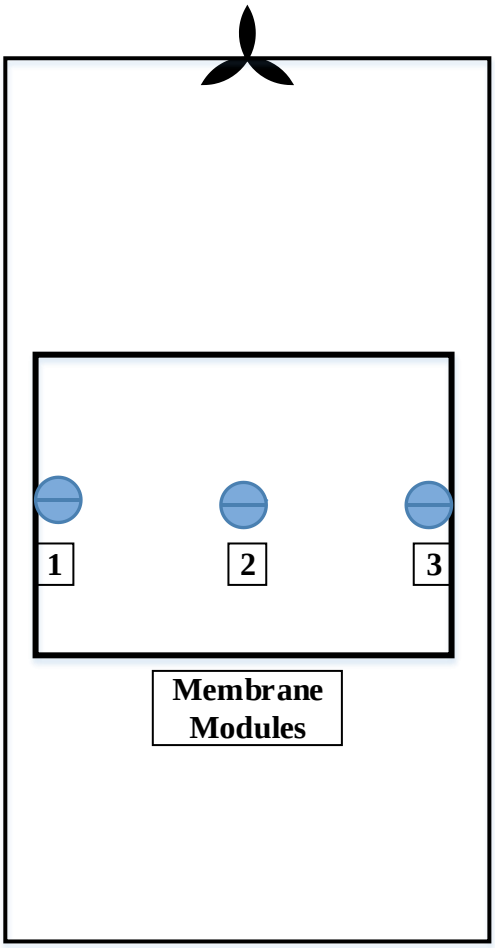

Figure 3.3: Measurement points of air velocity from front view

3.5 Membrane based water cooling system

The schematic drawing of water cooling system is shown in Figure 3.4.

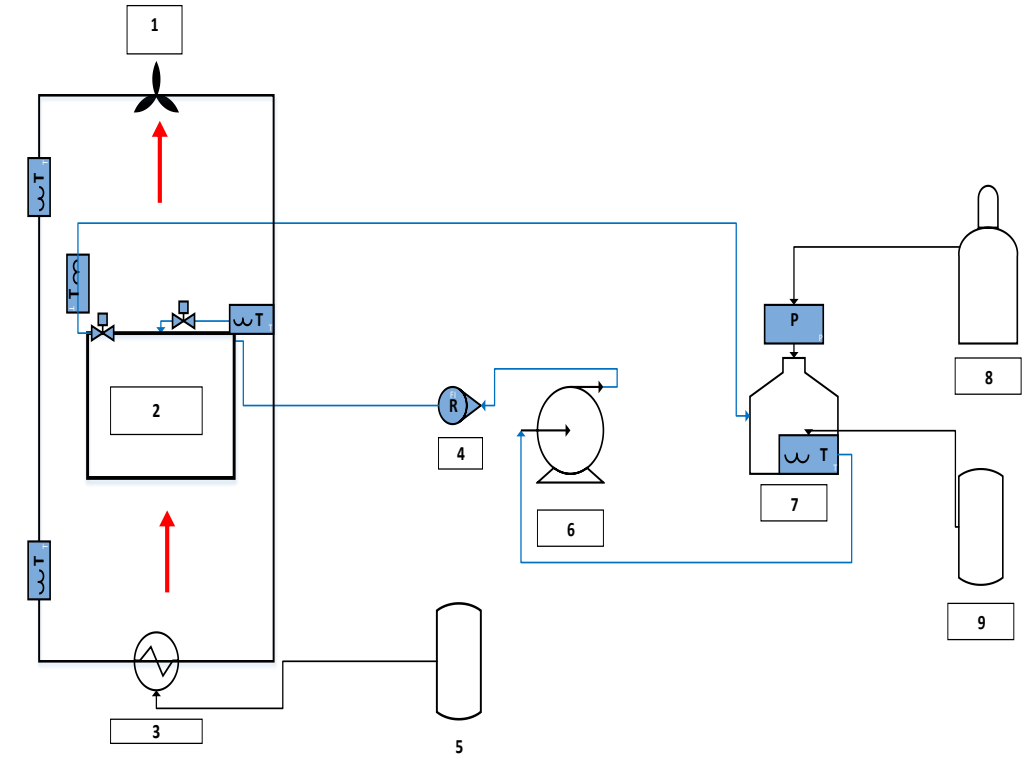

1- Air Fan	T: Thermocouple
2- Membrane Module	P: Pressure gauge
3- Heat Exchanger for Air Temperature Change	R:Rotameter
4- Rotameter	
5- Temperature Controller of Air	
6- Peristaltic Pump	
7- Feed Tank	
8- Gas Cylinder	
9- Temperature Controller of Water	

Figure 3.4: Scheme of membrane based water cooling system

The system is divided into two parts which are water and air side. In water side, there are water tank, peristaltic pump, mixer, temperature controller, rotameter and water thermocouples. Water tank shown as 7 in Figure 3.4, with the capacity of 700 mL is filled with distilled water. With peristaltic pump, water is fed to the distributor. Flow rate of the water can be arranged between 0-40 mL/min. From the distributor, water is distributed to the hollow fiber membrane pack. In the system, there are 18 pack spaces (3 horizontal, 6 vertical). Water flowing through the tube side of the membranes is recirculated to the tank. Tank can be pressurized by nitrogen (Linde 99% purity). The pressure is measured from pressure gauge (Keller 0-20 bar). In addition, water temperature in the tank is controlled by a temperature controller and is measured by thermocouple. To homogenize the water temperature, mixer is placed under the water tank with 250 rpm. All connections in the system are ¼'' polyurethane tubing and they are isolated by heat insulation material. Water temperature change between the inlet and outlet of the module is measured by J type thermocouples. Water temperature data is taken with two ways. For single module experiments, temperature data is measured directly from the inlet and outlet of the module. For multiple module experiments, data is measured from the inlet and outlet of the distributors as average. Taken data is digitally recorded.

Air side includes air fan, heat exchanger, temperature controller filter and air thermocouples. Air is flowing cross to the membranes. To eliminate the contamination on membrane surface, air filter (5 μm) is placed at the inlet of the air. The inlet temperature of the air is arranged by using temperature controller and heat exchanger. Air fan (suction) is installed at the top of the system and flow rate can be changed by switch. Inlet and outlet air temperature is measured by using J type thermocouples. Both wet and dry bulb temperature data were recorded with respect to time. To keep air flow constant over the membranes, system is surrounded by plexy cabins with size of 10 cm x 50 cm. Beside the temperature data, water level data is also taken with time to calculate the evaporated amount of water from the membranes for each experiment.

In the membrane based water cooling system, there are seven independent variables. They are inlet air temperature, inlet water temperature, air flow rate, water flow rate, module length, pack number and transmembrane pressure. The effect of these parameters on the water cooling performance is tested. For investigating inlet air temperature effect, one module with 4 fiber is placed into system. Water inlet temperature is 25°C, air pressure is 0 barg, water flow is 10 mL/min and air flow is 1.84 m/s during the experiment. Inlet air temperature is changed as 25, 30 and 40°C. With the same way, for the effect of inlet water temperature, one module is used. Air inlet temperature is 25°C, air pressure is 0 barg, water flow is 10 ml/min during the experiment. Inlet water temperature is changed as 20, 25, 30 and 40°C.

Air flow rate effect is tested by changing the air flow switch from 1 to 9 (0.64 m/s-3.32 m/s). Since air velocities are close to each other, measurements vary as 1, 3, 5, 7 and 9. The set temperatures of inlet air and water are 25°C. Other parameters are kept same. In water flow rate effect analysis, one module is placed into system. Water flow is changed between 10- 40 mL/min with air flow of 1.84 m/s, air pressure of 0 barg.

To investigate the module length effect, membrane modules are connected in series. In other parameter investigations, they were connected in parallel. Module length of 30 cm, 60 cm, 90 cm, and 120 cm are measured with the air flow of 1.84 m/s, water flow of 10 ml/min, air pressure of 0 barg and set temperatures of inlet air and water, 25°C. The effect of pack number on the water cooling performance is tested with 1, 9 and 18 packs in parallel. Other parameters are same with the module length experiments. Lastly, air pressure of the membranes are changed as 0, 0.1 and 0.2 barg in one module with air velocity of 1.84 m/s, water flow of 10 ml/min and set temperatures of 25°C. All experiments were repeated 3 times with different membrane packs prepared in different times.

After the experiments, hollow fiber membrane modules are left in a solution (500 ppm sodium hypochlorite) to prevent drying.

CHAPTER 4

RESULTS AND DISCUSSION

4.1 Membrane characterization

The membranes used in this study were commercial hollow-fiber ultrafiltration membranes that was made of polysulfone. Figure 4.1 shows the cross-sectional SEM image of a membrane. The membrane has an outer diameter of 900 μm and inner diameter of approximately 500 μm. The skin layer, which is responsible for the separation, is at the bore side with a thickness of 6.9 μm (Figure 4.2). The support side consists of large finger like pores that are expected to show low resistance to permeation.

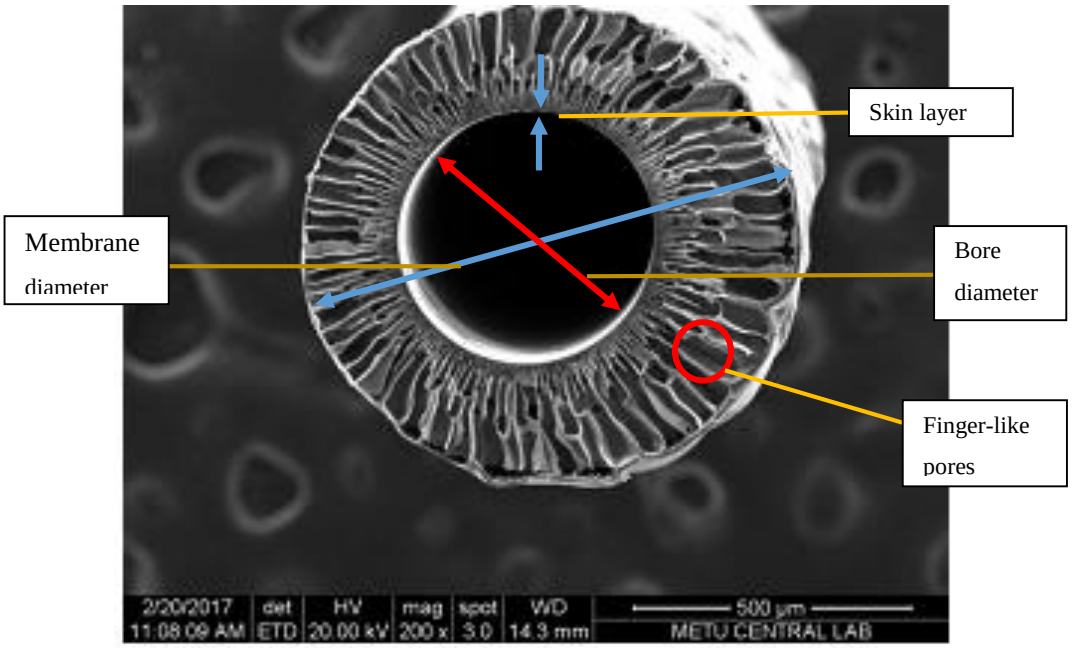

Figure 4.1: SEM image of commercial polysulfone hollow fiber membrane

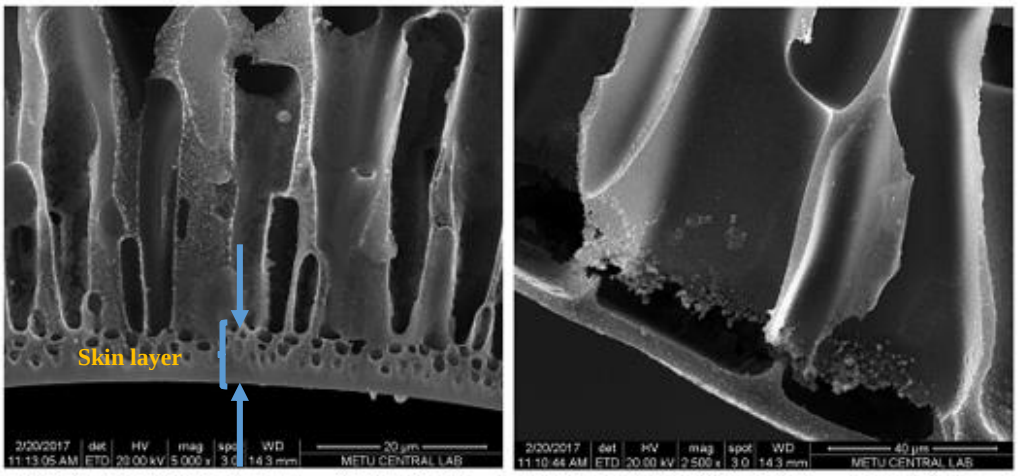

Figure 4.2: SEM images of inner (a) and outer portion (b) of fiber

4.2 Flux of water permeated through the membranes

The working principle of membrane based water-cooling system is evaporative cooling. Therefore, it is essential to know the amount of water permeated thorough the membrane and evaporated from the surface. It may not be possible to measure the rate of water permeation accurately during the cooling process because the water permeates across the membranes and evaporates from the surface simultaneously. For this reason, the pure water flux of membranes was determined without air flow at room temperature under a transmembrane pressure difference of 0.05 to 0.7 bars. The reason that pressure was not incremented further is it was not recommended.

The measurements were carried out with 10 pieces of 39-cm-length membranes (Figure 4.3). The membrane flux, which is in the range of $2x10^{-4}$ to $7x10^{-4}$ cm^3/cm^2-sec that is typical to ultrafiltration membranes, increased with transmembrane pressure as expected. The water permeation data were also tabulated in Appendix Table A1 and A2.

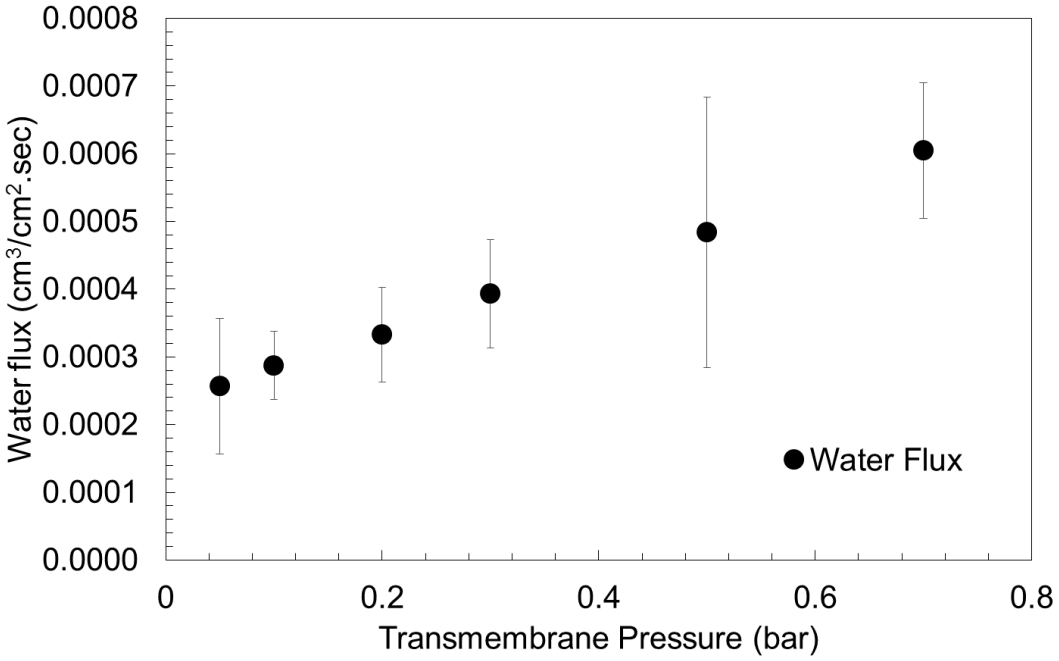

Figure 4.3: Water flux data points for various pressures

According to the given results in Figure 4.3, water flux permeating from the hollow fiber membrane is increasing with the pressure. During the experiments, water loss from the system is measured. Water flux measurement result is an important tool to compare evaporated amount from system with flux.

4.3 Calibration of air blower used in cooling system

Air flow rate of the system is measured by anemometer device. There are 10 different arrangements of flow enabled by the device via a switch. For each level, 10 measurements are conducted at three different locations around bundle.

Air velocity results are given in Appendix Table A.3 for three different zones which are at the ends of bundle and middle portion of the bundle. The average of these data are taken to find air velocities. Plot of air velocity with respect to air switch level is shown in Figure 4.4:

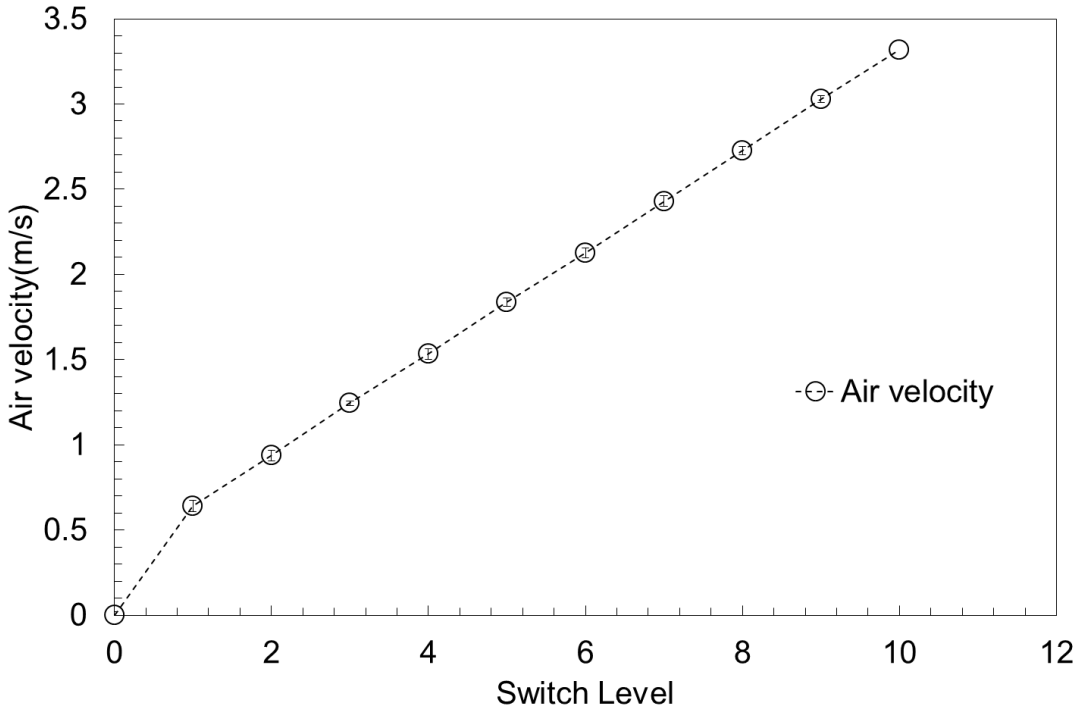

Figure 4.4: Plot of air velocity versus air switch level

For area of air flow of 0.05 m^2, volumetric air flow rates are obtained by air velocity data for each switch level and is given in Figure 4.5:

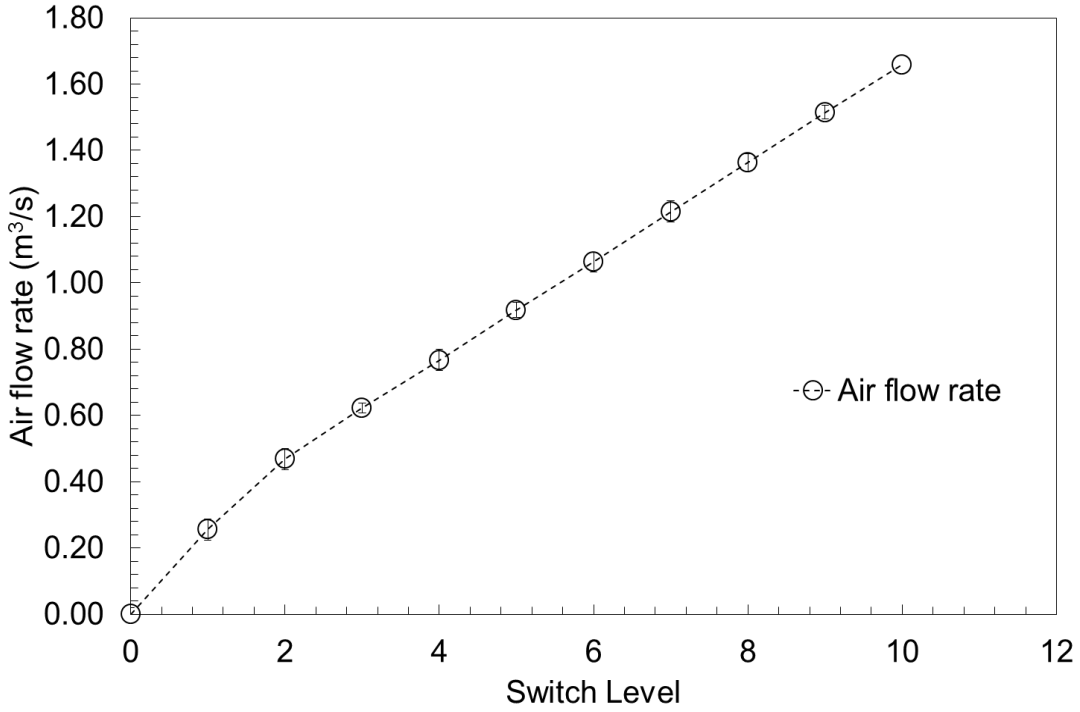

Figure 4.5: Plot of air flow rate change with switch level

4.4 Position of thermocouples in the membrane based cooling system

Figure 4.6 shows the positions of thermocouples used to measure the water, dry and wet bulb air temperatures and of other instruments used to measure the water level, flow rate and air velocity. Hereafter the same labels and numbers are used to indicate a particular temperature measurement.

The water, whose flow rate was measured by a flow meter (R), was recirculated between a large tank and the membrane module by a peristaltic pump. The tank water temperature, measured by thermocouple T9, was kept constant by an electric heater. The amount of water permeated through the membrane cannot be measured precisely due to evaporation during the cooling process, therefore the change of level of water in the tank (h) was measured to find the rate of permeation across the membrane. Throughout the study, dripping of water from the membrane surface was seldom observed, suggesting that the water that permeated through the membrane completely evaporates. Hence the decrease in the water level indicates the rate of evaporation since only water loss is resulted from the membranes in all system.

The hollow-fiber UF membranes was cut into 38-cm pieces and used to make a pack of 4 membranes, which are connected parallel to each other. 4-cm from each end was used to glue so that the active length of a pack was 30 cm with a total permeation area of 33.9 cm^2/pack (8.5 cm^2/piece). The water flows from the bore of the fibers, and air flows out of them. The membrane module consisted of a distributor plate (plates B) and a collector (plate B) as shown Figure 4.6. Those plates distribute the hot water (coming from the tank) among the membrane packs, and collect cold water (left from the membranes) before returning to the tank. The membrane module has 18 slots for membrane packs; therefore, the total permeation area can be changed between 33.9 cm^2 to 610.2 cm^2.

The water temperature is measured at the inlet of module (T7) and a membrane pack (T5). Although the T5, T7 and T9 are expected to be equal to each other, the heat loss along the tubing and plate B causes small differences. The water temperature is also measured at the exit of a membrane pack (T6) and module (T8). Therefore T6 represents the cooling performance of a single membrane pack and T8 shows the average performance of as many as 18 packs.

Throughout the study, air temperatures were also measured above and below the membrane module. The dry and wet bulb temperatures of air flowing into the module were T3 and T1, respectively. Those leaving the membrane module were T4 and T2. The humidity of air was determined by using dry and wet bulb temperatures.

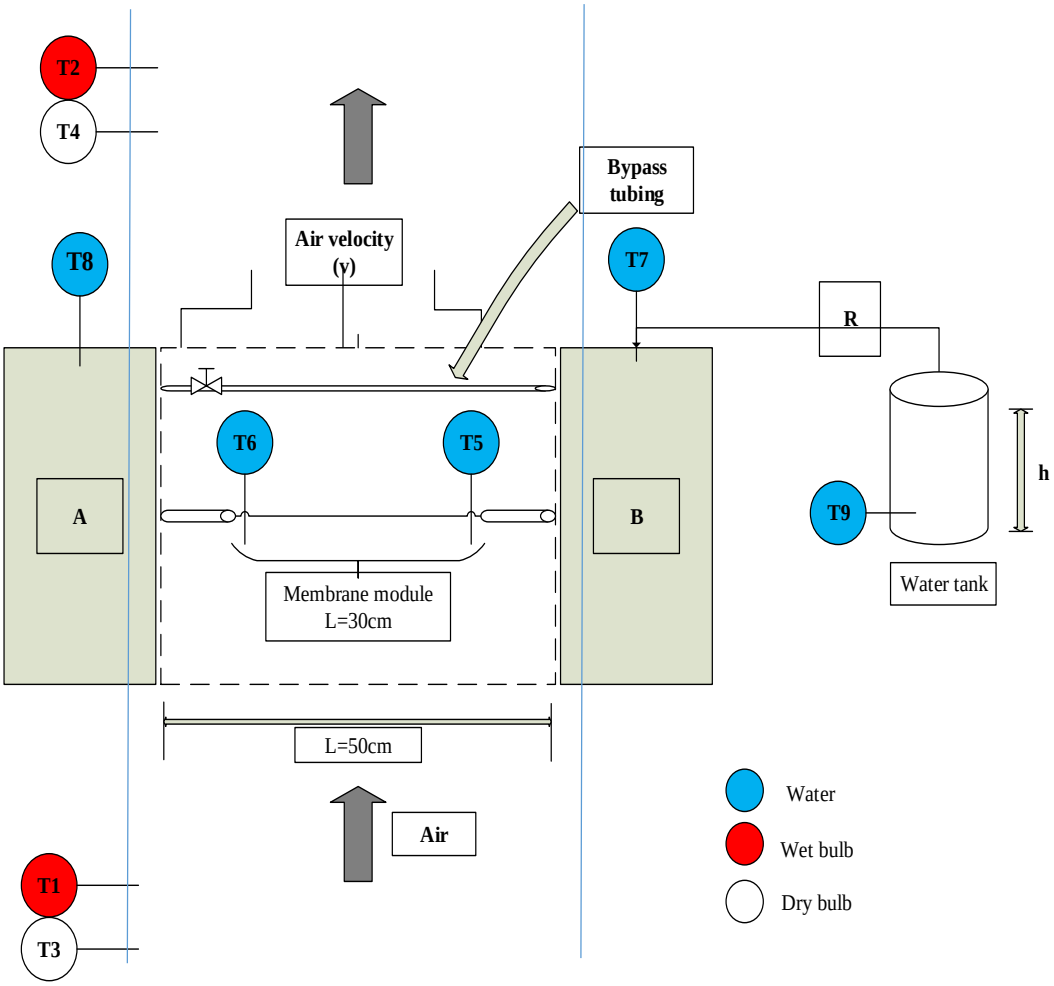

Figure 4.6: Positions of sensors around the membrane module in the membrane based water cooling system

4.5 The change of water and air temperatures with time

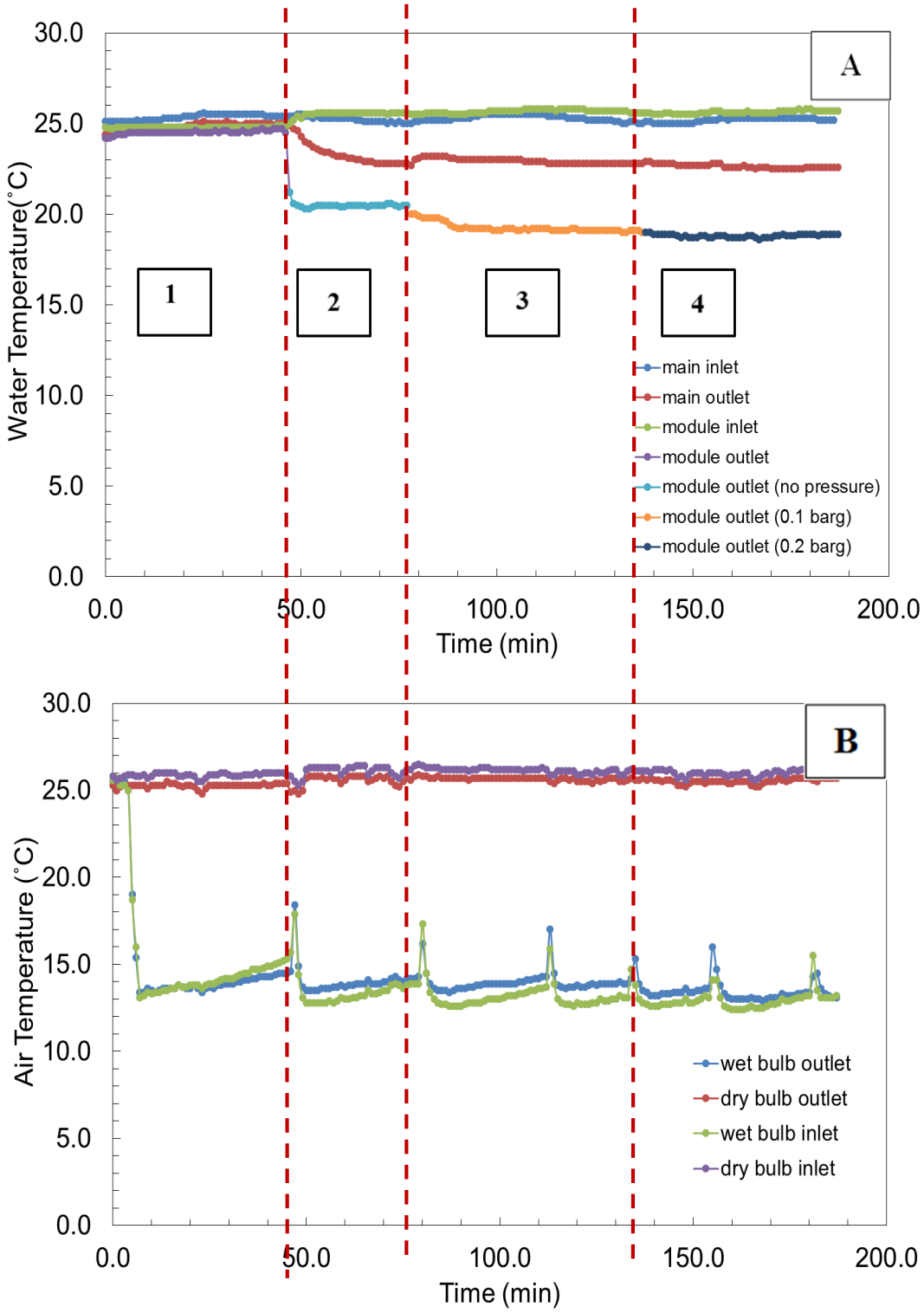

Figure 4.7: Change of water temperature (A) and air temperature (B) with time, 1 is bypass stage, 2-3-4 are different air pressures

In Figure 4.7, water temperature (A) and air temperature (B) changes are shown with time. Typical result belongs to transmembrane pressure change in one module system. In water temperature with time graph (A), water inlet and outlet temperatures are given as single module and main average. With increasing transmembrane pressure effect, temperature change is measured. In air temperature with time graph, dry bulb and wet bulb temperatures of air at inlet and outlet of the bundle are shown.

In the experiment, 30 cm membrane module placed in parallel. Bundle water inlet and air inlet dry bulb temperatures are arranged as 25˚C. Water flow through the membrane module is 10 mL/min and air flow rate is 1.84 m/s during the experiment. In Stage 1, water pumped into bypass tubing instead of membrane module. As it is seen from Figure 4.7 (A), at inlet and outlet of tubing temperatures of water are approximately same. Also, bundle water inlet and outlet temperatures recorded from the distributors are very close to each other. At the beginning of Stage 2, water is sent to module by closing bypass valve and instant water temperature difference is observed. Bundle water outlet temperature is above the module outlet temperature since exit distributor is effected by outside temperature with lack of insulation. In Stage 3, by keeping all parameters constant in the experiment, nitrogen pressure is turned to 0.1 barg. Pressure is measured by pressure gauge in the system. According to water temperature decrease, cooling performance becomes higher in this stage. Last, in Stage 4, pressure is arranged at 0.2 barg. Further rising in pressure causes water drop from the membrane module. For this reason, effect of transmembrane pressure is investigated up to 0.2 barg nitrogen pressure. In the air temperature graph, it is seen that both dry bulb and wet bulb temperature does not change during the experiment. There are fluctuations in wet bulb temperature. Since wet bulb temperature is measured by using wet cotton at tip of the thermocouple, dampness of the cotton will not be same during the experiments.

On the other hand, air flow rate is much higher than water flow rate in the system. Since evaporated amount of water determines the change in outlet dry bulb temperature of air, resulted temperatures are expected.

4.6 Investigating the effect of process variables on the performance of membrane based water cooling system- Experimental Work

In membrane based water cooling system, effect of seven different independent variables on water-cooling was investigated. These parameters are water flow rate, air flow rate, transmembrane pressure, module length, module number, inlet air temperature and inlet water temperature.

4.6.1 Effect of water flow rate on the cooling performance

In the system, water flow rate was changed between 10 and 40 mL/min. Inlet air temperature, water temperature, air velocity and tank pressure is 25°C, 25°C, 1.84 m/s and 0 barg, respectively. There were one membrane pack in the module.

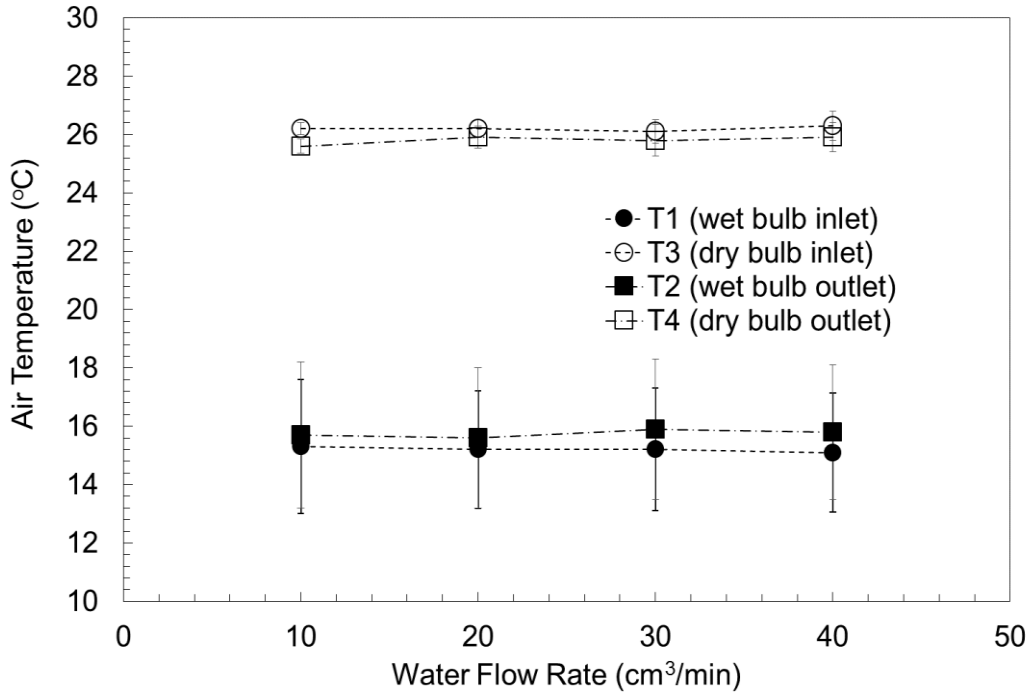

Figure 4.8: Air Temperature Change with Water Flow Rate, 1.84 m/s air velocity-0 barg air pressure-1 pack

Figure 4.8 shows the change of wet and dry bulb temperatures at the module exit as a function of water flow rate. Due to high flow rate of air, its temperature and humidity changes were negligible as expected so the wet bulb temperature at the exit (T2) is nearly the same as wet bulb temperature at the inlet (T1). It is an expected result since air flow rate is much higher than water flow rate. Hence air outlet temperature was not affected.

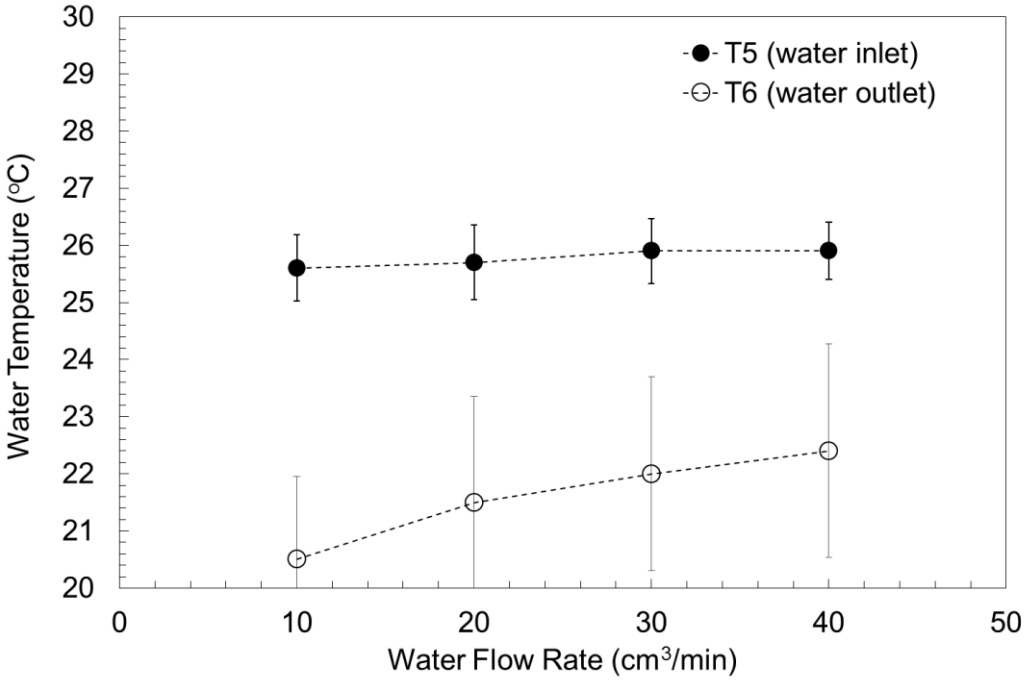

Figure 4.9: Water Temperature Change with Water Flow Rate, 1.84 m/s air velocity-0 barg air pressure-1pack

On the other hand, water temperature changes significantly as its flow rate increases (Figure 4.9). At a water flow rate of 10 cm^3/min, the cooling performance was higher so that its temperature decreased from 25.6˚C to 20.5˚C. At higher flow rates, the cooling performance decreased. For example, for water flow rate of 40 cm^3/min flow rate, temperature drops from 25.9 to only 22.4 ˚C.

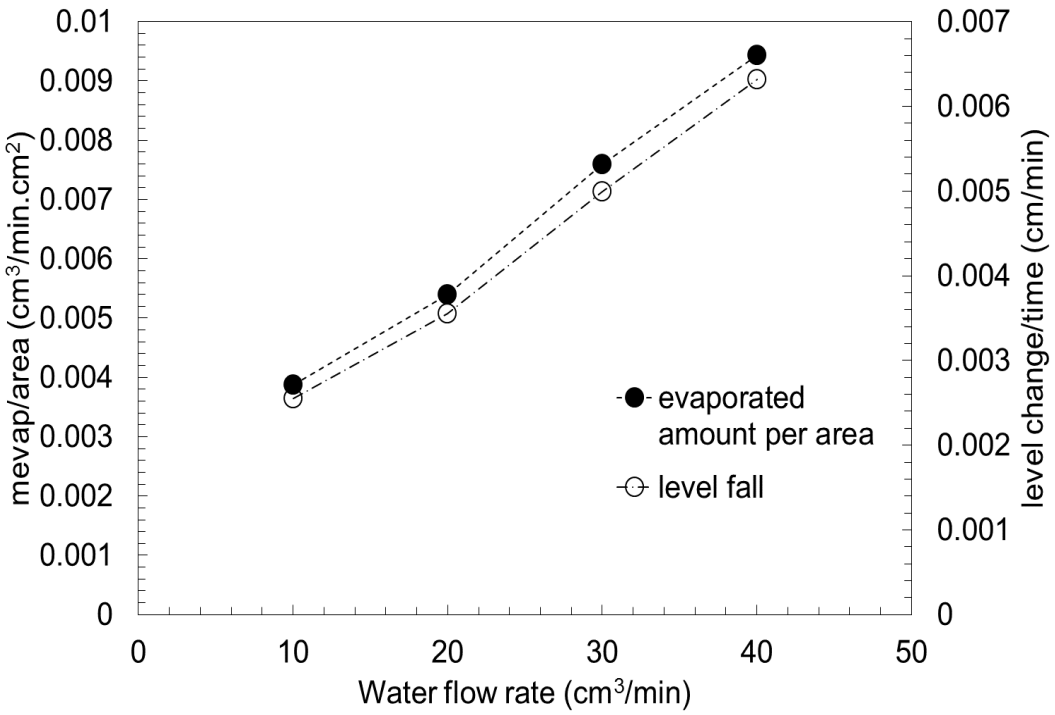

Figure 4.10: Evaporated Water Amount and Level Change with Water Flow Rate

In Figure 4.10, evaporated water amount change per area and level change per time is shown with four different water flow rates. Level change is measured from the water tank during the experiment with time by using millimeter paper and evaporated water amount is calculated from amount of water loss from the tank per membrane outer surface area. Although from the result, water loss is increasing, it does not mean all water droplets are evaporated from the surface.

4.6.2 Effect of air flow rate on cooling performance

In Figure 4.11, wet and dry bulb air temperature change is given with changing air velocity. T1 and T2 represent wet bulb inlet and outlet temperatures, T3 and T4 show the dry bulb temperatures at inlet and outlet of the module.

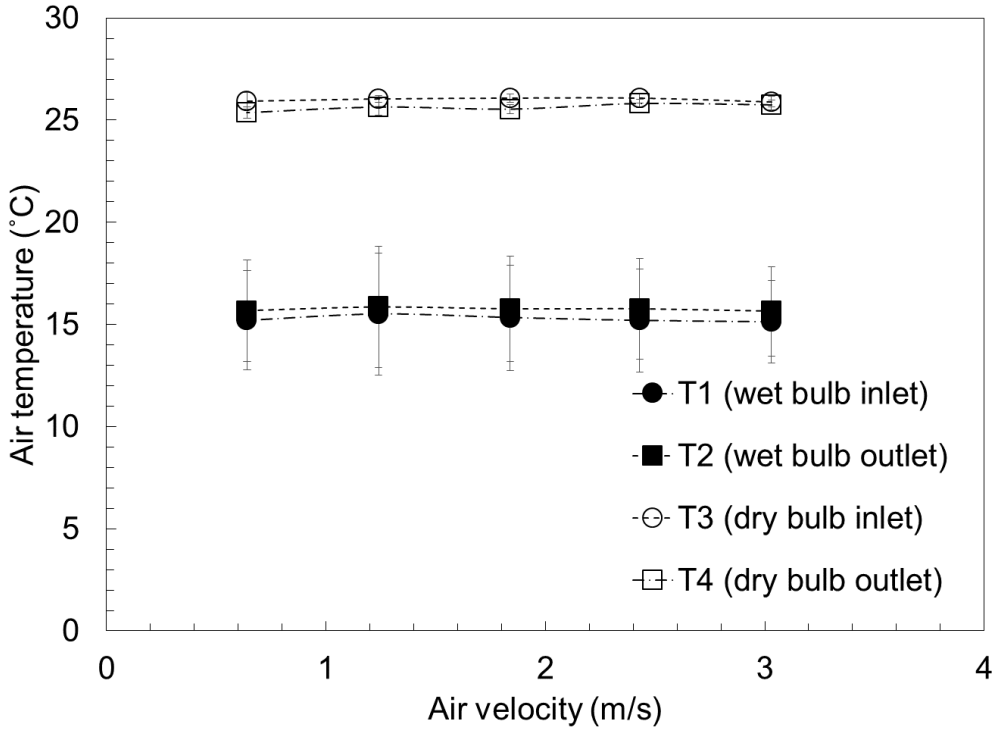

Figure 4.11: Air Temperature Change with Air Velocity, 10cm^3/min water flow- 0 barg air pressure-1 pack

According to results, outlet air temperatures are nearly constant in the one pack experiment. Since air flow rate is much higher than water flow rate and evaporation, air temperatures are not affected.

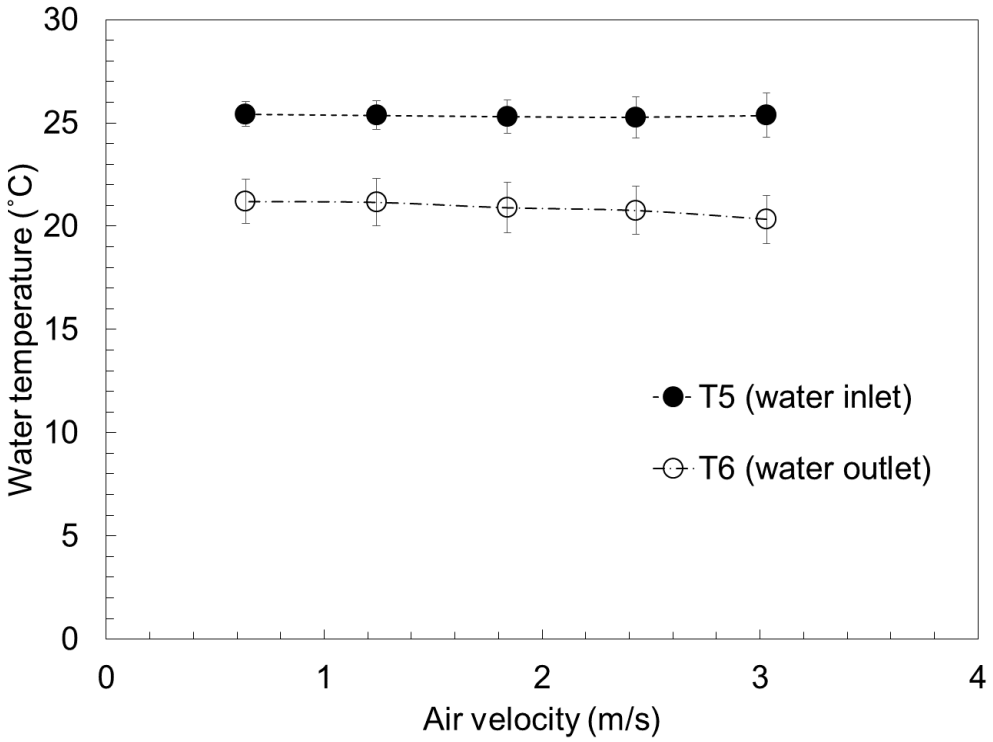

Figure 4.12: Water Temperature Change with Air Velocity, 10cm^3/min water flow-0 barg air pressure-1 pack

In Figure 4.12, with increasing air velocity, water temperature change is shown. Under five different air velocity, water inlet and outlet temperatures are measured. With decreasing air velocity from 3.32 m/s to 0.64 m/s, inlet water temperatures are 25.4, 25.3, 25.3, 25.4 and 25.4 ˚C and outlet water temperatures are 20.3, 20.8, 20.9, 21.2 and 21.2˚C. Cooling of water cannot be distinguished clearly between close air velocities. Yet, if highest and smallest air flow are compared each other, it is observed that cooling performance is higher with high air flow rates. It is expected result since increasing air velocity causes decrease water vapor amount in air flow. Hence driving force of vaporization grows into higher.

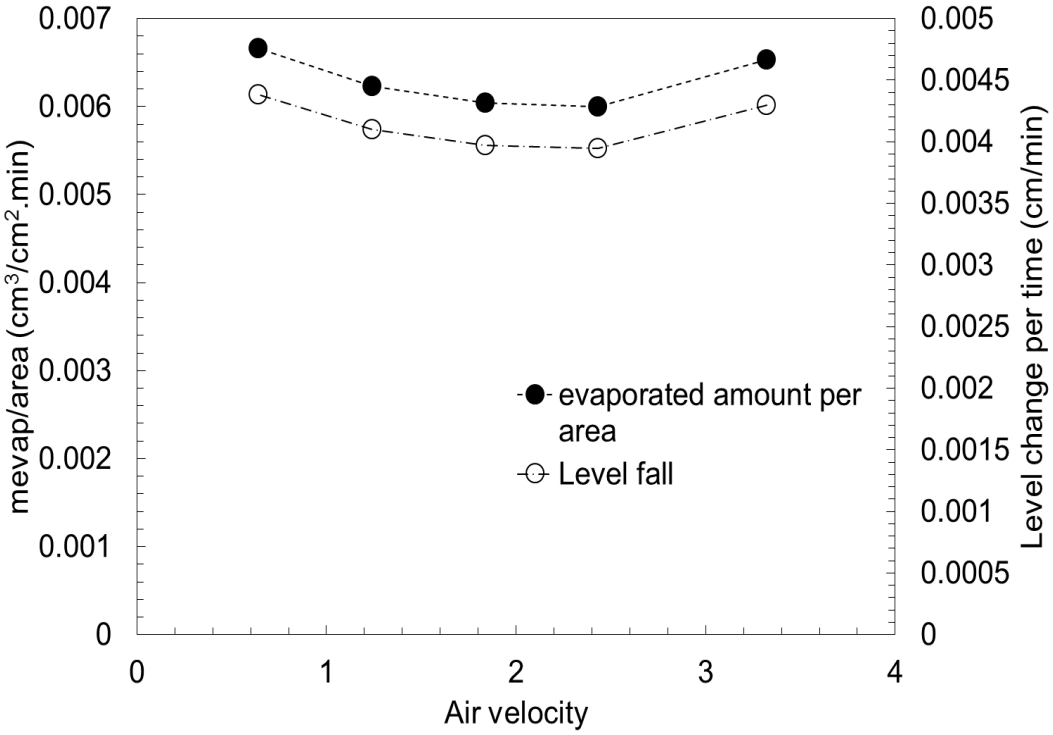

Figure 4.13: Evaporated water and level change with air velocity

In Figure 4.13, evaporated water amount data and level change during the experiment is demonstrated with air velocity effect. In the plot, evaporation trend is nearly constant with changing air velocity. The trend is same as the plot of water temperature with air velocity. Since evaporation amount affects the decrease in water temperature, it is an expected result.

4.6.3 Effect of transmembrane pressure on cooling performance

Figure 4.14 gives the air temperature change data with increasing air pressure in the membrane based cooling system. With experiments conducted by using 1 pack and constant water flow rate, air velocity, dry bulb and wet bulb temperatures are measured.

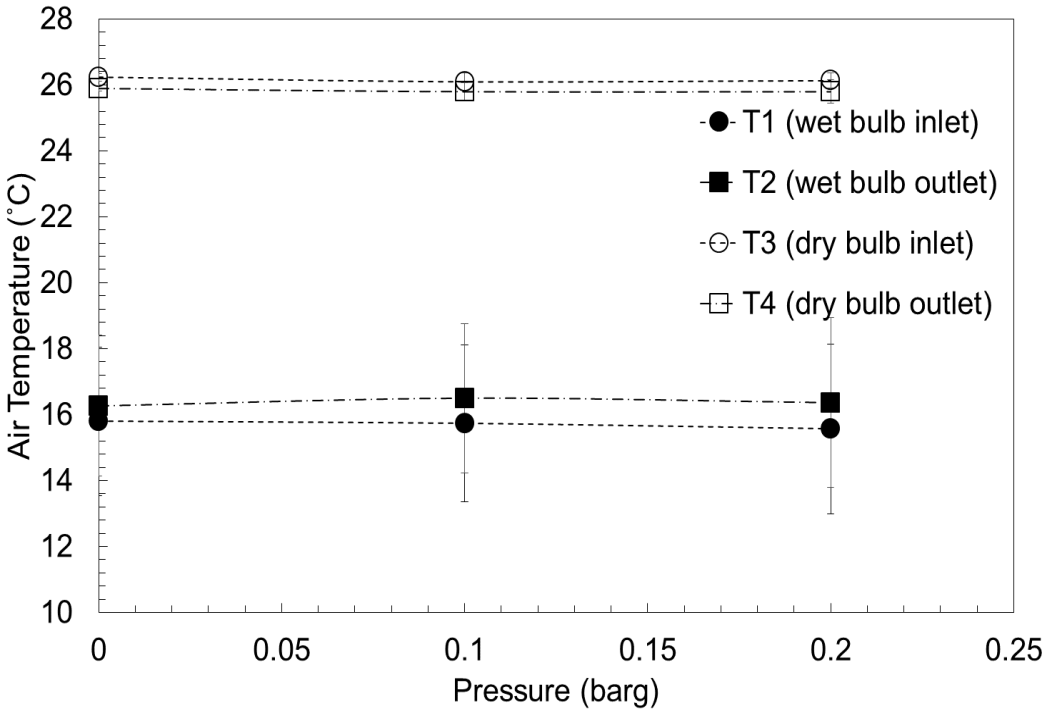

Figure 4.14: Air temperature change with transmembrane pressure, 10 cm^3/min water flow rate-1.84m/s air velocity-1pack

According to the plot in Figure 4.14, both wet bulb and dry bulb temperatures show slight changes. Air flowing over membrane module is away from saturation. The evaporation amount of water was not enough to change the outlet air temperature in one pack experiment.

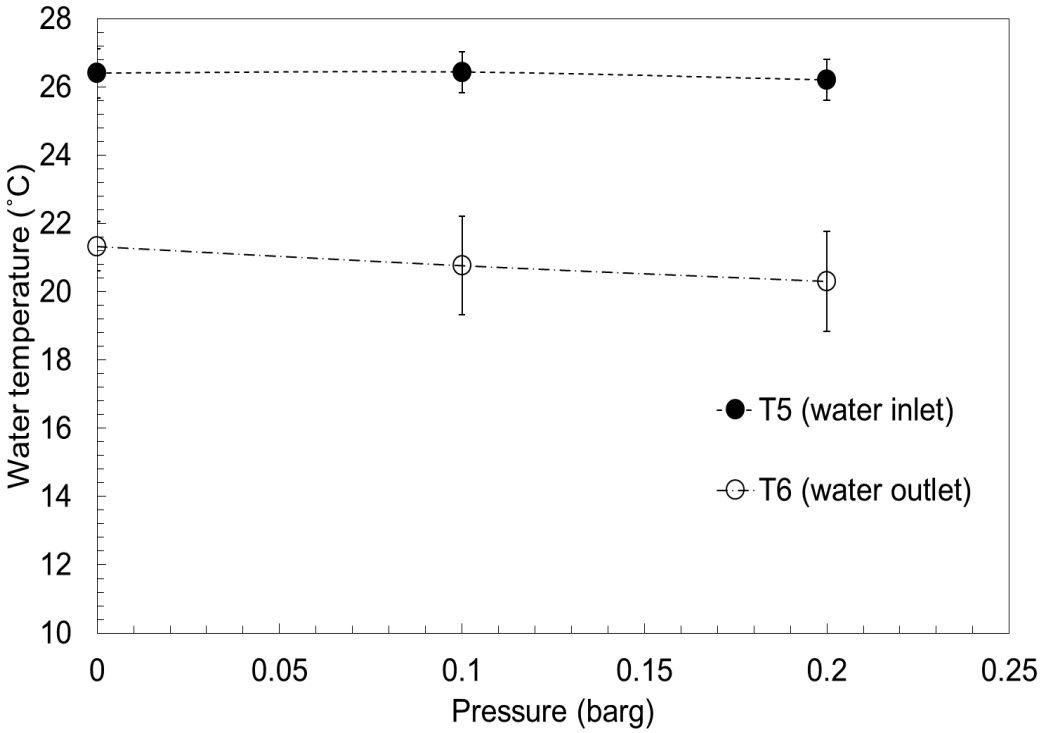

Figure 4.15: Water temperature change with transmembrane pressure, 10 cm^3/min water flow rate-1.84m/s air velocity-1pack

Module inlet and outlet temperatures with three different air pressures are plotted in Figure 4.15. For 0 barg, 0.1 barg and 0.2 barg air pressures, inlet water temperatures are 26.6, 26.5 and 26.2˚C. Outlet temperatures of water are 21.3, 20.8 and 20.3˚C. With elevation of air pressure on membrane modules, it can be interpreted that cooling performance develops. Rise in transmembrane pressure causes increase in water permeance. Hence vaporization of water increases and it affects the water outlet temperatures.

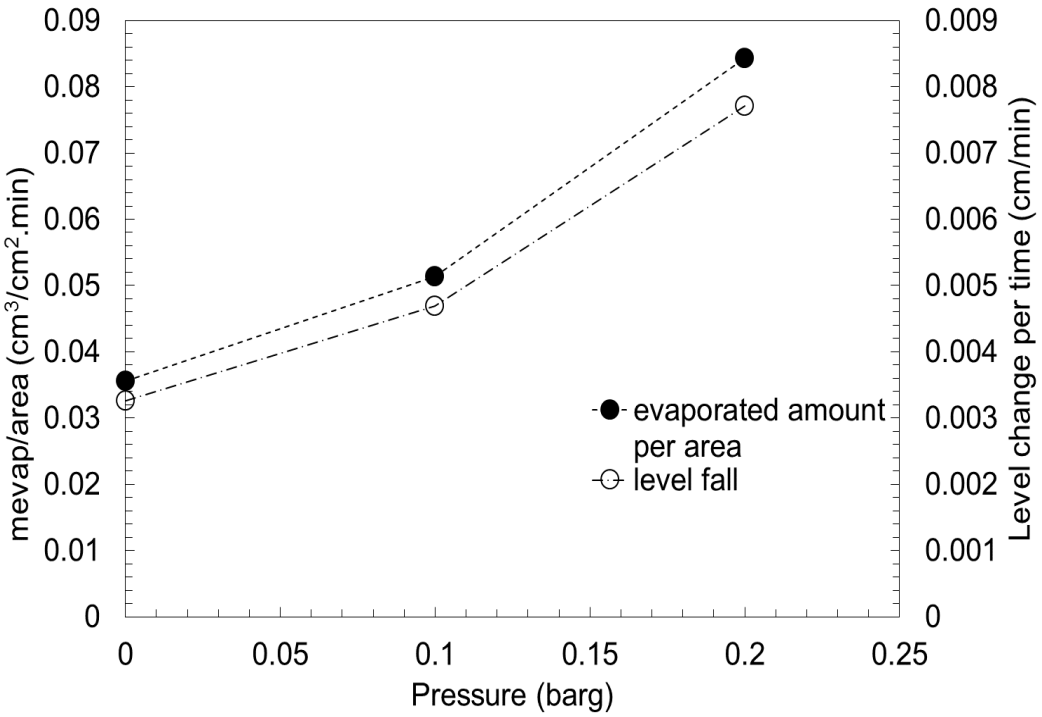

Figure 4.16: Evaporated water and level change with time

In Figure 4.16, for one polysulfone hollow fiber pack, evaporated water amount per membrane lateral area with respect to air pressure is given. According to resulted plot, amount water evaporation trend is increasing with elevation of air pressure. Water outlet temperature fall resulted from the evaporation so that it is an expected result.

4.6.4 Effect of module length on cooling performance

For investigation of length effect on membrane based cooling system, by keeping water flow rate, air flow rate and pressure constant, module length becomes 30, 60, 90 and 120 cm. Since, commercial hollow fiber length is limited, membrane modules of 30 cm are added to each other in series with proper fittings.

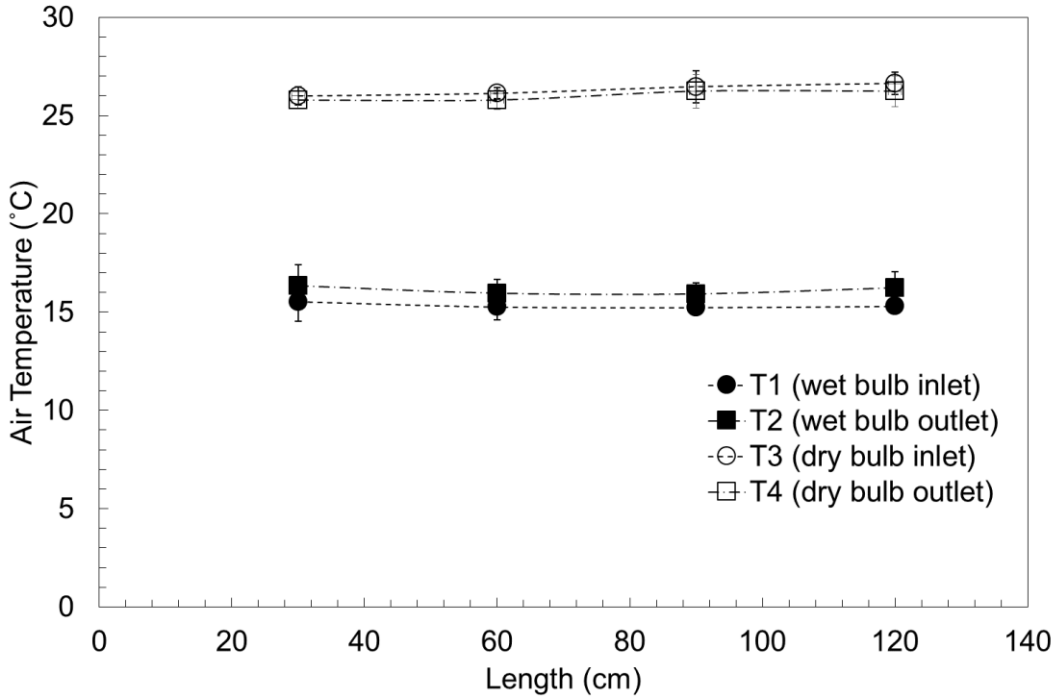

Figure 4.17: Air temperature change with length, 10 cm^3/min water flow rate-1.84m/s air velocity-0 barg air pressure

The results of air temperature change at inlet and outlet of the membrane module are shown in Figure 4.17 with increasing length. Increasing length of membrane bundle resulted in slight decrease in dry bulb temperature and slight increase in wet bulb temperature. It is expected since membrane contact surface area increases with connection in series. Rise in vaporization amount of water results in slight changes in outlet air temperatures.

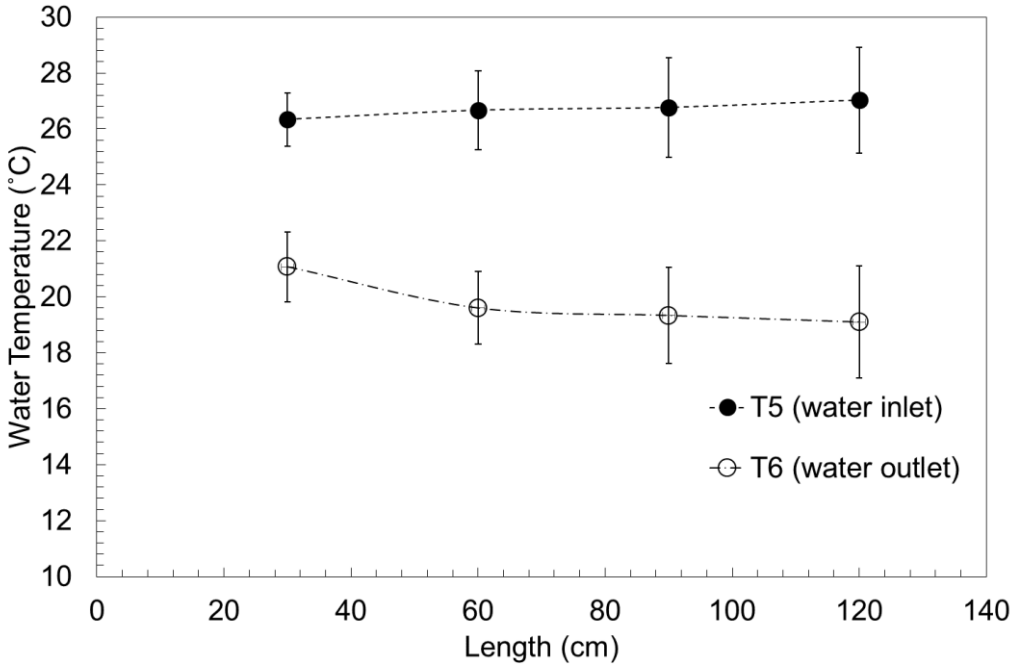

Figure 4.18: Water temperature change with length, 10 cm^3/min water flow rate-1.84 m/s air velocity-0 barg air pressure

In Figure 4.18, water inlet and water outlet temperature trends are shown with increasing module length from 30cm to 120cm. According to plot, inlet water temperatures are 26.3, 26.6, 26.4 and 26.6˚C for 30, 60, 90, 120 cm length, respectively. Also, outlet water temperatures are 21.1, 19.6, 19.3 and 19.1 ˚C. The difference between inlet and outlet water temperatures indicate that, length increase affects the cooling performance in positive way. On the other hand, the decrease in water temperature is not linearly proportional with length. Experimentally, it is observed that above 120 cm module length, water flow was not continuous. For this reason, length was not incremented further.

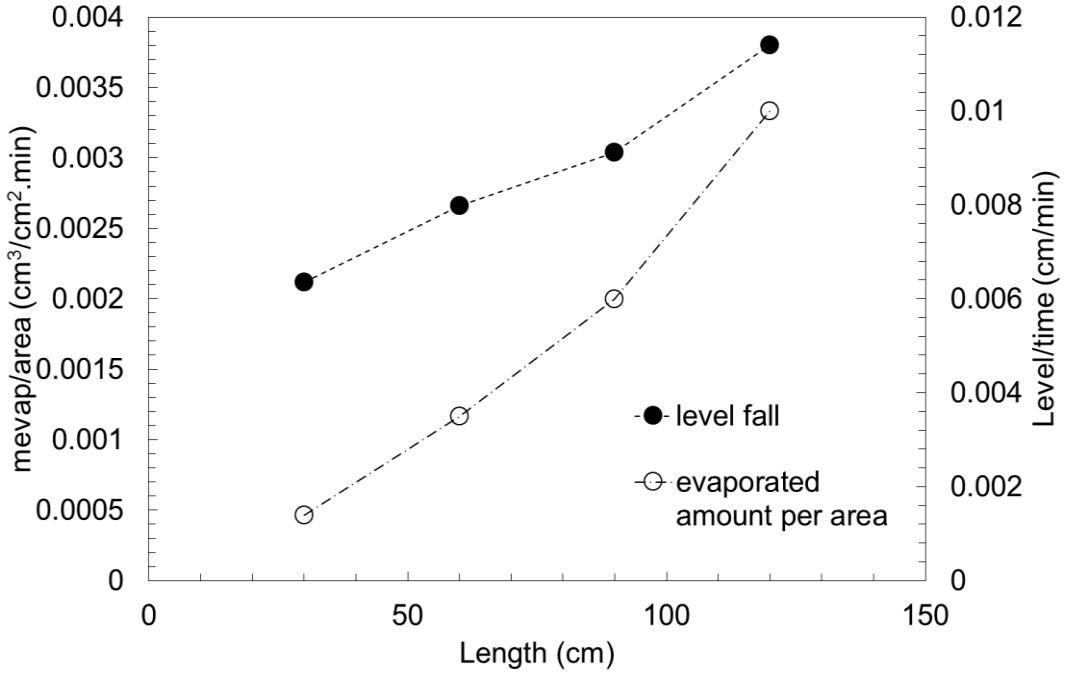

Figure 4.19: Plot of evaporated water and level change with length

Figure 4.19 shows level decrease and evaporated water amount with change in module length. With increasing membrane bundle surface area in water cooling system, evaporation amount is increased with increasing module length. Theoretical results have same trend with water temperature change in one pack experiment.

4.6.5 Effect of number of fiber on cooling performance

In Figure 4.20, dry bulb and wet bulb air temperatures are shown at the inlet and outlet of bundle with respect to module number. Module number effect is observed by using 1, 9 and 18 membrane packs.

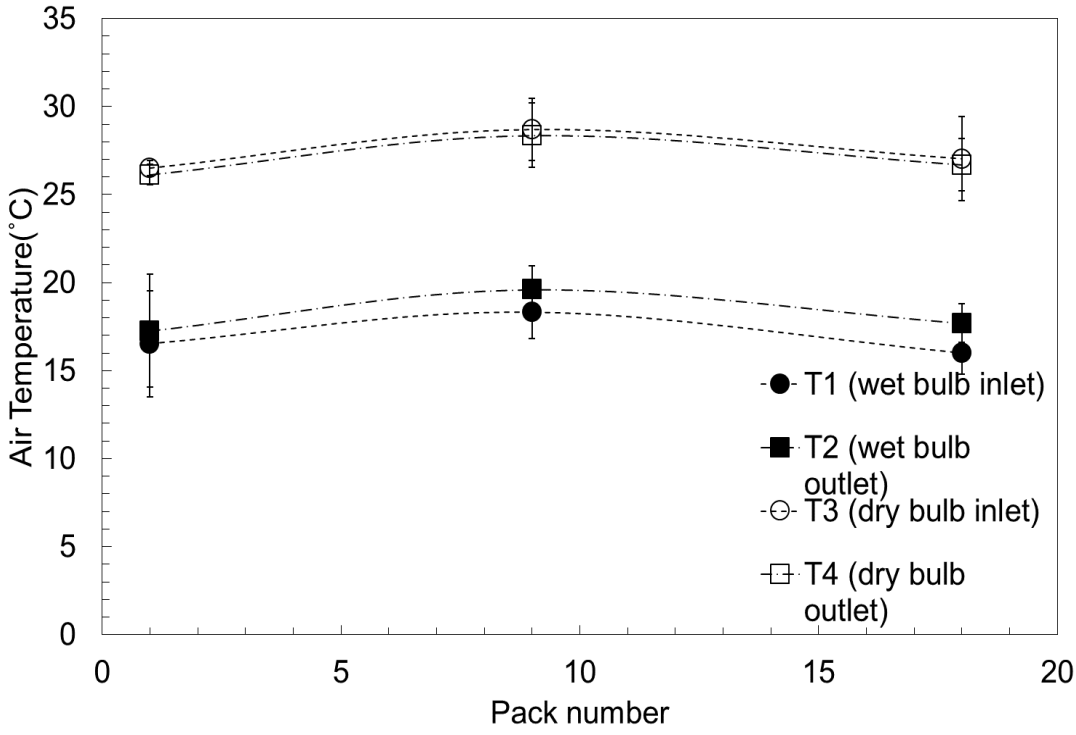

Figure 4.20: Plot of air temperature change with pack number, 10 cm^3/min water flow rate-1.84m/s air velocity-0 barg air pressure

Increasing number of fibers cause a certain change between inlet and outlet wet bulb temperatures. Increasing wet bulb temperature at the outlet of the bundle shows humidification in air. Between 1 pack experiment and 18 pack experiment, difference between inlet wet bulb temperature and outlet wet bulb temperature can be seen clearly.

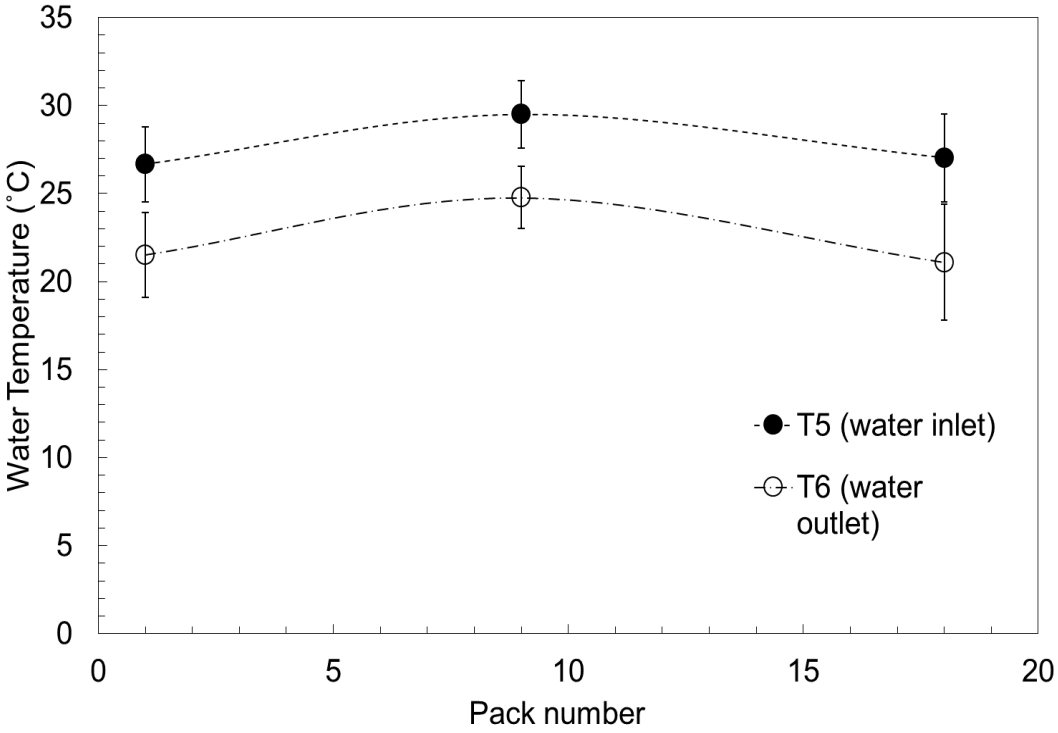

Figure 4.21: Plot of water temperature change with pack number, 10 cm^3/min water flow rate-1.84m/s air velocity-0 barg air pressure

Figure 4.21 shows the water temperature trend at inlet and outlet with respect to pack number. According to results, inlet water temperatures are 26.7, 29.5 and 27.0 ˚C. On the other hand, outlet water temperatures are 21.5, 24.8 and 21.1˚C for 1, 9 and 18 pack, respectively. The difference between inlet water and outlet water temperatures are similar to each other with changing in pack number. Since modules are connected in parallel, this in an expected result.

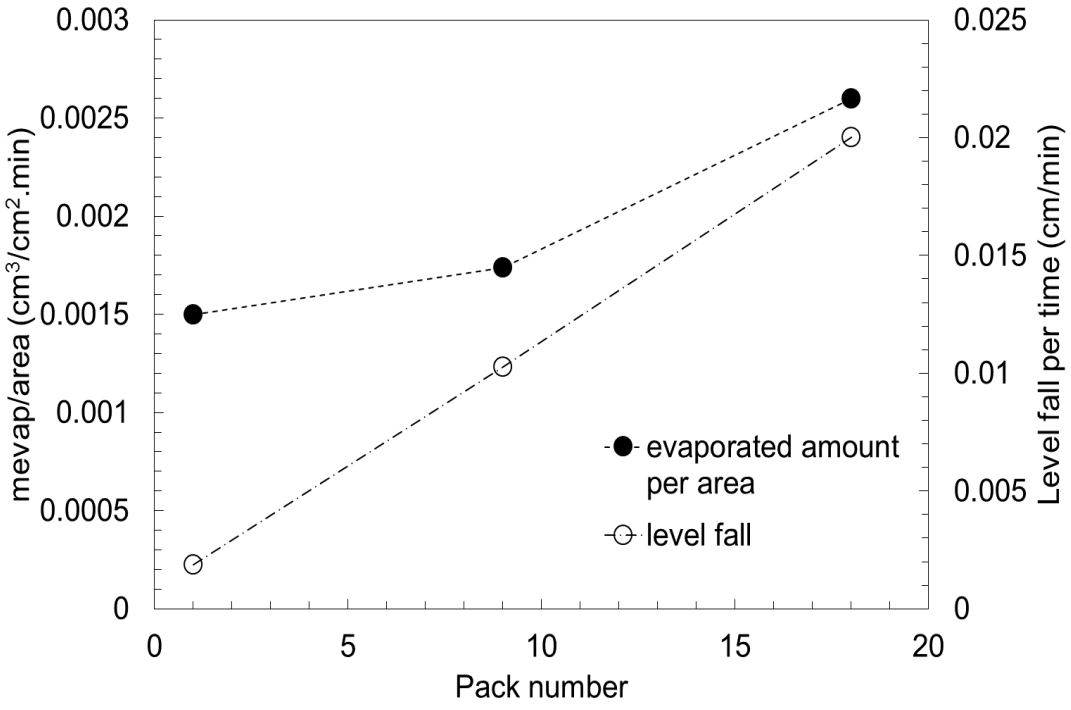

Figure 4.22: Plot of evaporated water and level change with pack number

In Figure 4.22, evaporated water amount and level change with respect to module number is shown. According to plot, water loss from the system is increasing with module number. Actually, increasing water loss from the system is an expected result with increasing of pack number. Since outlet water temperatures are similar to each other, all permeance cannot be evaporated in the system.

4.6.6 Effect of inlet air temperature on cooling performance

Another topic that is investigated for the effect on cooling performance in membrane based system is air inlet temperature. In Figure 4.23, dry bulb and wet bulb air temperature changes are given. Since dry bulb temperature is increased by heater, wet bulb temperature is also rising.

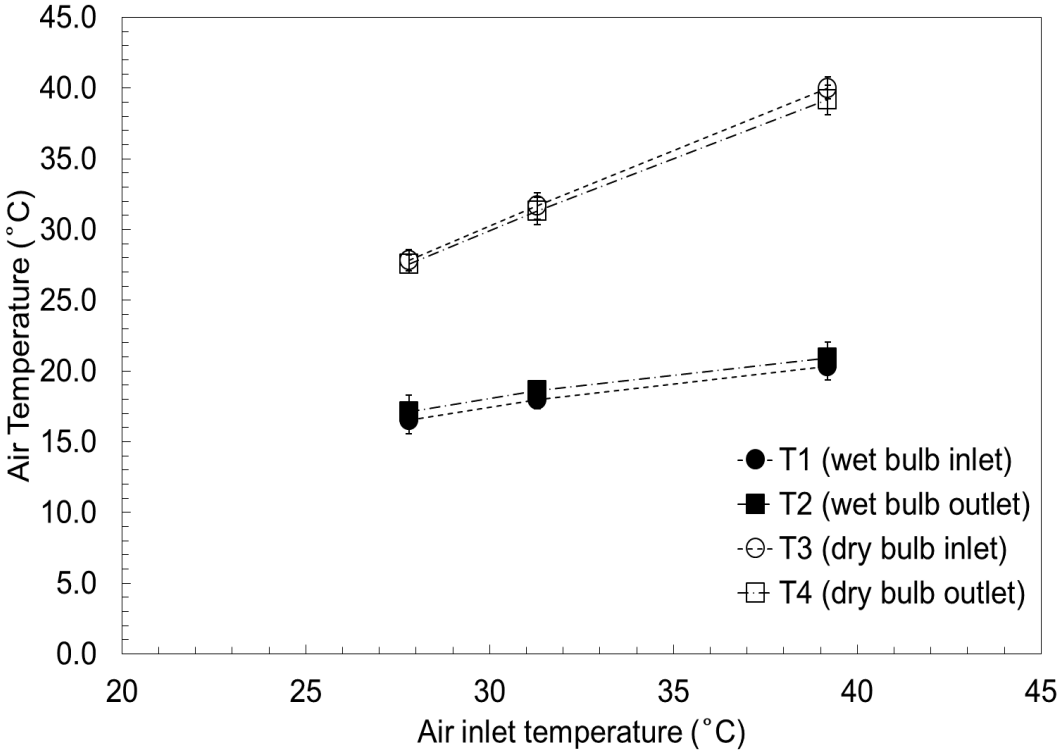

Figure 4.23: Plot of air temperature change with air inlet temperature, 10 cm^3/min water flow rate-1.84m/s air velocity-0 barg air pressure-1 pack

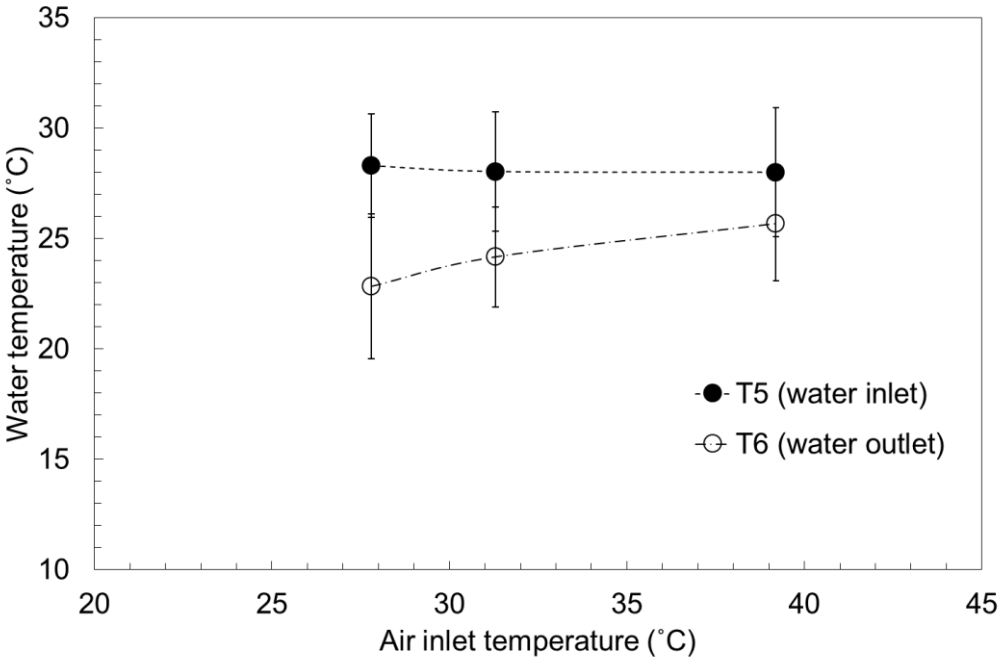

Figure 4.24: Plot of water temperature change with air inlet temperature, 10 cm^3/min water flow rate-1.84m/s air velocity-0 barg air pressure-1 pack

Effect of changing air inlet dry bulb temperature on water temperature is demonstrated in Figure 4.24. In the experiments, while inlet water temperatures are 28.3, 28.0 and 28.0˚C, water outlet temperatures are 22.8, 24.2 and 25.7˚C with increasing air inlet temperature. According to temperature differences between water at inlet and outlet of the module, cooling performance is affected negatively. With rise in air inlet temperature, sensible heat transferring to the water side will be higher and water will start to warm up.

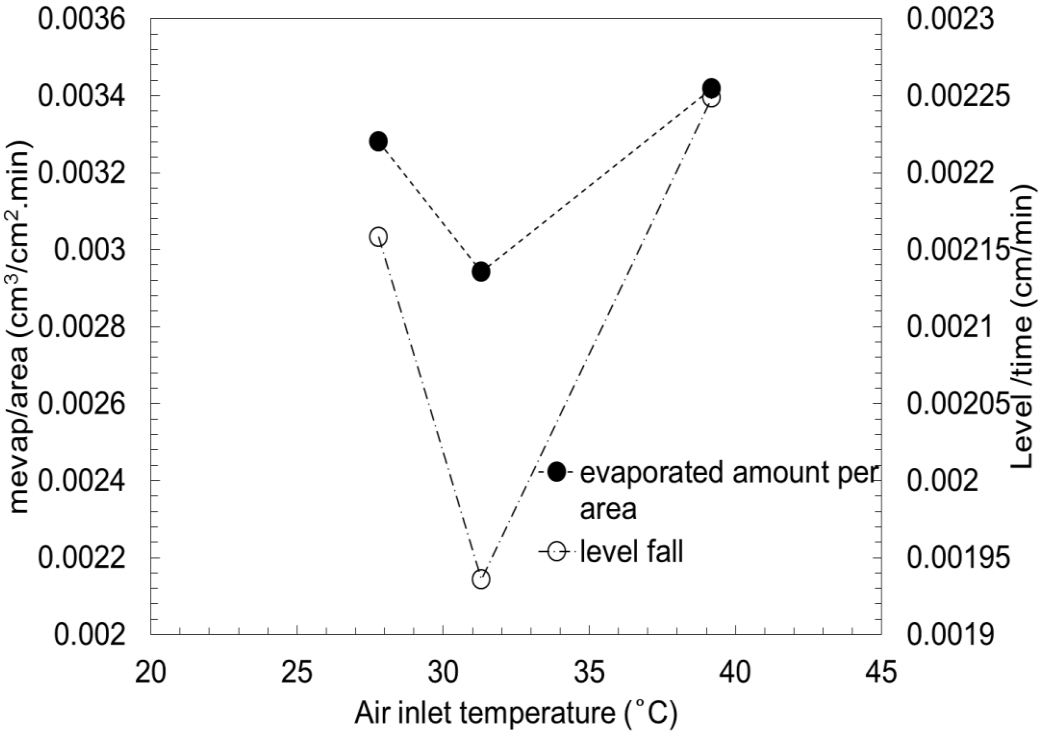

Figure 4.25: Plot of evaporated water and level change with air inlet temperature

In Figure 4.25, plot of evaporation amount change and level change with respect to inlet dry bulb increase in membrane based system. According to plot, the values are close to each other and the difference can be caused from water cannot totally evaporated from membrane surface.

4.6.7 Effect of inlet water temperature on cooling performance

For inlet water temperature effect on membrane based system, same parameters are used as inlet air temperature effect. In this part, rather than inlet air temperature, inlet water temperature are increased during the experiments.

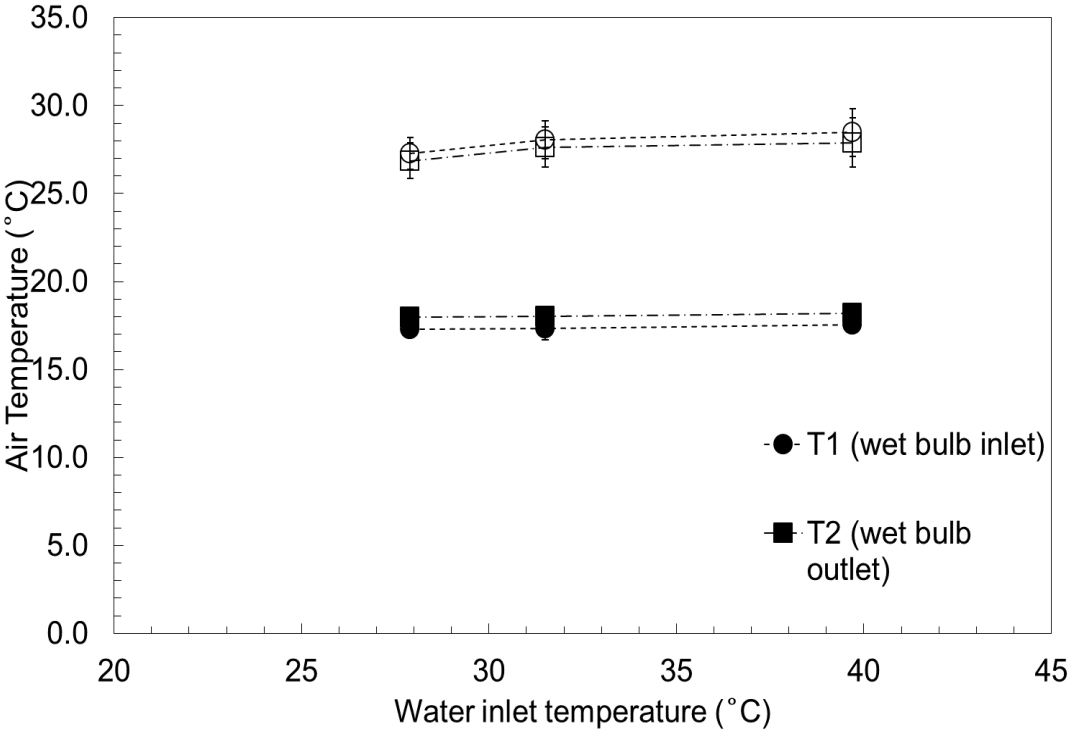

Figure 4.26: Plot of air temperature change with water inlet temperature, 10 cm^3/min water flow rate-1.84m/s air velocity-0 barg air pressure-1 pack

In Figure 4.26, dry bulb and wet bulb air temperatures at inlet and outlet of the bundle is shown. Dry bulb temperature are slightly increased with elevation of water temperature. Since air flow rate is much higher than water flow rate, the impact of change inlet temperature is not high as Figure 4.24.

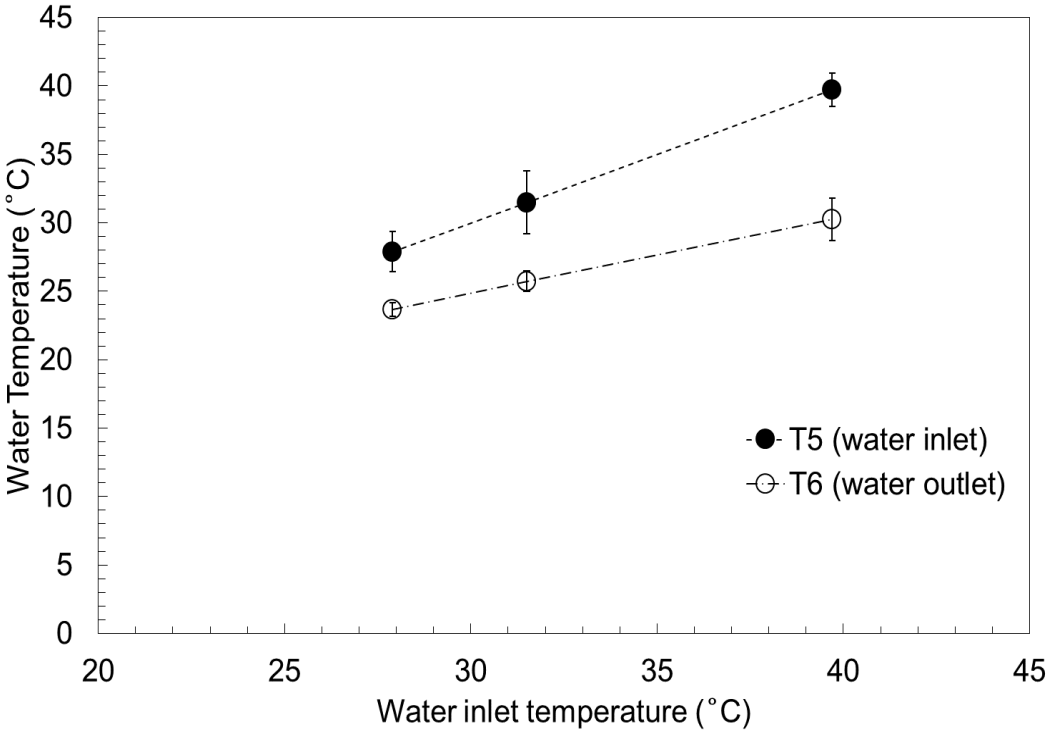

Figure 4.27: Plot of water temperature change with water inlet temperature, 10 cm^3/min water flow rate-1.84m/s air velocity-0 barg air pressure-1 pack

In Figure 4.27, water inlet and outlet temperatures are given. Since the effect of inlet water temperature change is investigating, water inlet temperature is rising in the plot. This increase also brings sensible heat exchange through air side. Thus, water temperature difference between inlet and outlet is getting higher.

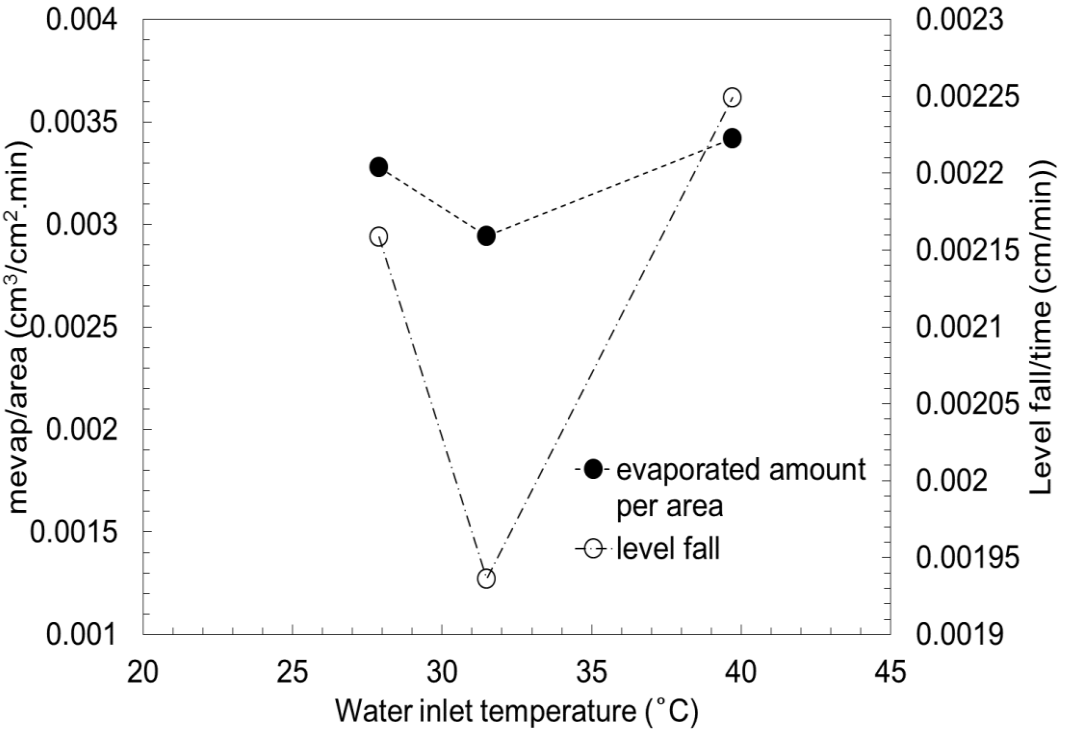

Figure 4.28: Plot of evaporated water and level change with water inlet temperature

In Figure 4.28, evaporated amount of water and level change plots are shown with respect to differ in inlet water temperature. As in Figure 4.25, resulted values are close to each other but the difference between them can be resulted from level measurement which has 0.1 cm deviation. Also, another reason can be all water permeated from membrane cannot not be vaporized during the experiment.

4.7 Theoretical approach for membrane based cooling system

In Figure 4.29, differential element of hollow fiber membrane is given with two directions of r and z. Modelling of the system is conducted with heat and mass transfer equations.

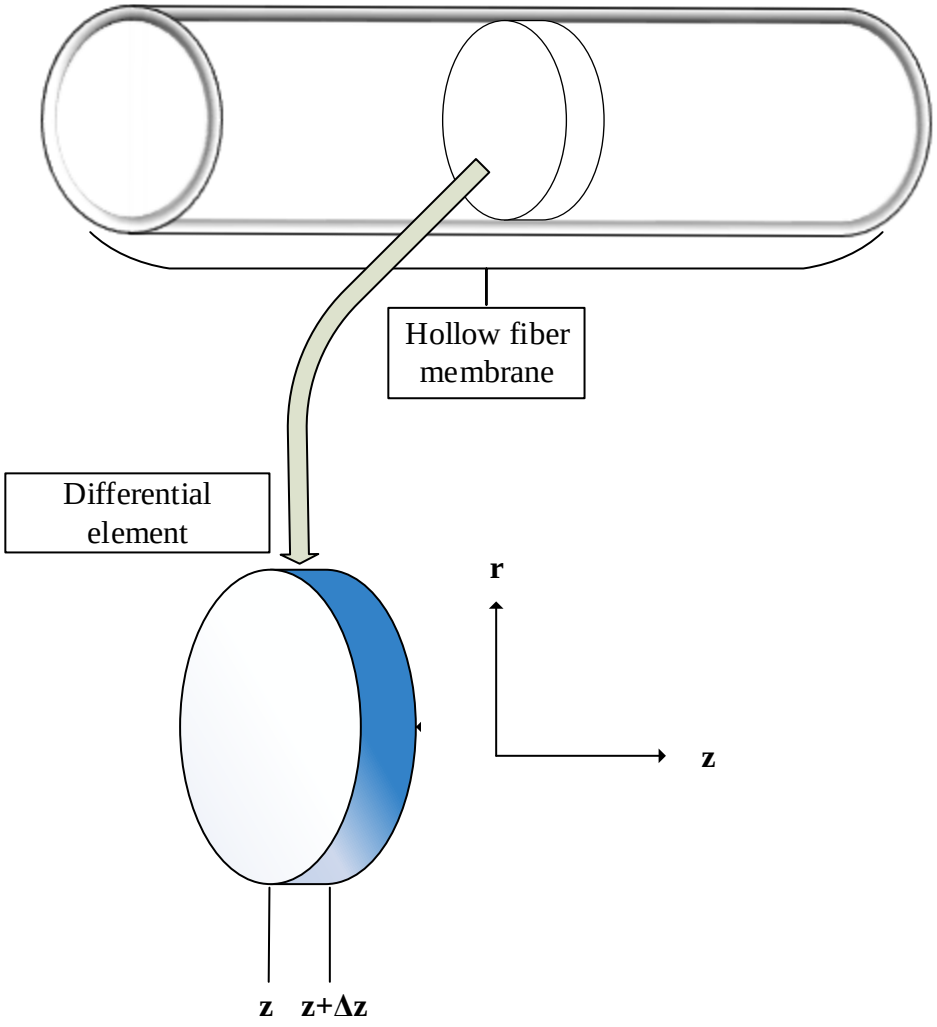

Figure 4.29: Differential element of hollow fiber membrane

In mathematical modelling, heat and mass transfer equations are shown for two different systems. These are water in the capillary and membrane with certain thickness. The aim is to estimate outlet water temperature from the module. Firstly, water in the capillary is chosen as system.

For the chosen system, the main assumption is steady state system. Steady state means system is independent from time. Another assumption is r direction is neglected in equations. The reason is length of the fiber is much higher than diameter. Hence, temperature change in r direction shown in Figure 4.29 is neglected with respect to flow direction (z).

$$\dot{m}_{in}Cp\left(T_z - T_{ref}\right) - \dot{m}_{out}Cp\left(T_{z+\Delta z} - T_{ref}\right) - h_i A_i (T_z - T_{wi}) - \mathrm{P}\Delta P \pi D_i \Delta z Cp\left(T_z - T_{ref}\right) = 0 \qquad \text{Equation 4-1}$$

In Equation 4-1, heat transfer equation around differential element is shown. In equation, first and second term is heat transferred between z and z+Δz. Third term is convective heat transfer through membrane wall and last term is heat loss caused from water permeation.

In inlet and outlet water flow rates are assumed as same since permeance is much lower than, water flow rate in a capillary as shown in Equation 4-2:

$$\mathrm{P}\Delta P \pi D_i \Delta z \ll \dot{m}_{in} \rightarrow \dot{m}_{in} = \dot{m}_{out} = \dot{m} \qquad \text{Equation 4-2}$$

With this assumption, Equation 4-1 is transformed in to differential equation of Equation 4-3:

$$-\dot{m}Cp\frac{dT}{dz} - h_i\pi D_i(T - T_{wi}) = 0 \qquad \text{Equation 4-3}$$

For inner heat transfer coefficient calculation (hi), flow is assumed as laminar. Laminar flow assumption is valid since in experiments, water flow is low. Also, wall temperature of membrane is assumed as equal to air temperature.

In membrane based water cooling system, for mathematical modelling, system can be chosen as membrane with certain thickness. The chosen system is assumed as steady state which does not change with time. For membrane polymer, thermal conductivity of the polymer is high and heat capacity is low. Hence, heat capacity is assumed as negligible.

With given assumptions, r and z direction heat transfer equation is given in Equation 4-4. In this equation, only conduction is taken into consideration and convective heat transfer is neglected because heat transfer equations are for solid membrane. Also, velocities are neglected.

$$(2\pi r\Delta z q_r)_r - (2\pi r\Delta z q_r)_{r+\Delta r} + (2\pi r_i \Delta r q_z)_z - (2\pi r_i \Delta r q_z)_{z+\Delta z} = 0$$

Equation 4-4

Equation 4-4 is divided to Δr , Δz and become Equation 4-5:

$$-\frac{\partial}{\partial r}(rq_r) - r_i\frac{\partial q_z}{\partial z} = 0 \qquad \text{Equation 4-5}$$

With isotropic assumption, conduction term is given below in Equation 4-6 and 4-7:

$$q_r = -k\frac{\partial T}{\partial r} \qquad \text{Equation 4-6}$$

$$q_z = -k\frac{\partial T}{\partial z} \qquad \text{Equation 4-7}$$

If q terms in Equation 4-6 and 4-7 are placed into Equation 4-5, it became Equation 4-8 and T^p shows the polymer temperature.

$$\frac{1}{r_i}\frac{\partial}{\partial r}\left(r\frac{\partial T^p}{\partial r}\right) + \frac{\partial^2 T^p}{\partial z^2} = 0 \qquad \text{Equation 4-8}$$

Boundary conditions:

$$1)@r = r_i \quad h_i(T - T^p) = -k\frac{\partial T^p}{\partial r}$$

$$2)@r = r_o \quad h_o(T_{air} - T^p) - \mathrm{P}\Delta P\lambda = k\frac{\partial T^p}{\partial r}$$

$$3)@z = 0 \quad (T^p) = T_{w,in}$$

$$3)@z = L \quad (T^p) = T_{w,out}$$

Since diameter of capillary is much lower than length r direction is neglected in equations. In membrane based system, diameter is 0.9 cm and fiber length is 30 cm. According to given magnitudes, assumption is valid and Equation 4-8 become Equation 4-9.

$$\frac{\partial T^p}{\partial r} \ll \frac{\partial T^p}{\partial z}$$

$$\frac{\partial^2 T^p}{\partial z^2} = 0 \qquad \text{Equation 4-9}$$

In modelling of membrane based water cooling system, the aim is to find and compare outlet water temperature with experimental results. For this reason rather than polymer temperature, model system is chosen as water in capillary. After system is chosen for mathematical modelling, Equation 4-3 is rewritten with consideration of membrane and air side. Then, h_i term which is heat transfer coefficient for water side became U_i which is overall heat transfer coefficient. Also, in Equation 4-10, third term should be included since this term shows the permeation from the system.

$$-\dot{m}Cp\frac{dT}{dz} - U_i\pi D_i(T - T_{wi}) - \mathrm{P}\Delta P\lambda\rho D_i\pi = 0 \qquad \text{Equation 4-10}$$

Equation 4-10 is ordered as Equation 4-11:

$$\frac{dT}{dz} = \frac{-\mathrm{P}\Delta P\lambda D_i\pi}{\dot{m}Cp} - \frac{U_i\pi D_i}{\dot{m}Cp}(T - T_{wi}) \qquad \text{Equation 4-11}$$

In Equation 4-11, first term in right side is called A and coefficient of T term is called B. Equation 4-12 is given below:

$$\frac{dT}{dz} = A + B(T - T_{wi}) \qquad \text{Equation 4-12}$$

The solution of Equation 4-12 is given in Equation 4-13:

$$T = \frac{-A}{B} + \frac{A}{B}e^{Bz} + T_{wi} \qquad \text{Equation 4-13}$$

After solution is complete, temperature of water at outlet will be found by using method which has the algorithm given in Figure 4.30. In first calculation, inlet water temperature is used.

In this method, a fiber with 30 cm length is divided into 100 fragments. Since these fragments are very small, Equation 4-11 becomes Equation 4-14:

$$\frac{\Delta T}{\Delta z} = \frac{T - T_{w,in}}{\Delta z} = \frac{-\mathrm{P}\Delta P \rho \lambda D_i \pi}{\dot{m} Cp} - \frac{U_i \pi D_i}{\dot{m} Cp}\left(T - T_{wi}\right)$$

Equation 4-14

In Equation 4-14, PΔPρ term is equal to evaporated amount of water. In any T, evaporation is given in Equation 4-15:

$$\mathrm{P}\Delta P \rho = m$$

$$m_{evap} = k(P_T^* - P_\infty)$$ Equation 4-15

In Equation 4-14, another unknown beside the temperature is overall heat transfer coefficient. Overall heat transfer coefficient is found by Equation 4-16.

$$\frac{1}{U_i A_i} = \frac{1}{A_i h_i} + \frac{\ln\left(\frac{A_o}{A_i}\right)}{2\pi L k} + \frac{1}{A_o h_o}$$ Equation 4-16

To find heat transfer coefficients for water and air side, proper correlations are used. For inner side water flow, Hausen correlation for laminar flow through cylinder is used and for outer side air flow over cylinder Zukauskas correlation is used (Incorpera, 2013). Physical properties are assumed constant in calculations. Also, membrane thickness is not neglected. Correlation used for air side heat transfer calculations, is given in Equation 4-17. The constants in equation are proper for Reynold and Prandtl numbers in membrane based system.

$$Nu = 0.683Re^{0.466}Pr^{1/3}$$ Equation 4-17

The relationship of Nusselt number and heat transfer coefficient is in Equation 4-18:

$$Nu = \frac{hD}{k}$$ Equation 4-18

By using Equation 4-18, heat transfer coefficient can be calculated. In Equation 4-14, overall heat transfer coefficient can be placed accordingly. After that, to find outlet water temperature, an algorithm is used and it is shown in Figure 4-30.

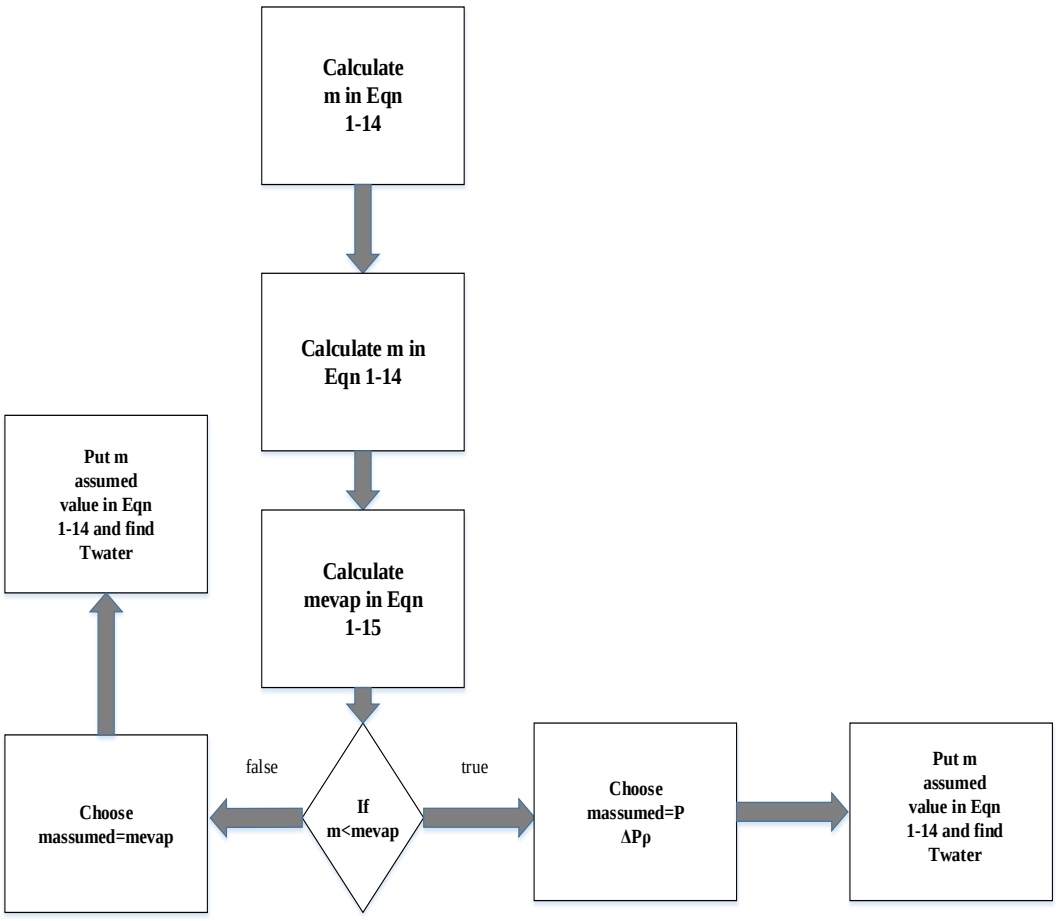

Figure 4.30: Algorithm of calculation

4.7.1 Comparison of experimental work and modelling results

In the modelling of membrane based water cooling system, by using algorithm given in Figure 4.30, outlet water temperatures are found for different parameters. In this study, there are seven factors that are investigated and for these parameters, theoretical outlet water temperature values are found.

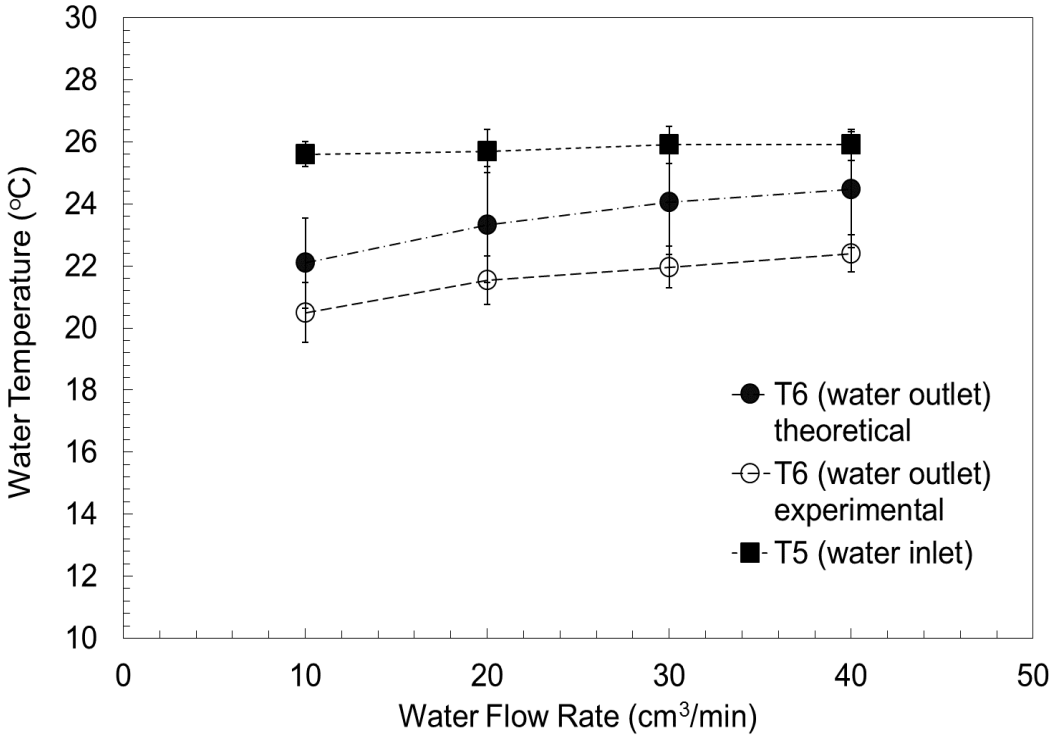

Figure 4.31: Comparison of Theoretical and Experimental Water Temperatures for Water Flow Rate Effect

After experimental process of the membrane based water cooling system, theoretical analysis are completed to compare experimental results with theoretical. For water flow rate effect, in Figure 4.31, theoretical and experimental water outlet temperature are given. Both results are close to each other. Also, they have same increasing trend with increasing water flow rate.

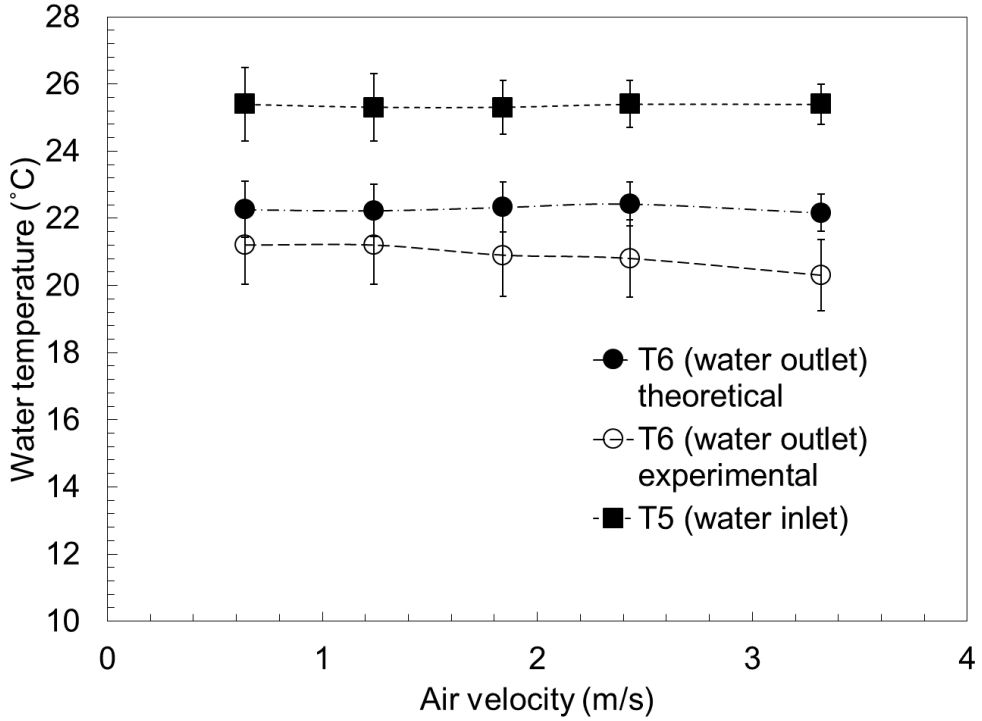

Figure 4.32: Comparison of Theoretical and Experimental Water Temperatures for Air Flow Rate Effect

For comparison of air flow rate effect on membrane based cooling system experimentally and theoretically, the graph is plotted in Figure 4.32. According to graph, in theoretical results, there are slight changes. The effect of air flow rate cannot be observed obviously. Yet, water outlet temperature values are close to each other.

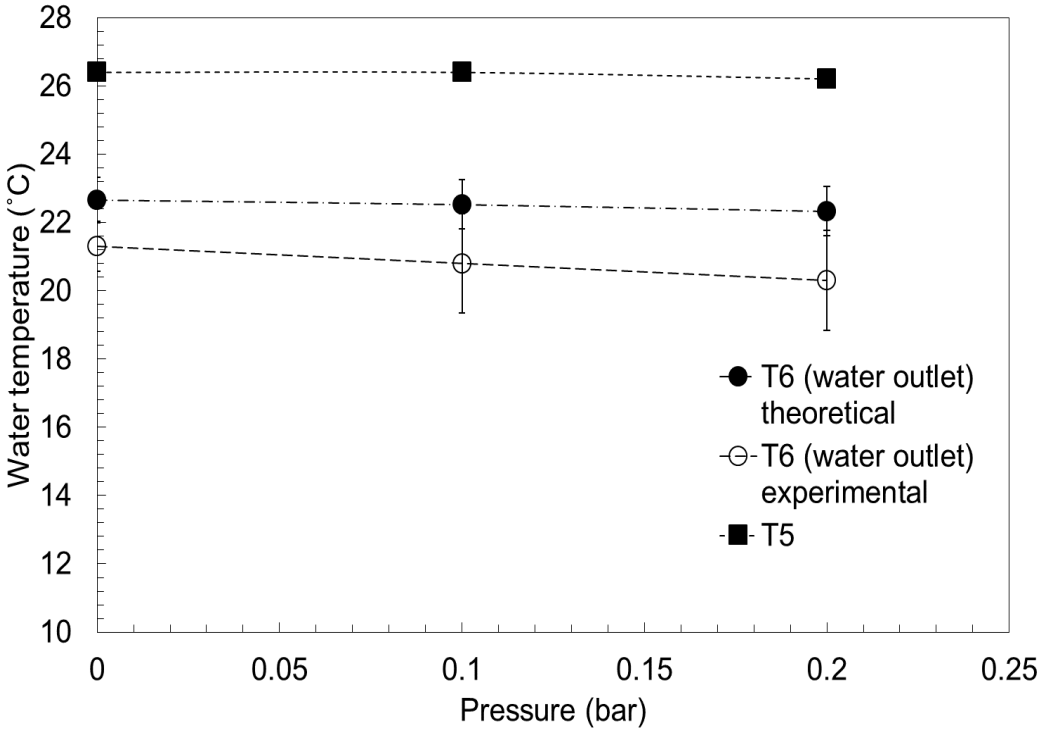

Figure 4.33: Comparison of Theoretical and Experimental Water Temperatures for Pressure Effect

Figure 4.33 shows the water temperatures at inlet and outlet of the module experimentally and theoretically with pressure change. In theoretical water outlet results, with increasing air pressure, cooling performance becomes higher as same as the experimental results.

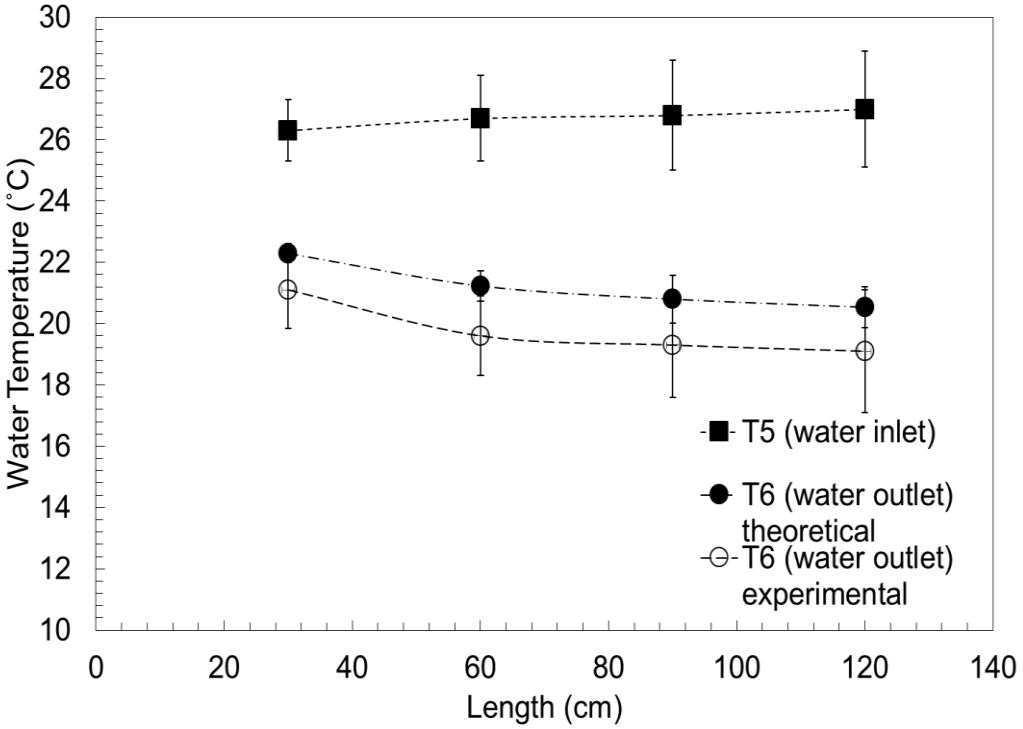

Figure 4.34: Comparison of Theoretical and Experimental Water Temperatures for Module Length Effect

In Figure 4.34, water temperature at inlet and outlet of module are given with length experimentally and theoretically. Results are promising since the trends of experimental and theoretical are very similar.

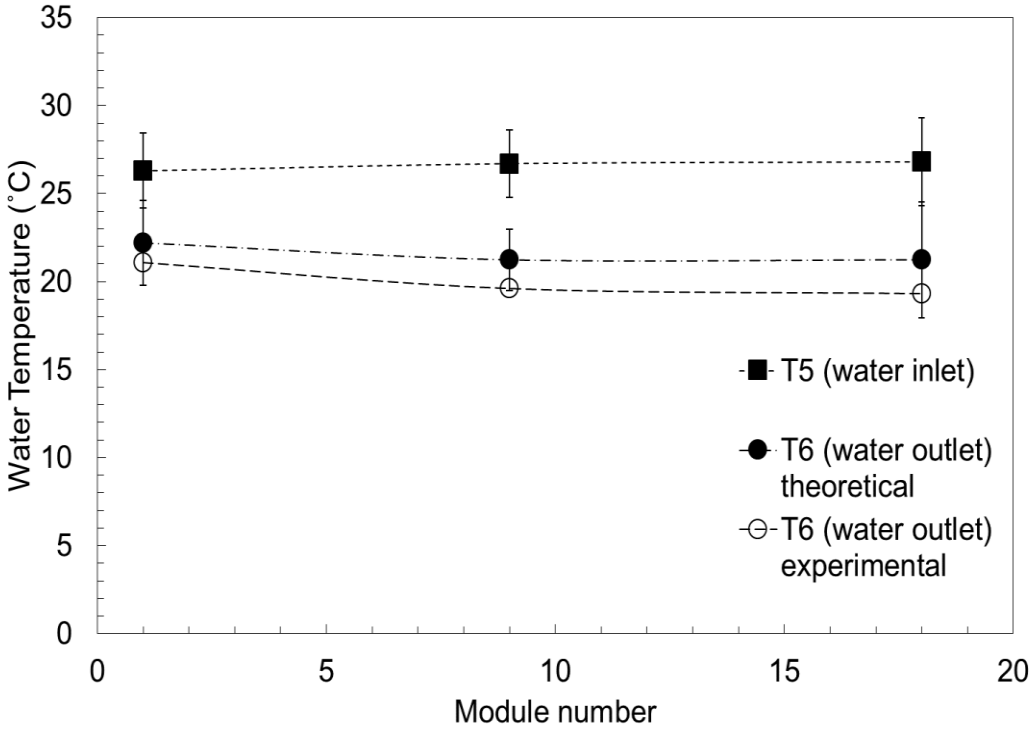

Figure 4.35: Comparison of Theoretical and Experimental Water Temperatures for Pack Number Effect

Pack number affects air temperature rather than water temperature. The reason is, although number of fibers are increasing, the driving force between two ends of membrane module does not change since modules are connected in parallel. In experimental investigation of this effect, results were similar to each other. .for theoretical approach, compassion of results are given in Figure 4.35. According to plot, theoretical temperature results are similar to experimental results.

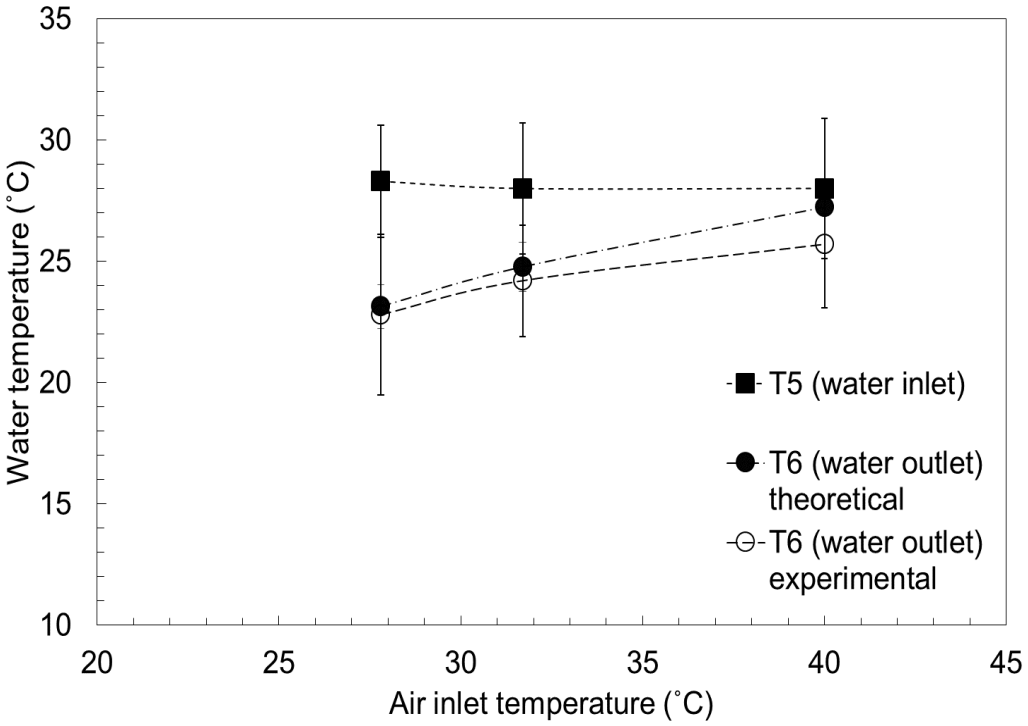

Figure 4.36: Comparison of Theoretical and Experimental Water Temperatures for Inlet Air Temperature Effect

In Figure 4.36, theoretical and experimental results of inlet air temperature effect is demonstrated. Both experimental and theoretical approaches have same trend which is cooling performance decreases with increasing inlet air temperature effect. Water outlet temperatures are also very close to each other except last inlet air temperature. The separation at this point can be resulted from lower effect of sensible heat transfer.

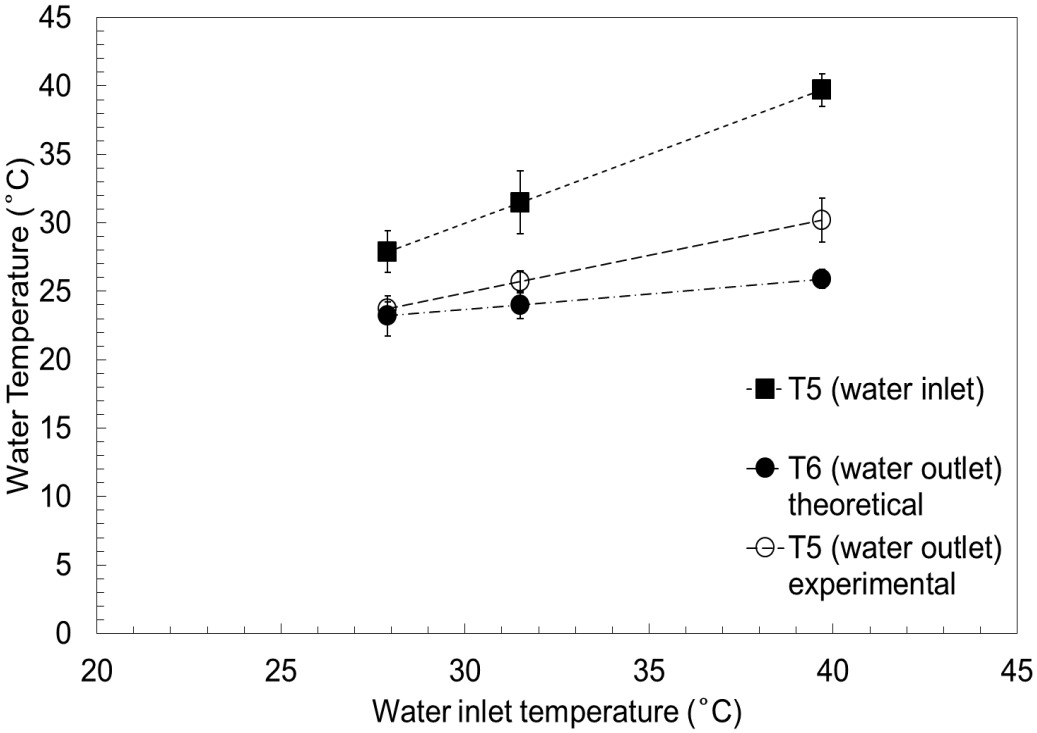

Figure 4.37: Comparison of Theoretical and Experimental Water Temperatures for Inlet Water Temperature Effect

In Figure 4.37, theoretical and experimental water inlet and outlet temperatures are plotted. In the graph, both experimental data and theoretical data have similar trends. At last water inlet temperature, theoretical result implements higher cooling performance.

CHAPTER 5

CONCLUSIONS

In the membrane based water cooling system, there are seven independent variables that are investigated. These are water and air flow rates, transmembrane pressure, module length and pack number, inlet air and water temperatures. Conclusions are given with respect to experimental parameters.

1. Water flow rate increase causes decrease in cooling performance.
2. Air flow rate elevation results in slight decrease in water temperature.
3. Transmembrane pressure effect is directly proportional to cooling performance.
4. With elongation in module length, watertemperature difference increases.
5. Inlet air temperature factor affects cooling performance negatively.
6. Inlet water temperature factor affects temperature fall in positive way.
7. Theoretical results are very similar to experimental results obtained from membrane based system so that model is valid.

In this study, water temperature are reduced between 4-9˚C for different parameters. Although this temperature decrease is lower than cooling tower performance, membrane based water cooling system is very efficient system because water cooling occurs in very small membrane areas. Scale up of this system can be provided by changing length for water cooling applications. For air cooling, increasing fiber number will directly affects the cooling results. Since in industrial applications, process water cooling would require an extra step in heat exchanger, membrane based water cooling should be improved. This improvement can be provided by changing polymer or using longer fibers.

REFERENCES

[1] Cooling Tower Efficiency.. Retrieved from http://www.engineeringtoolbox.com/cooling-tower-efficiency-d_699.html Retrieved date 2017, July12

[2] Fisenko, S., Petruchik, A., & Solodukhin, A. (2002). Evaporative cooling of water in a natural draft cooling tower. *International Journal of Heat and Mass Transfer, 45*(23), 4683-4694. doi:10.1016/s0017-9310(02)00158-8

[3] Fisenko, S., Brin, A., & Petruchik, A. (2004). Evaporative cooling of water in a mechanical draft cooling tower. *International Journal of Heat and Mass Transfer*, *47*(1), 165-177. doi:10.1016/s0017-9310(03)00409-5

[4] Chaudhari, B. D., Sonawane, T. R., Patil, S. M., & Dube, A. (2015). International Journal of Research in Advent Technology. *A Review on Evaporative Cooling Technology*, *3*.

[5] Psychrometric Chart Use (inner frame). (n.d.). Retrieved from http://web.uconn.edu/poultry/NE-127/NewFiles/psychrometric_inset.html

[6] Schwedler, M. (2014). Effect of Heat Rejection Load and Wet Bulb on Cooling Tower Performance. *ASHRAE Journal*.

[7] *Legionellois*. (2008). Retrieved from Cooling Technology Institute website: http://www.cti.org/pub/cticode.php Retrieved date 2017 July12

[8] Baker, R. (2013). *Membrane technology and applications*. Hoboken, NJ: Wiley

[9] Gabelman, A., & Hwang, S. (1999). Hollow fiber membrane contactors. *Journal of Membrane Science, 159*(1-2), 61-106. doi:10.1016/s0376-7388(99)00040-x

[10] Zhang, L. (2011). An Analytical Solution to Heat and Mass Transfer in Hollow Fiber Membrane Contactors for Liquid Desiccant Air Dehumidification. *Journal of Heat Transfer*, *133*(9), 092001. doi:10.1115/1.4003900

[11] Comparison of Ceramic and Polymeric Membranes for Micro- and Ultrafiltration | AIChE. (n.d.). Retrieved from https://www.aiche.org/chenected/2011/10/comparison-ceramic-and-polymeric-membranes-micro-and-ultrafiltration

[12] Sarkar, A., & Kellogg, G. (2010). Hydrophobicity - Shake Flasks, Protein Folding and Drug Discovery. *Current Topics in Medicinal Chemistry*, *10*(1), 67-83. doi:10.2174/156802610790232233

[13] Properties of Polysulfones. (n.d.). Retrieved from http://polymerdatabase.com/polymer%20classes/Polysulfone%20type.html

[14] Mittal, A., Kataria, T., Das, G. K., & Chatterjee, S. G. (2006). Evaporative Cooling of Water in a Small Vessel Under Varying Ambient Humidity. *International Journal of Green Energy*, *3*(4), 347-368. doi:10.1080/01971520600704654

[15] CHARLES, N., & JOHNSON, D. (2008). The occurrence and characterization of fouling during membrane evaporative cooling. *Journal of Membrane Science, 319*(1-2), 44-53. doi:10.1016/j.memsci.2008.03.022

[16] Velasco Gómez, E., Rey Martínez, F., Varela Diez, F., Molina Leyva, M., & Herrero Martín, R. (2005). Description and experimental results of a semi-indirect ceramic evaporative cooler. International Journal of Refrigeration, 28(5), 654-662. doi:10.1016/j.ijrefrig.2005.01.004

[17] Johnson, D. W., Yavuzturk, C., & Pruis, J. (2003). Analysis of heat and mass transfer phenomena in hollow fiber membranes used for evaporative cooling. Journal of Membrane Science, 227(1-2), 159-171. doi:10.1016/j.memsci.2003.08.023

[18] Woods, J. (2014). Membrane processes for heating, ventilation, and air conditioning. *Renewable and Sustainable Energy Reviews*, *33*, 290-304. doi:10.1016/j.rser.2014.01.092

[19] LOEB, S. (2003). Membrane Evaporative Cooling to 30°C or Less. *Annals of the New York Academy of Sciences*, *984*(1), 515-527. doi:10.1111/j.1749-6632.2003.tb06024.x

[20] Bhatia, A. (2012). *Principles of evaporative cooling* [PDF]. Retrieved from https://pdhonline.com/courses/m231/m231.htm

[21] Buecker, B. (2010). *Cooling Tower Heat Transfer 101*. Power engineering.

[22] Zhang, L. (2006). Mass Diffusion in a Hydrophobic Membrane Humidification/Dehumidification Process: the Effects of Membrane Characteristics. *Separation Science and Technology*, *41*(8), 1565-1582. doi:10.1080/01496390600634723

[23] Dohnal, M., Vesely, T., & Raudensky, M. (2012). Low cost membrane contactors based on hollow fibres. *EPJ Web of Conferences*, *25*, 01009. doi:10.1051/epjconf/20122501009

[24] Johnson, D. W., Yavuzturk, C. C., & Rangappa, A. S. (2010). Formaldehyde removal from air during membrane air humidification evaporative cooling: Effects of contactor design and operating conditions. *Journal of Membrane Science*, *354*(1-2), 55-62. doi:10.1016/j.memsci.2010.02.075

[25] Li, D., Wang, R., & Chung, T. (2004). Fabrication of lab-scale hollow fiber membrane modules with high packing density. *Separation and Purification Technology*, *40*(1), 15-30. doi:10.1016/j.seppur.2003.12.019

[26] Chiari, A. (2000). Air humidification with membrane contactors: experimental and theoretical results. International Journal of Ambient Energy, 21(4), 187-195. doi:10.1080/01430750.2000.9675373

[27] Ter verkrijging van. (2003). *WATER VAPOR AND GAS TRANSPORT THROUGH POLYMERIC MEMBRANES*. Retrieved from https://core.ac.uk/download/pdf/11457309.pdf

[28] Halasz, B. (1998). A general mathematical model of evaporative cooling devices. *Revue Générale de Thermique*, *37*(4), 245-255. doi:10.1016/s0035-3159(98)80092-5

[29] Zhang, L. (2012). Coupled heat and mass transfer in an application-scale cross-flow hollow fiber membrane module for air humidification. International Journal of Heat and Mass Transfer, 55(21-22), 5861-5869. doi:10.1016/j.ijheatmasstransfer.2012.0

APPENDICES

APPENDIX A

Calibration results and experimental parameter data

Table A.1: Water flux results with pressure for each membrane

Press. (barg)	Mem 1	Mem 2	Mem 3	Mem 4	Mem5	Mem 6	Mem 7	Mem 8	Mem 9	Mem10	Avr.	Std.
0.05 bar	0.85	0.87	0.89	0.78	0.8	0.83	0.87	0.86	0.85	0.85	0.85	0.033
0.1 bar	0.95	0.92	0.93	0.9	0.97	0.98	0.98	0.98	0.97	0.96	0.95	0.028
0.2 bar	1.1	1	1.2	1.15	1.25	1.21	1	0.96	0.95	0.98	1.08	0.115
0.3 bar	1.3	1.25	1.37	1.4	1.25	1.29	1.38	1.3	1.25	1.24	1.30	0.060
0.5 bar	1.6	1.6	1.5	1.45	1.5	1.7	1.8	1.5	1.55	1.6	1.58	0.106
0.7 bar	2	2.5	2.1	2.2	1.85	1.84	1.8	1.9	1.5	2.4	2.01	0.299

Table A.2: Average water flux values with various air pressures

Pressure (barg)	**Permeate (cm^3)**	**Time (sec)**	**Area (cm^2)**	**Water Flux ($cm^3/cm^2.s$)**
0.05	0.85	300	11.03	$7.72x10^{-4}$
0.1	0.95	300	11.03	$8.63x10^{-4}$
0.2	1.10	300	11.03	$9.99x10^{-4}$
0.3	1.30	300	11.03	$1.18x10^{-3}$
0.5	1.60	300	11.03	$1.45x10^{-3}$
0.7	2.00	300	11.03	$1.82x10^{-3}$

Table A.3: Air flow rate calibration results

Air	**Zone 1 (m/s)**	**Zone 2 (m/s)**	**Zone 3 (m/s)**	**Average (m/s)**	
1	0.62	0.66	0.64	0.640	±0.02
2	0.90	0.95	0.96	0.936	±0.03
3	1.28	1.22	1.23	1.243	±0.03
4	1.55	1.53	1.52	1.533	±0.02
5	1.80	1.86	1.85	1.836	±0.03
6	2.10	2.14	2.14	2.126	±0.02
7	2.43	2.40	2.46	2.430	±0.03
8	2.69	2.75	2.74	2.726	±0.03
9	3.00	3.05	3.04	3.030	±0.03
10	3.31	3.30	3.34	3.316	±0.02

Water flow rate effect on cooling performance in membrane based system

Table A.4: Experiment parameters and temperature results for water flow effect for 1.84 m/s air velocity and 1 pack parallel connection

	Run	10 mL/min	20 mL/min	30 mL/min	40 mL/min	L cm	Air pressure barg
Wet bulb inlet temperature (T_1)	1	13.6	13.8	13.6	13.5	30	0
	2	14.4	14.3	14.5	14.5	30	0
	3	17.8	17.5	17.6	17.4	30	0
	Avr.	15.3	15.2	15.2	15.1		
	Std.	±2.2	±2.0	±2.1	±2.1		
Wet bulb outlet temperature (T_2)	1	13.8	14.0	14.2	14.0	30	0
	2	14.8	14.4	14.9	15.0	30	0
	3	18.6	18.4	18.7	18.3	30	0
	Avr..	15.7	15.6	15.9	15.8		
	Std.	±2.5	±2.4	±2.4	±2.3		
Dry bulb inlet temperature (T_3)	1	26.3	26.5	26.0	26.7	30	0
	2	26.0	25.9	25.7	25.7	30	0
	3	26.4	26.3	26.5	26.5	30	0
	Av.	26.2	26.2	26.1	26.3		
	Std.	±0.2	±0.3	±0.4	±0.5		
Dry bulb outlet temperature (T_4)	1	25.6	26.1	26.0	26.0	30	0
	2	25.4	25.5	25.2	25.4	30	0
	3	25.9	26.2	26.2	26.3	30	0
	Avr.	25.6	25.9	25.8	25.9		
	Std.	±0.3	±0.4	±0.5	±0.5		
Water inlet temperature (T_5)	1	25.3	25.7	26.0	26.0	30	0
	2	25.3	25.0	25.3	25.4	30	0
	3	26.3	26.3	26.4	26.4	30	0
	Avr.	25.6	25.7	25.9	25.9		
	Std.	±0.4	±0.7	±0.6	±0.5		

Water outlet temperature (T_6)	1	19.0	19.8	20.3	20.7	30	0
	2	20.6	21.3	21.9	22.1	30	0
	3	21.9	23.5	23.7	24.4	30	0
	Avr.	20.5	21.5	22.0	22.4		
	Std.	±1.5	±1.5	±1.7	±1.7		

Air temperature and water temperature graphs with time are in Figure A.1 and Figure A.2:

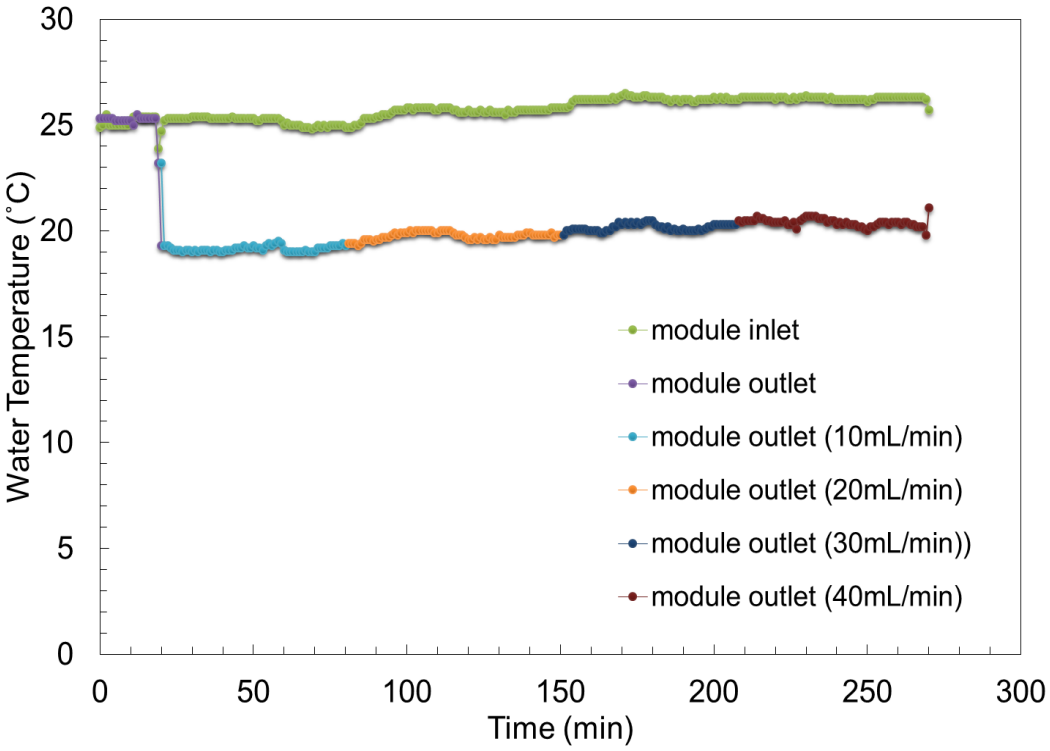

Figure A.1: Plot of water temperature change with time for Run1

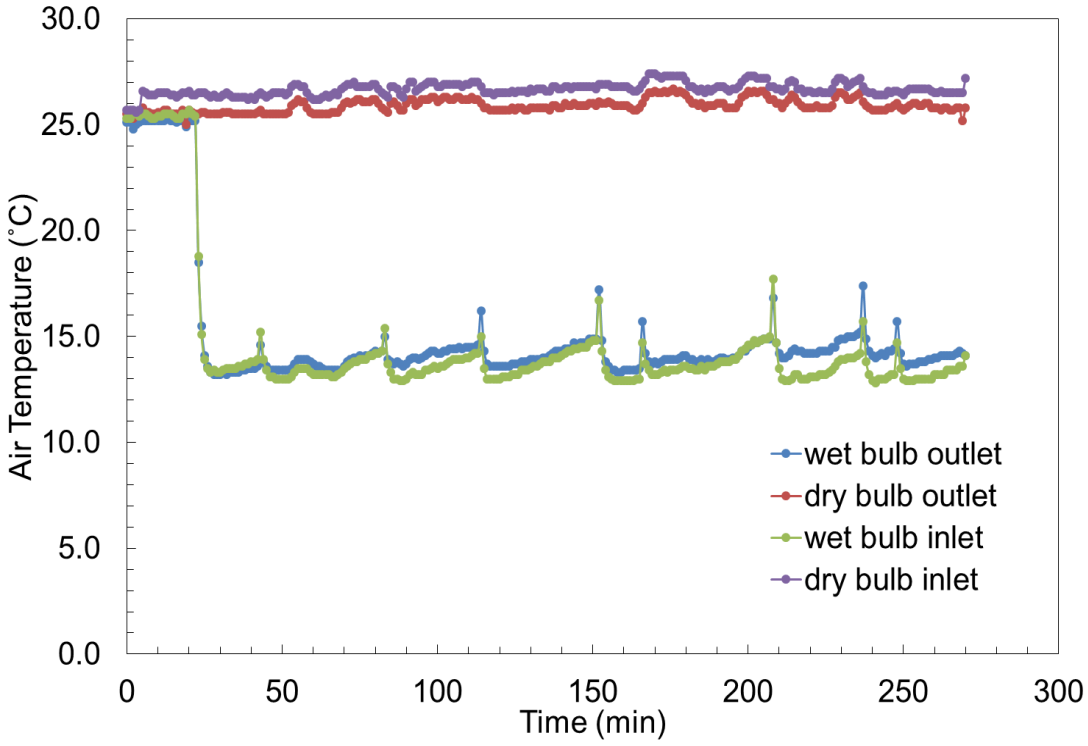

Figure A.2: Plot of air temperature change with time for Run1

Air temperature and water temperature graphs with time are in Figure A.3 and A.4 for Run 2:

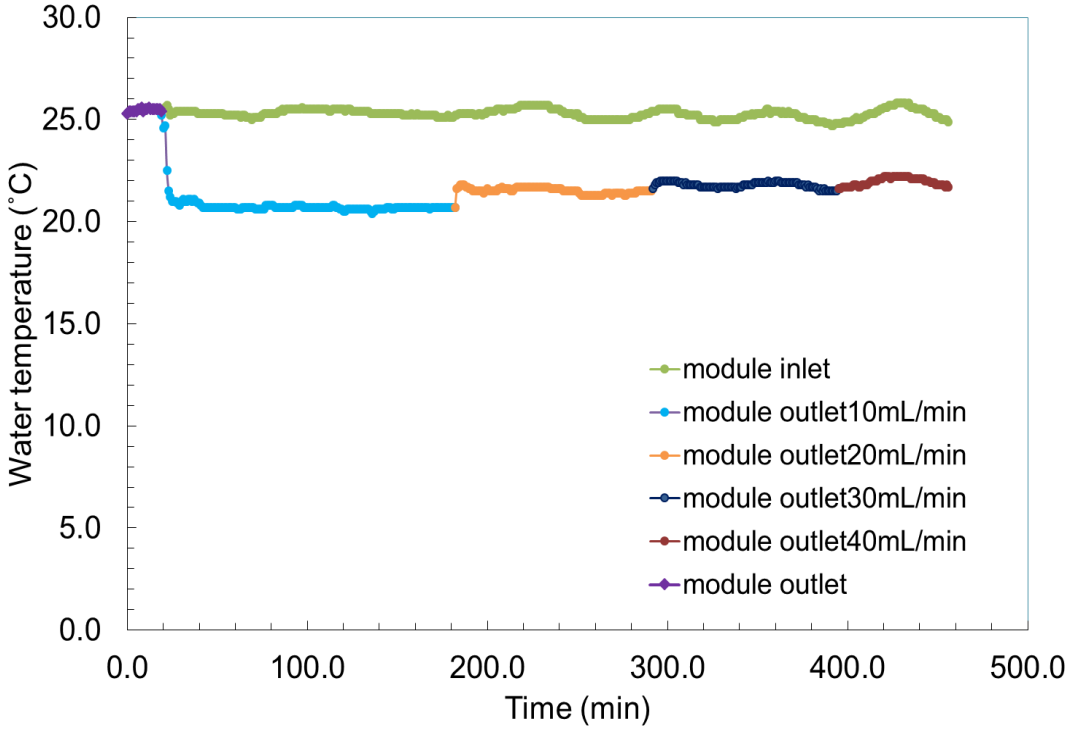

Figure A.3: Plot of water temperature change with time for Run2

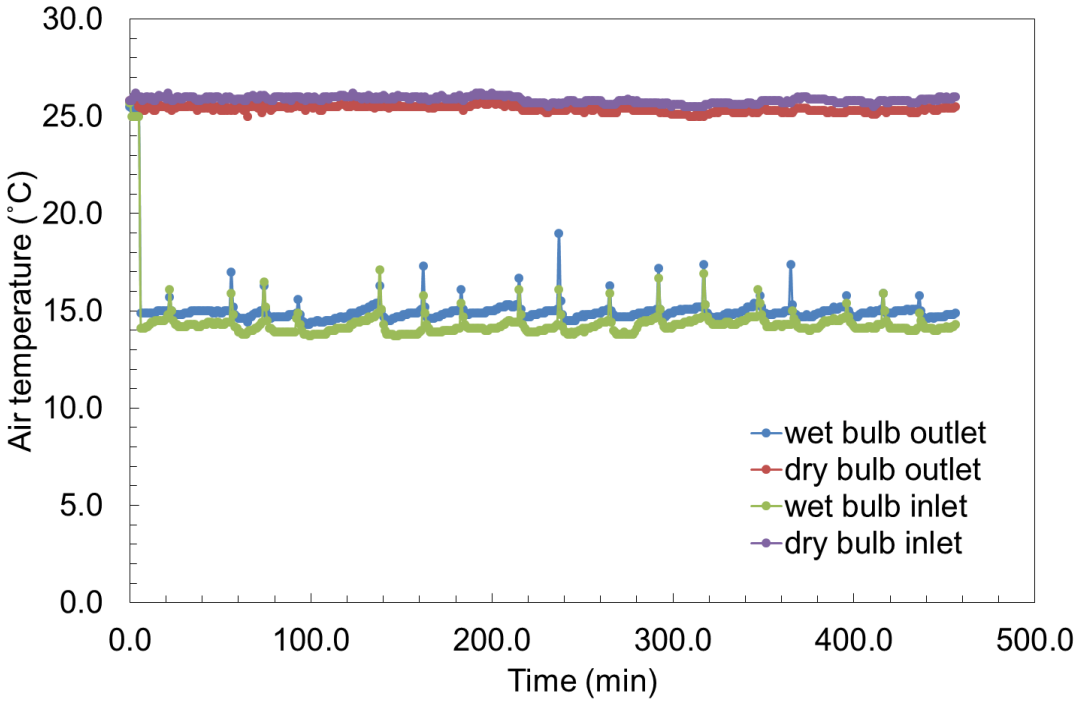

Figure A.4: Plot of air temperature change with time for Run2

Air temperature and water temperature graphs with time are in Figure A.5 and A.6 for Run 3:

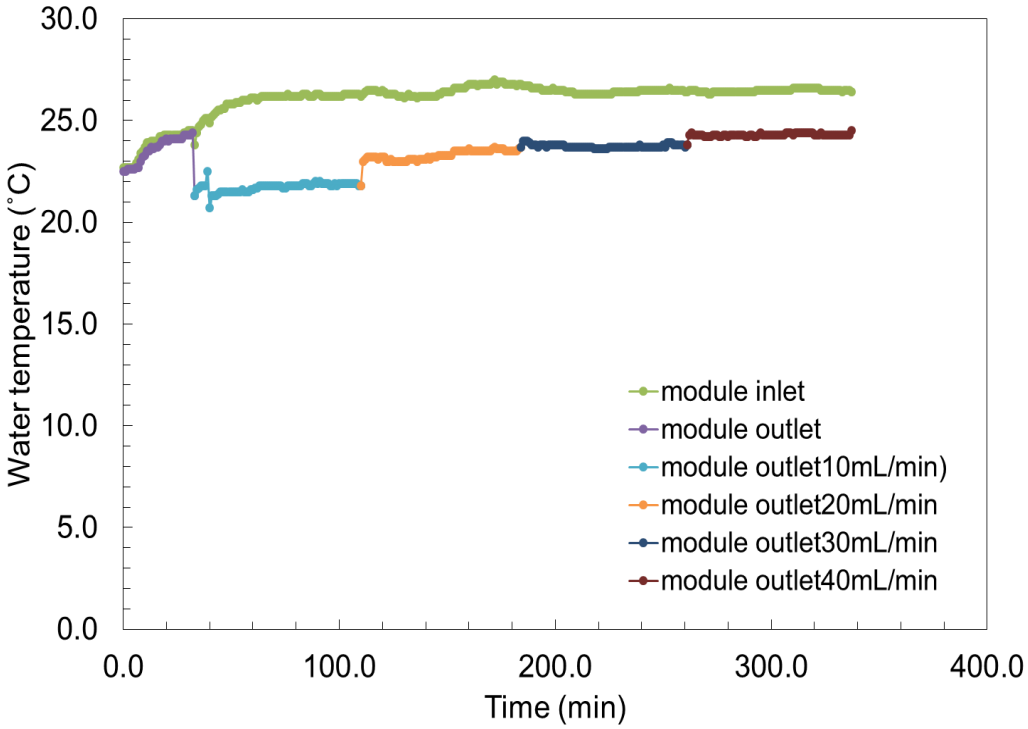

Figure A.5: Plot of water temperature change with time for Run3

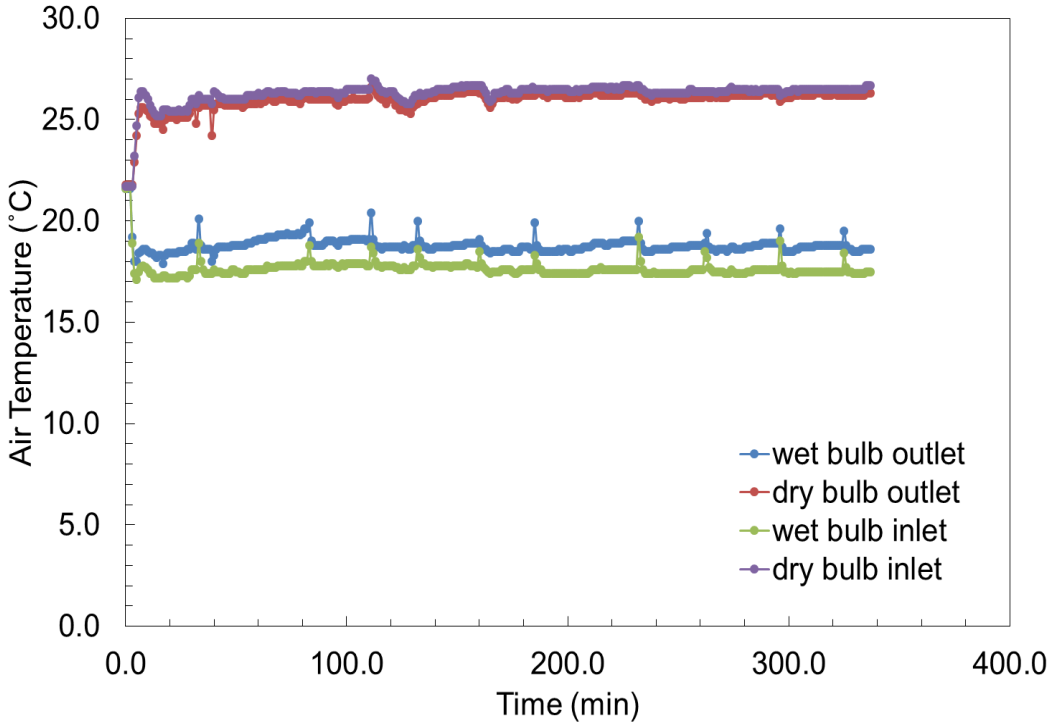

Figure A.6: Plot of air temperature change with time for Run3

Air flow rate effect on cooling performance in membrane based system

Table A.5: Experiment parameters and temperature results for air flow effect for 1 pack and parallel connection

	Run	Air switch (9)	Air switch (7)	Air switch (5)	Air switch (3)	Air switch (1)	L (cm)	Air pressure (barg)
Wet bulb inlet temperature (T_1)	4	13.5	13.1	13.0	12.8	13.0	30	0
	5	14.5	14.5	14.9	15.0	14.8	30	0
	6	17.4	18.0	18.1	18.7	17.8	30	0
	Avr.	15.1	15.2	15.3	15.5	15.2		
	Std.	±2.0	±2.5	±2.6	±3.0	±2.4		
Wet bulb outlet temperature (T_2)	4	13.7	13.5	13.4	13.1	13.4	30	0
	5	15.2	15.4	15.4	15.5	15.3	30	0
	6	18.0	18.4	18.5	19.0	18.3	30	0
	Avr.	15.6	15.8	15.8	15.9	15.7		

	Std.	±2.2	±2.5	±2.6	±3.0	±2.5		
Dry bulb inlet temperature (T_3)	4	26.0	26.2	25.9	26.0	26.0	30	0
	5	25.6	25.8	26.0	25.9	25.5	30	0
	6	26.1	26.2	26.3	26.2	26.3	30	0
	Avr.	25.9	26.1	26.1	26.0	25.9		
	Std.	±0.3	±0.2	±0.2	±0.2	±0.4		
Dry bulb outlet temperature (T_4)	4	25.7	26.0	25.3	25.2	25.2	30	0
	5	25.5	25.8	25.7	25.7	25.2	30	0
	6	26.0	25.6	25.6	26.0	25.7	30	0
	Avr.	25.7	25.8	25.5	25.6	25.4		
	Std.	±0.3	±0.2	±0.2	±0.4	±0.3		
Water inlet temperature (T_5)	4	24.7	24.8	25.0	25.3	25.5	30	0
	5	24.8	24.6	24.7	24.7	24.8	30	0
	6	26.6	26.4	26.2	26.1	26.0	30	0
	Avr.	25.4	25.3	25.3	25.4	25.4		
	Std.	±1.1	±1.0	±0.8	±0.7	±0.6		
Water outlet temperature (T_6)	4	19.3	19.9	20.0	20.5	20.8	30	0
	5	20.1	20.3	20.4	20.5	20.4	30	0
	6	21.6	22.1	22.3	22.5	22.4	30	0
	Avr.	20.3	20.8	20.9	21.2	21.2		
	Std.	±1.2	±1.2	±1.2	±1.2	±1.1		

Air temperature and water temperature graphs with time are in Figure A.7 and A.8 for Run 4:

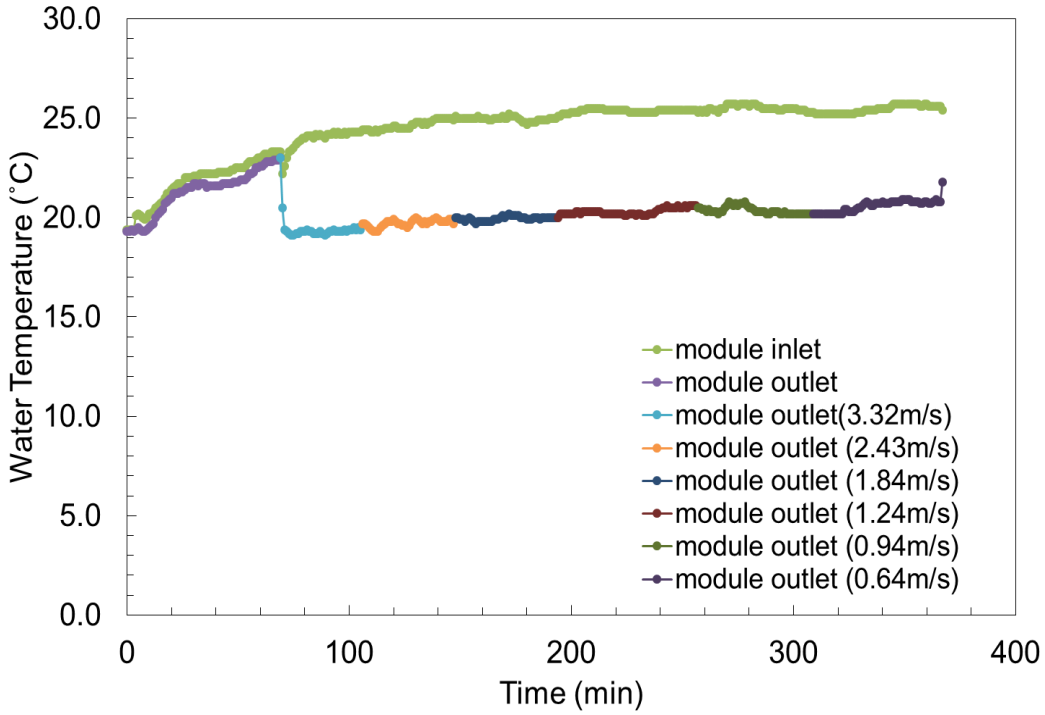

Figure A.7: Plot of water temperature change with time for Run4

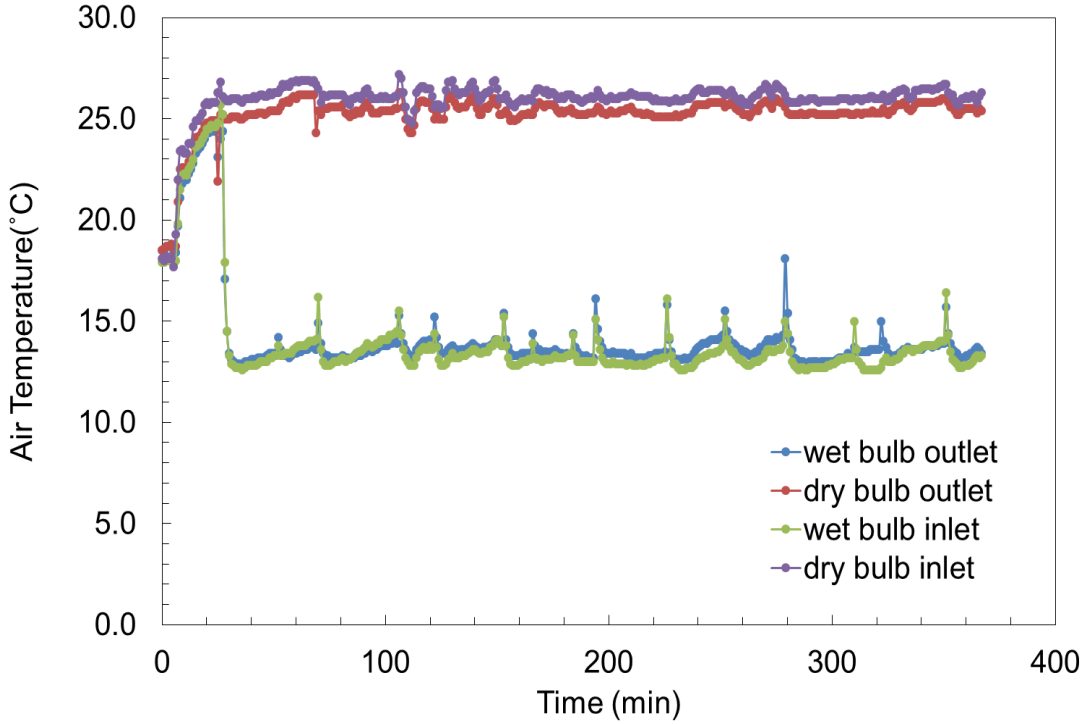

Figure A.8: Plot of air temperature change with time for Run4

Air temperature and water temperature graphs with time are in Figure A.9 and A.10 for Run 5:

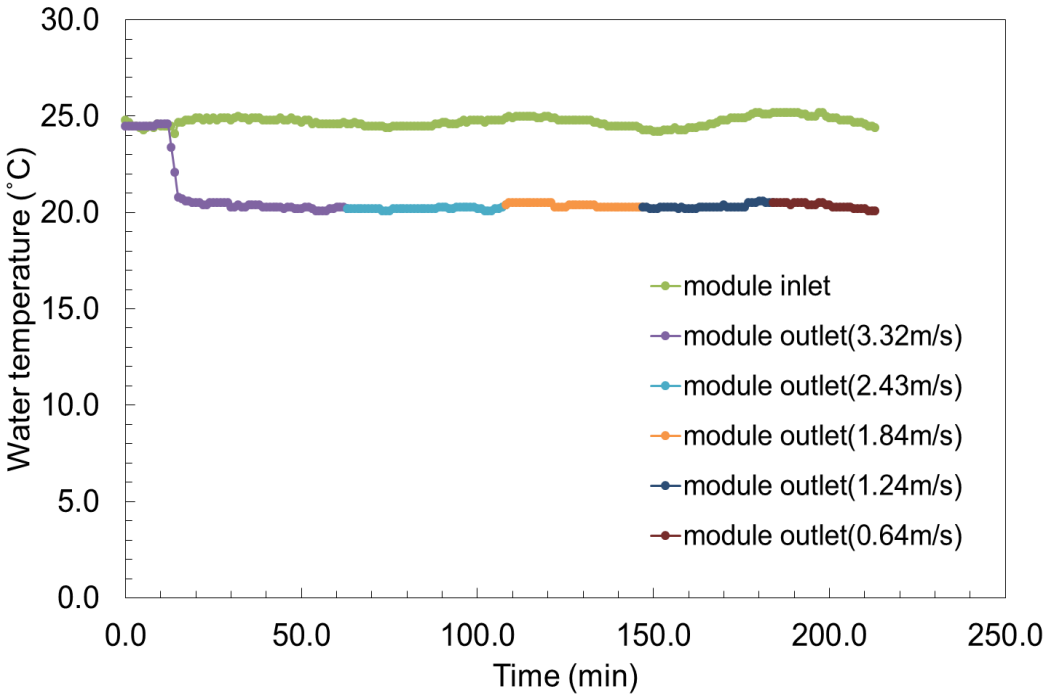

Figure A.9: Plot of water temperature change with time for Run5

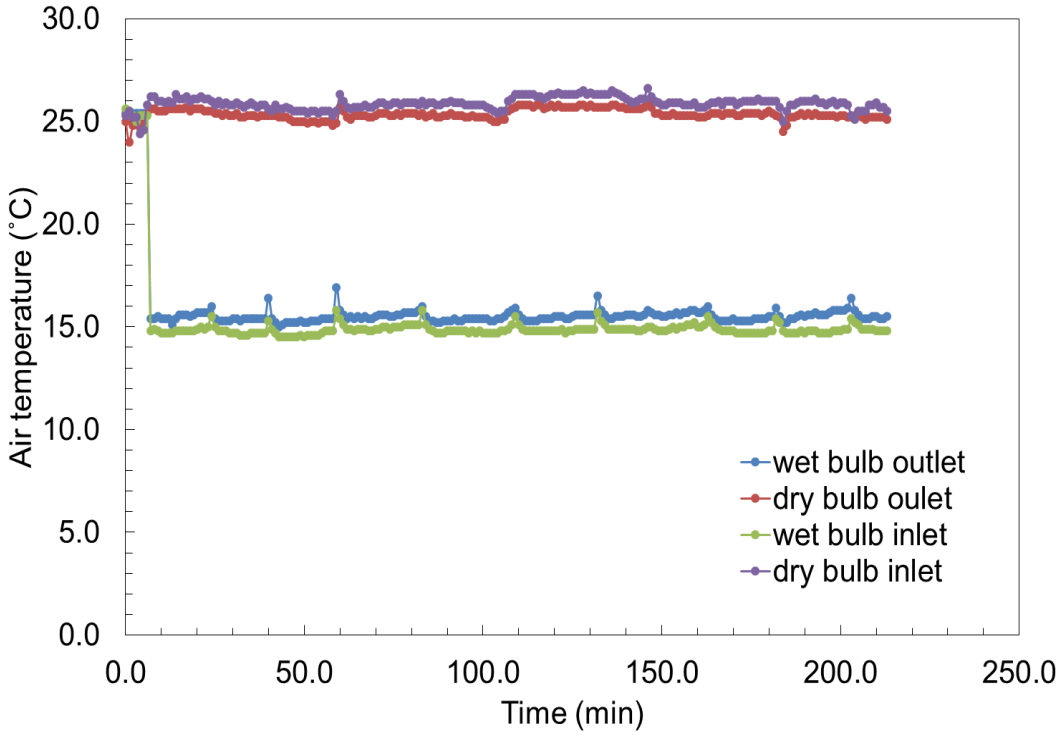

Figure A.10: Plot of air temperature change with time for Run5

Air temperature and water temperature graphs with time are in Figure A.11 and Figure A.12 for Run 6:

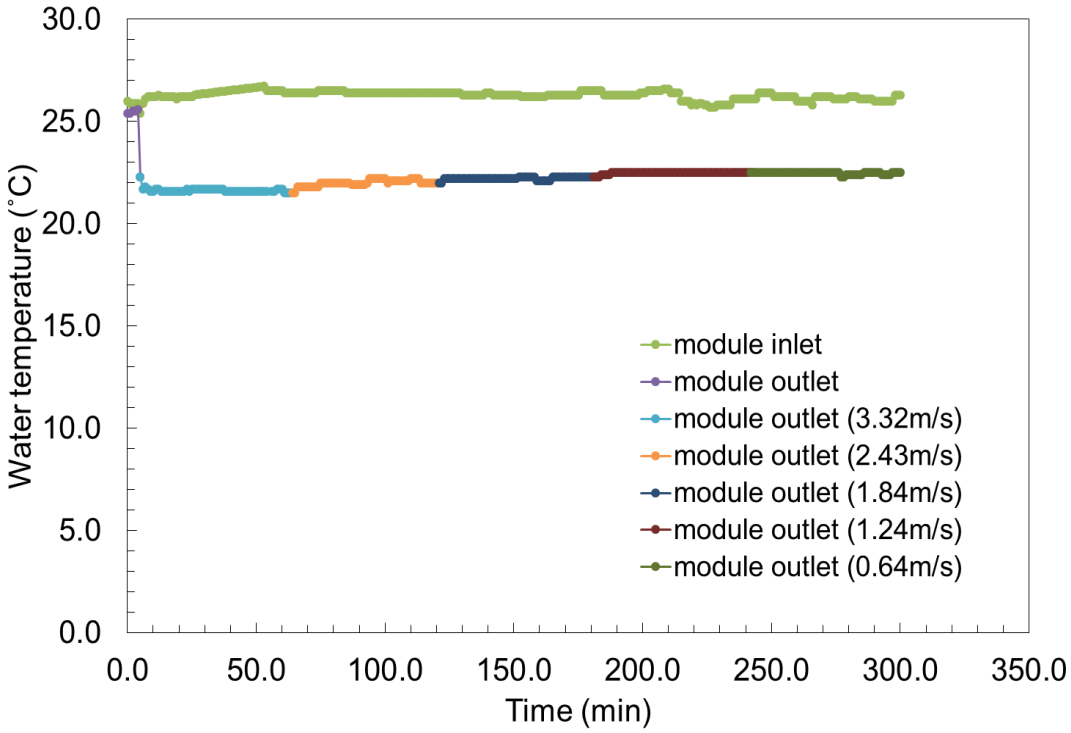

Figure A.11: Plot of water temperature change with time for Run6

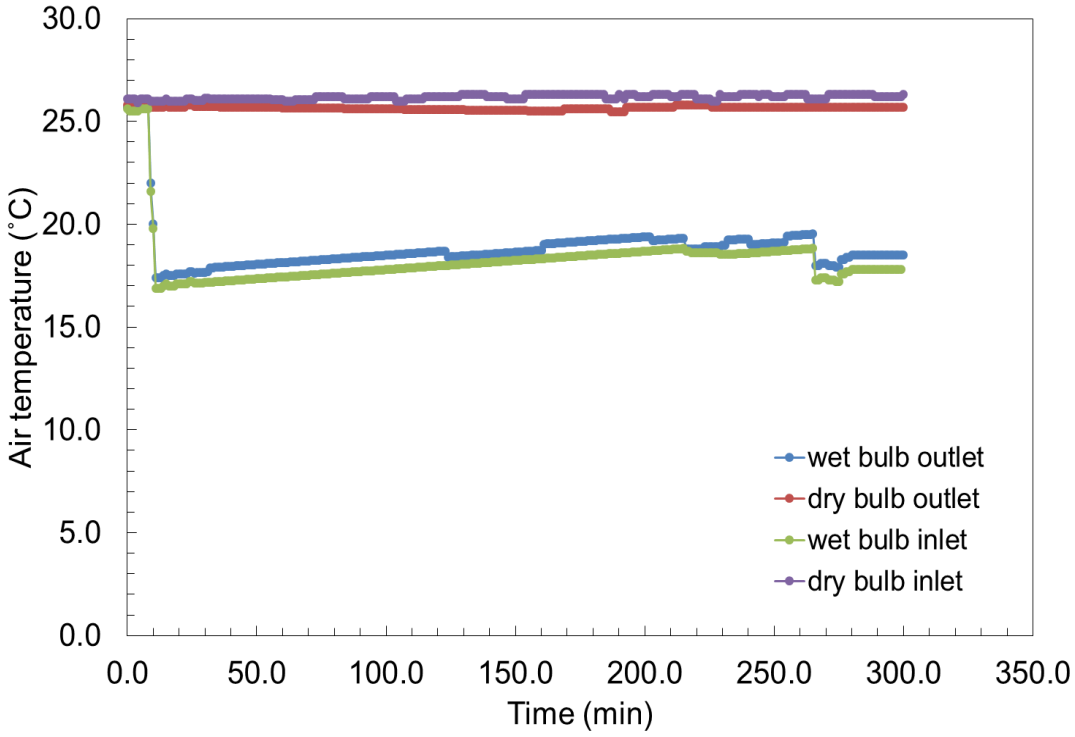

Figure A.12: Plot of air temperature change with time for Run6

Transmembrane pressure effect on cooling performance in membrane based system

Table A.6: Experiment parameters and temperature results for pressure effect for 1 pack in parallel connection

	Run	0barg	0.1barg	0.2barg	Air switch	Water flow rate (mL/min)	L (cm)
Wet bulb inlet temperature (T_1)	7	13.2	13.0	12.6	5	10	30
	8	17.0	17.3	17.2	5	10	30
	9	17.2	16.9	16.9	5	10	30
	Avr.	15.8	15.7	15.6			
	Std.	±2.3	±2.4	±2.6			
Wet bulb outlet	7	13.8	13.9	13.4	5	10	30
	8	17.5	18.0	17.7	5	10	30
	9	17.5	17.6	18.0	5	10	30

temperature (T_2)							
	Avr.	16.3	16.5	16.4			
	Std.	±2.1	±2.3	±2.6			
Dry bulb inlet temperature (T_3)	7	26.1	25.9	26.0	5	10	30
	8	26.3	26.4	26.0	5	10	30
	9	26.3	26.0	26.4	5	10	30
	Avr.	26.2	26.1	26.1			
	Std.	±0.1	±0.3	±0.2			
Dry bulb outlet temperature (T_4)	7	25.8	25.5	25.6	5	10	30
	8	25.9	26.0	25.6	5	10	30
	9	26.0	25.9	26.2	5	10	30
	Avr.	25.9	25.8	25.8			
	Std.	±0.1	±0.3	±0.4			
Water inlet temperature (T_5)	7	25.6	25.8	25.6	5	10	30
	8	26.6	26.5	26.2	5	10	30
	9	27.0	27.0	26.8	5	10	30
	Avr.	26.4	26.4	26.2			
	Std.	±0.7	±0.6	±0.4			
Water outlet temperature (T_6)	7	20.5	19.1	18.7	5	10	30
	8	21.7	21.5	20.6	5	10	30
	9	21.8	21.7	21.6	5	10	30
	Avr.	21.3	20.8	20.3			
	Std.	±0.7	±1.5	±1.5			

Air temperature and water temperature graphs with time are Figure A.13 and A.14 for Run 7:

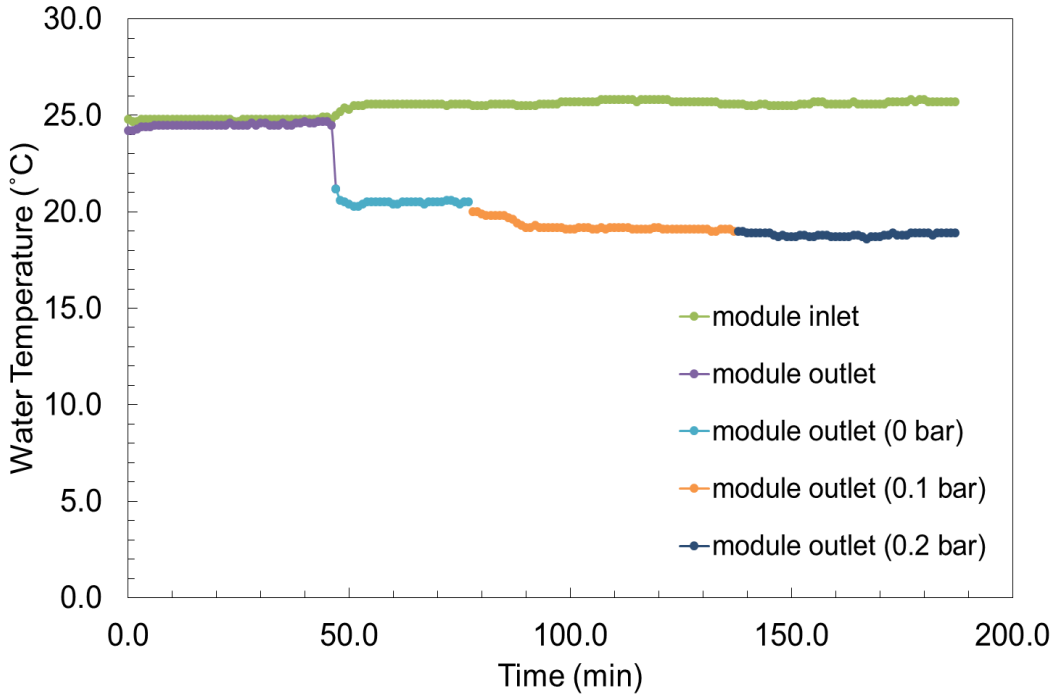

Figure A.13: Plot of water temperature change with time for Run7

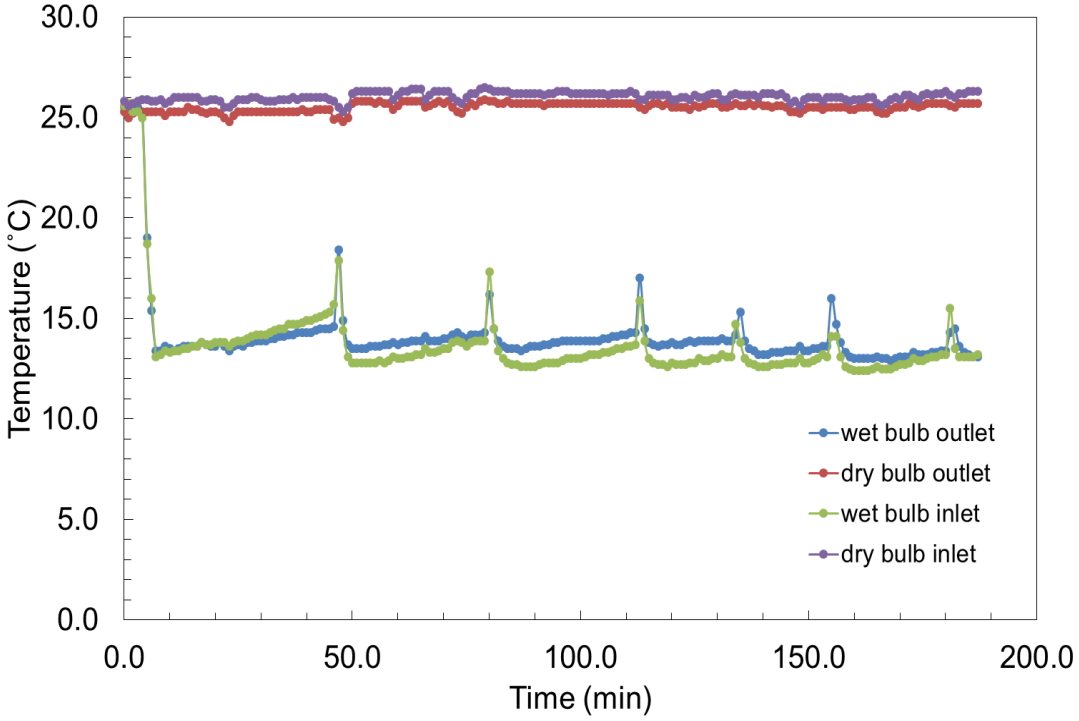

Figure A.14: Plot of air temperature change with time for Run7

Air temperature and water temperature graphs with time are in Figure A.15 and Figure A.16 for Run 8:

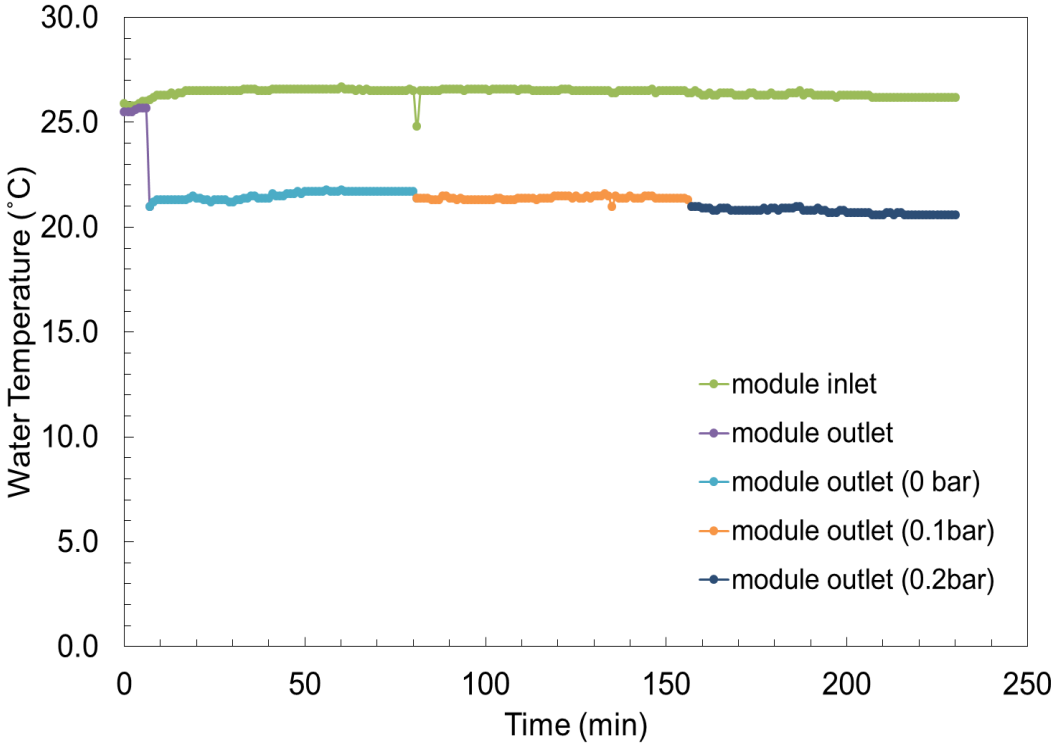

Figure A.15: Plot of water temperature change with time for Run8

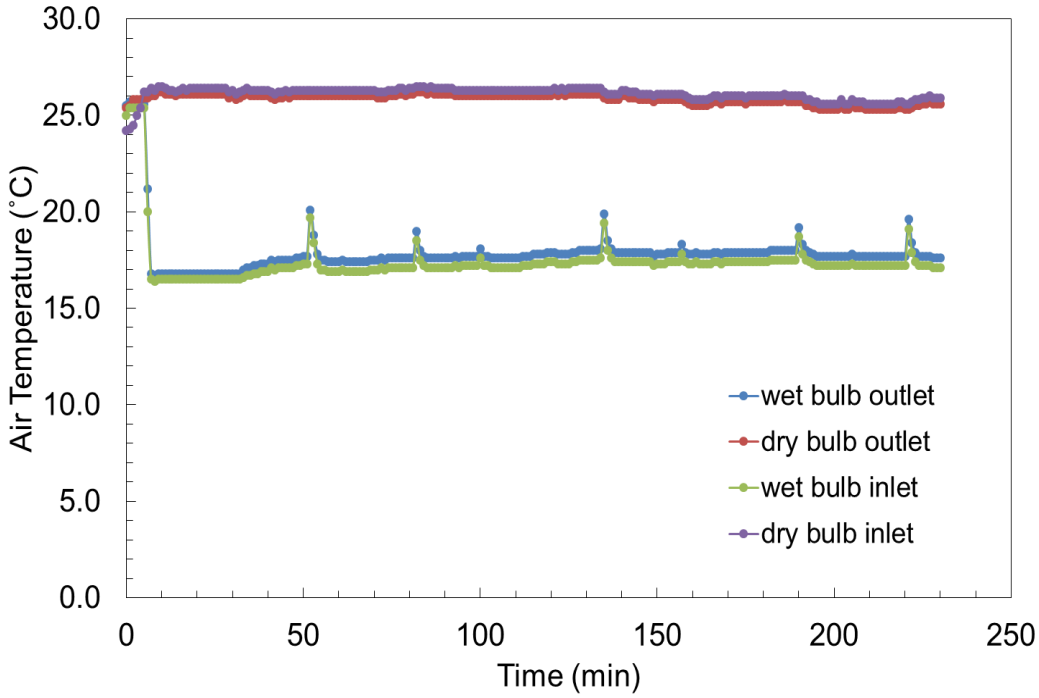

Figure A.16: Plot of air temperature change with time for Run8

Air temperature and water temperature graphs with time are in Figure A.17 and Figure A.18 for Run 9:

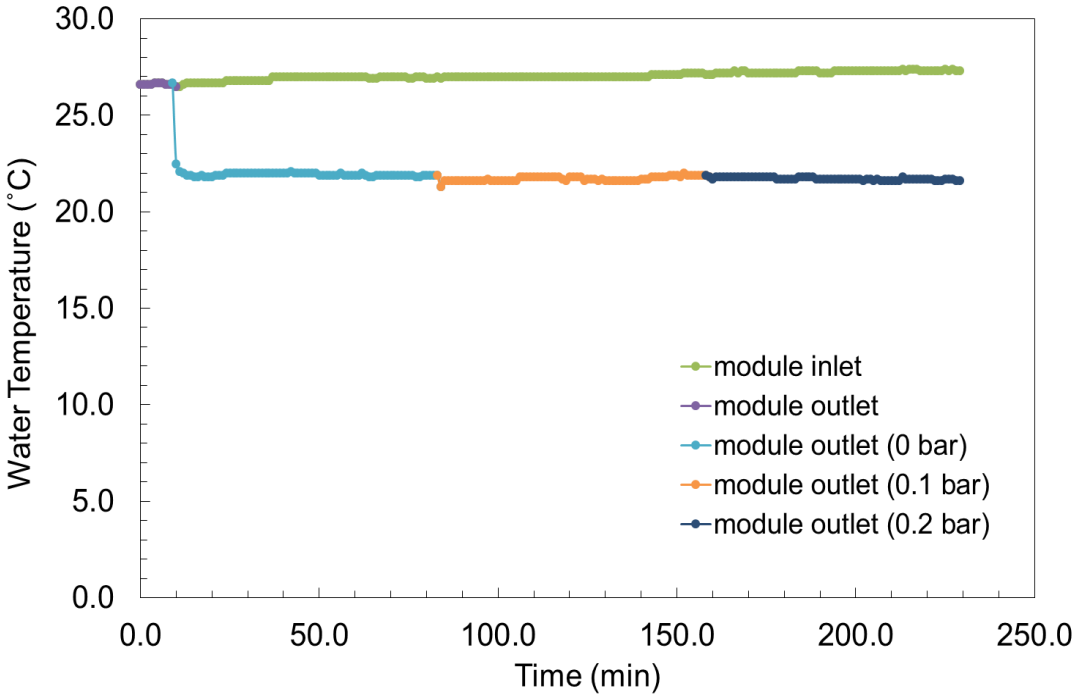

Figure A.17: Plot of water temperature with time for Run9

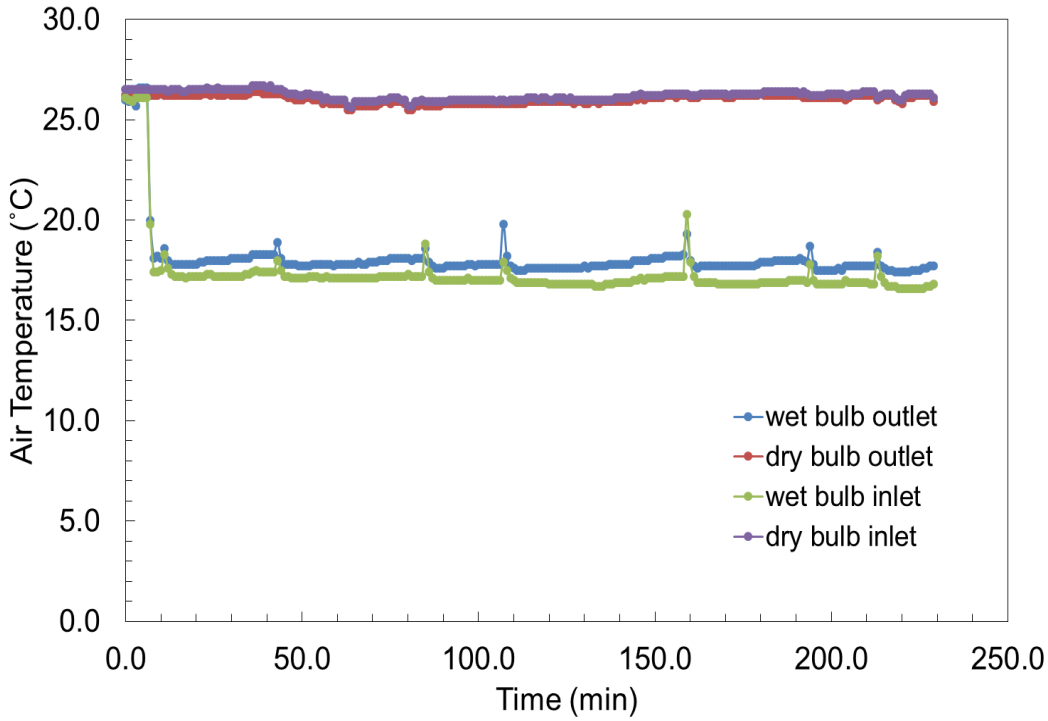

Figure A.18: Plot of air temperature change with time for Run9

Length effect on cooling performance in membrane based system

Table A.7: Experiment parameters and temperature results for length effect for 1.84 m/s air velocity and series connection

	Run	30cm	60 cm	90 cm	120 cm	Water flow rate (mL/min)	P(barg)	Number of module
Wet bulb inlet temperature (T_1)	10	14.4	14.5	15.0	15.0	10	0	1-4
	11	15.9	15.5	15.6	15.2	10	0	1-4
	12	16.3	15.8	15.1	15.7	10	0	1-4
	Avr.	15.5	15.3	15.2	15.3			
	Std.	±1.0	±0.7	±0.3	±0.4			
Wet bulb outlet temperature (T_2)	10	15.1	15.2	15.3	15.4	10	0	1-4
	11	16.9	16.2	16.3	16.3	10	0	1-4
	12	17.0	16.5	16.2	17.0	10	0	1-4
	Avr.	16.3	16.0	15.9	16.2			
	Std	±1.1	±0.7	±0.6	±0.8			
Dry bulb inlet temperature (T_3)	10	26.4	25.8	25.9	26.3	10	0	1-4
	11	26.1	26.3	26.1	26.3	10	0	1-4
	12	25.5	26.3	27.4	27.3	10	0	1-4
	Avr.	26.0	26.1	26.5	26.6			
	Std.	±0.5	±0.3	±0.8	±0.6			
Dry bulb outlet temperature (T_4)	10	26.3	25.3	25.8	26.0	10	0	1-4
	11	25.7	25.8	25.7	25.6	10	0	1-4
	12	25.4	26.3	27.2	27.1	10	0	1-4
	Avr.	25.8	25.8	26.2	26.2			
	Std.	±0.5	±0.5	±0.8	±0.8			
Water inlet temperature (T_5)	10	25.4	25.3	25.2	25.4	10	0	1-4
	11	26.3	26.6	26.4	26.6	10	0	1-4
	12	27.3	28.1	28.7	29.1	10	0	1-4
	Avr.	26.3	26.7	26.8	27.0			

	Std.	±1.0	±1.4	±1.8	±1.9			
Water outlet temperature (T_6)	10	20.5	18.8	18.5	18.2	10	0	1-4
	11	20.2	18.9	18.2	17.7	10	0	1-4
	12	22.5	21.1	21.3	21.4	10	0	1-4
	Avr.	21.1	19.6	19.3	19.1			
	Std.	±1.3	±1.3	±1.7	±2.0			

Air temperature and water temperature graphs with time are in Figure A.19 and Figure A.20 for Run 10:

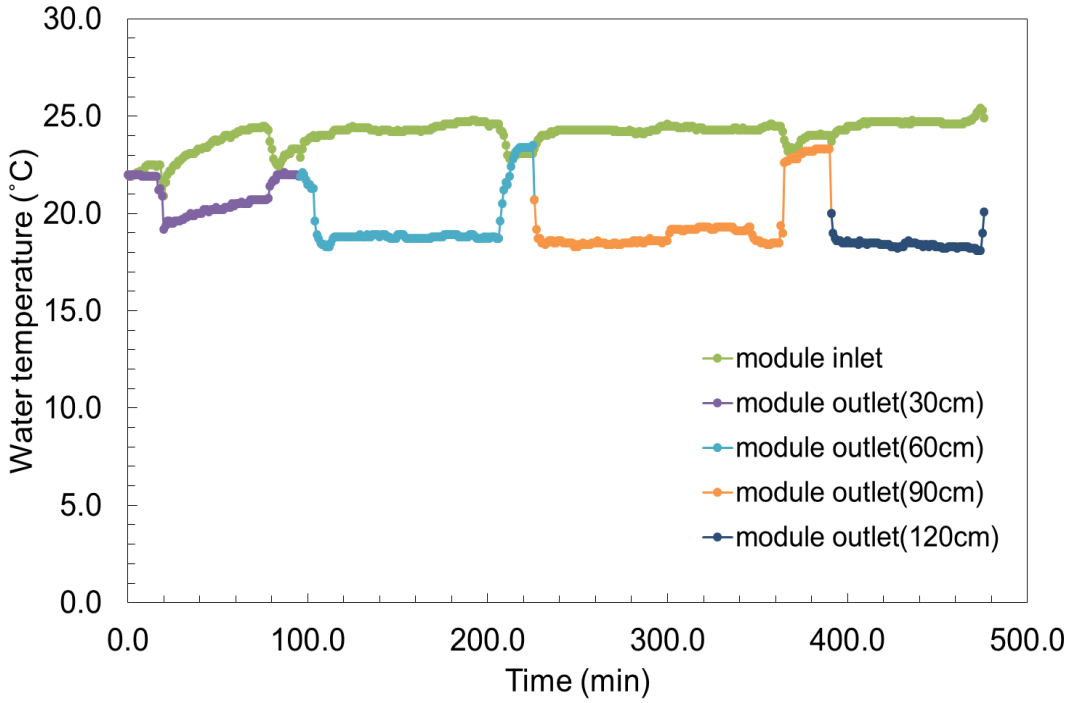

Figure A.19: Plot of water temperature change with time for Run10

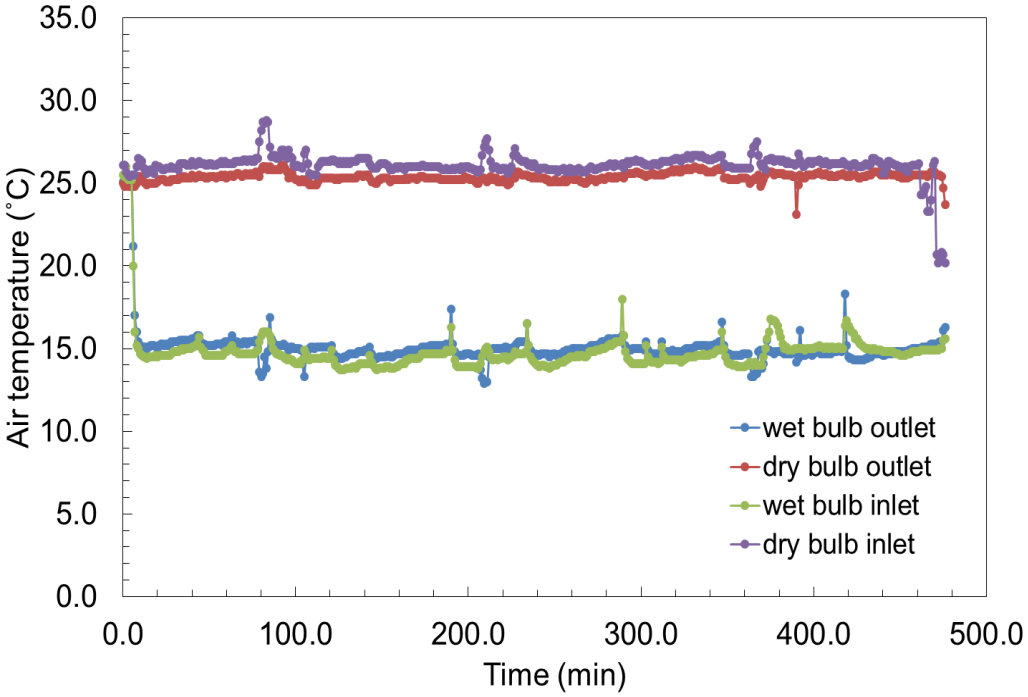

Figure A.20: Plot of air temperature change with time for Run10

Air temperature and water temperature graphs with time are in Figure A.21 and A.22 for Run 11:

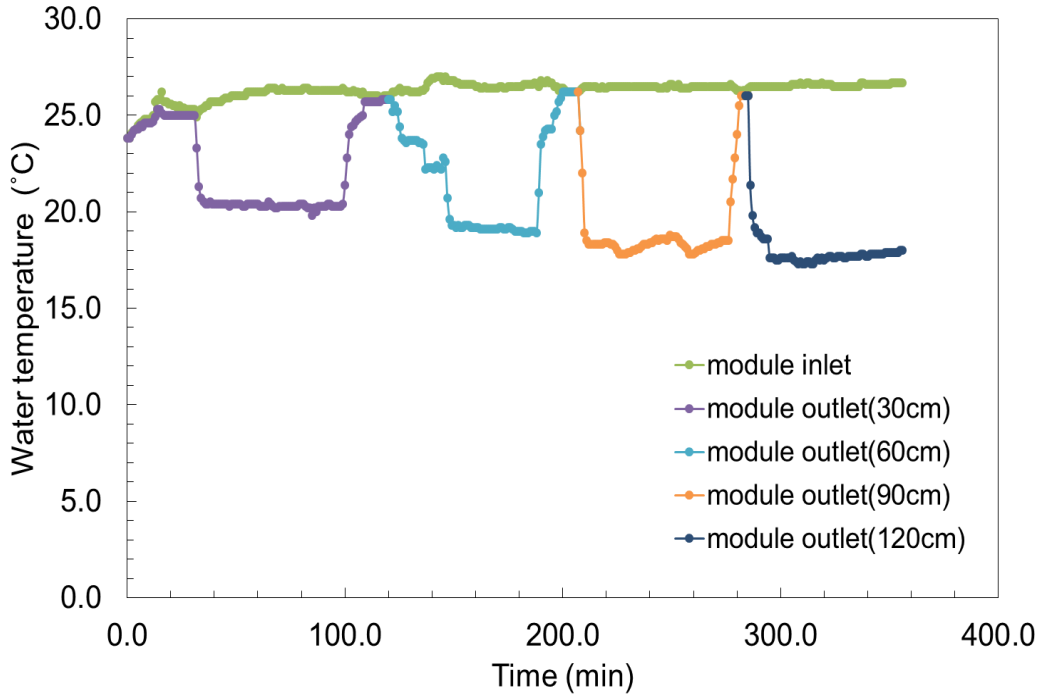

Figure A.21: Plot of water temperature change with time for Run11

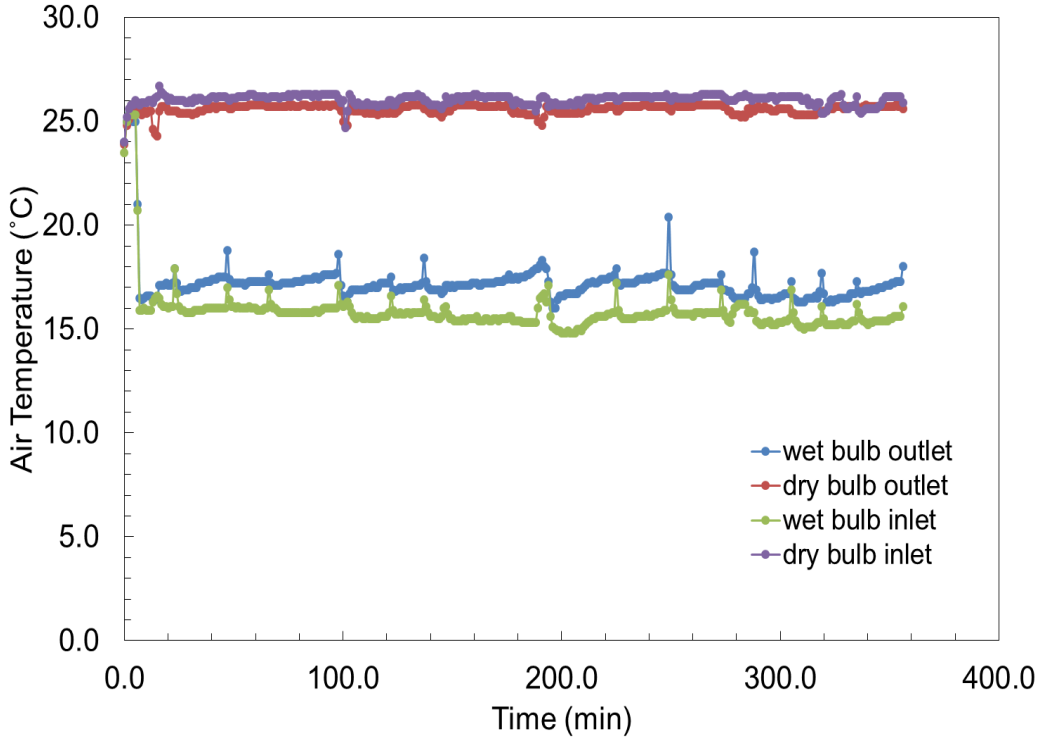

Figure A.22: Plot of air temperature change with time for Run11

Air temperature and water temperature graphs with time are in Figure A.23 and Figure A.24 for Run 12:

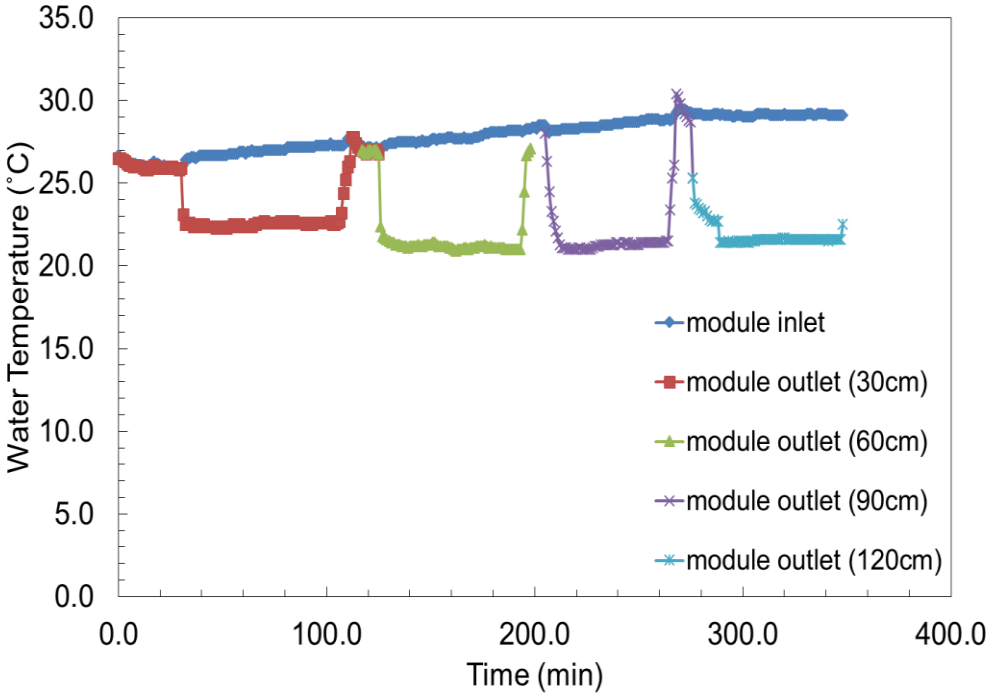

Figure A.23: Plot of water temperature change with time for Run12

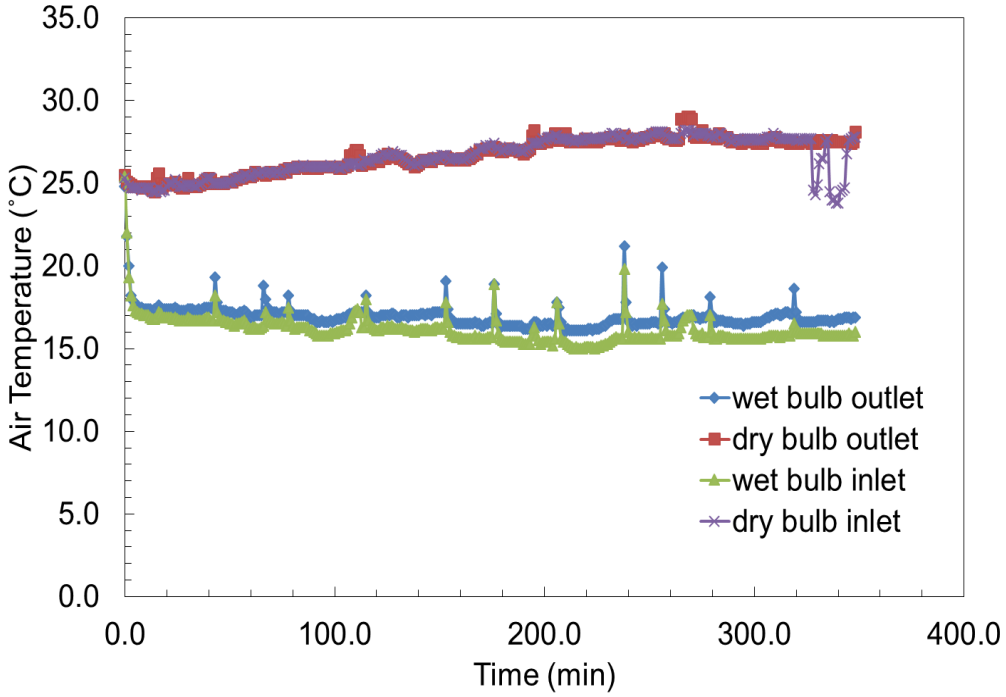

Figure A.24: Plot of air temperature change with time for Run12

Pack number effect on cooling performance in membrane based system

Table A.8: Experiment parameters and temperature results for pack number effect for 1.84 m/s air velocity and parallel connection

	Run	1 pack	9 pack	18 pack	P(bar)	Water flow rate (mL/min)	L (cm)
Wet bulb inlet temperature (T_1)	13	13.1	18.4	16.7	0	10	30
	14	17.8	16.8	14.6	0	10	30
	15	18.7	19.8	16.7	0	10	30
	Avr.	15.5	15.3	15.2			
	Std.	±1.0	±0.7	±0.3			
Wet bulb outlet temperature (T_2)	13	15.1	15.2	15.3	0	10	30
	14	16.9	16.2	16.3	0	10	30
	15	17.0	16.5	16.2	0	10	30

	Avrr.	16.3	16.0	15.9			
	Std.	±1.1	±0.7	±0.6			
Dry bulb inlet temperature (T_3)	13	26.4	25.8	25.9	0	10	30
	14	26.1	26.3	26.1	0	10	30
	15	25.5	26.3	27.4	0	10	30
	Avr.	26.0	26.1	26.5			
	Std.	±0.5	±0.3	±0.8			
Dry bulb outlet temperature (T_4)	13	26.3	25.3	25.8	0	10	30
	14	25.7	25.8	25.7	0	10	30
	15	25.4	26.3	27.2	0	10	30
	Avr.	25.8	25.8	26.2			
	Std.	±0.5	±0.5	±0.8			
Water inlet temperature (T_5)	13	25.4	25.3	25.2	0	10	30
	14	26.3	26.6	26.4	0	10	30
	15	27.3	28.1	28.7	0	10	30
	Avr.	26.3	26.7	26.8			
	Std.	±1.0	±1.4	±1.8			
Water outlet temperature (T_6)	13	20.5	18.8	18.5	0	10	30
	14	20.2	18.9	18.2	0	10	30
	15	22.5	21.1	21.3	0	10	30
	Avr.	21.1	19.6	19.3			
	Std.	±1.3	±1.3	±1.7			

In investigation of pack number effect on cooling of water, experiments are conducted in different times. Air and water temperature graphs will be given as 1 pack, 9 pack and 18 pack.

For Run 13 and 1 pack measurement, air and water temperature graphs are same as the Run 1 for water flow rate of 10 cm^3/min.

Air and water temperature plots with time will be given in A.25 and A.26for Run 13 and 9 module:

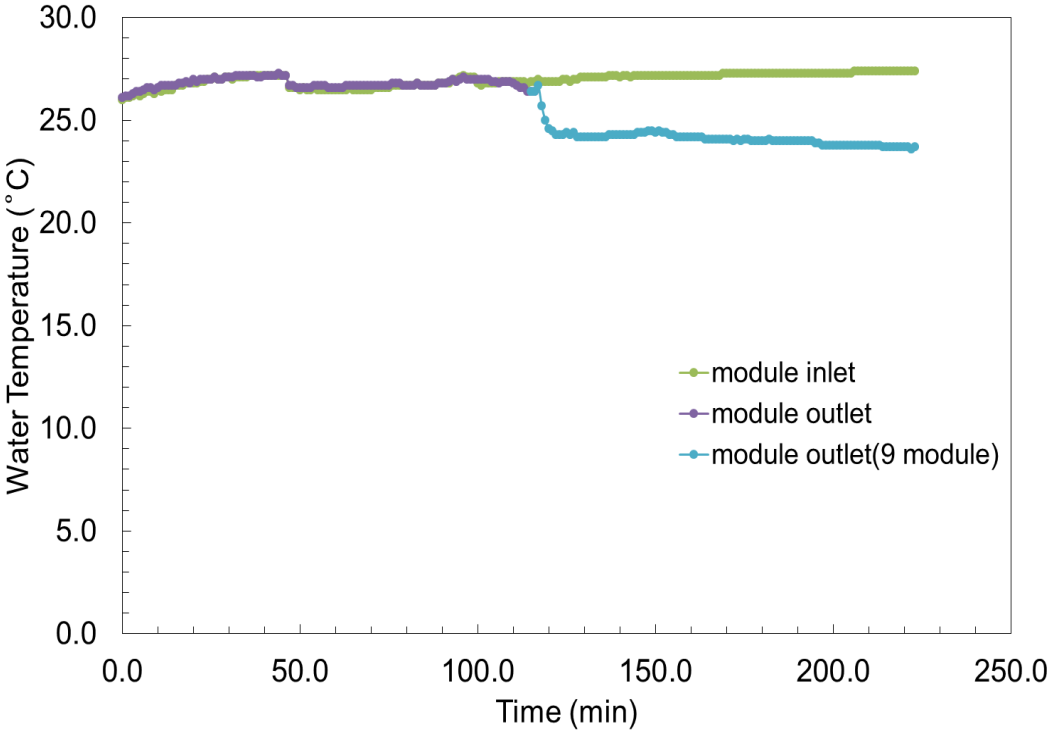

Figure A.25: Plot of water temperature with time for Run 13, 9 module

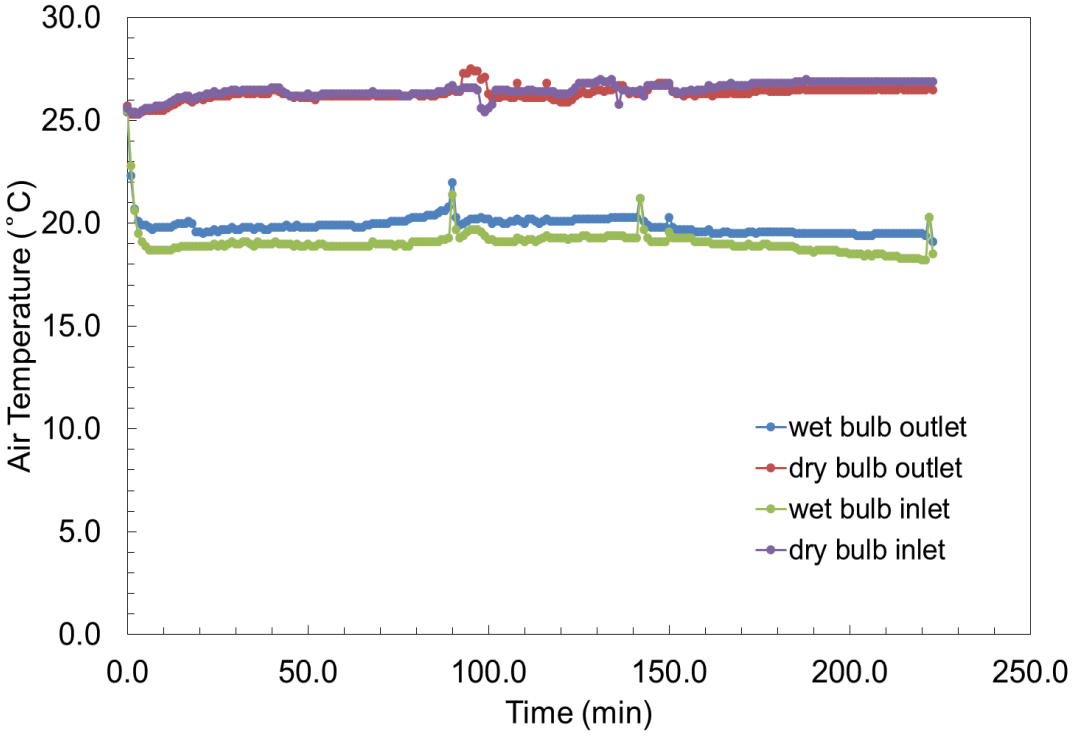

Figure A.26: Plot of air temperature with time for Run 13, 9 module

Run 13, 18 pack air and water temperature graphs with time are shown in Figure A.27Figure A.27 and Figure A.28:

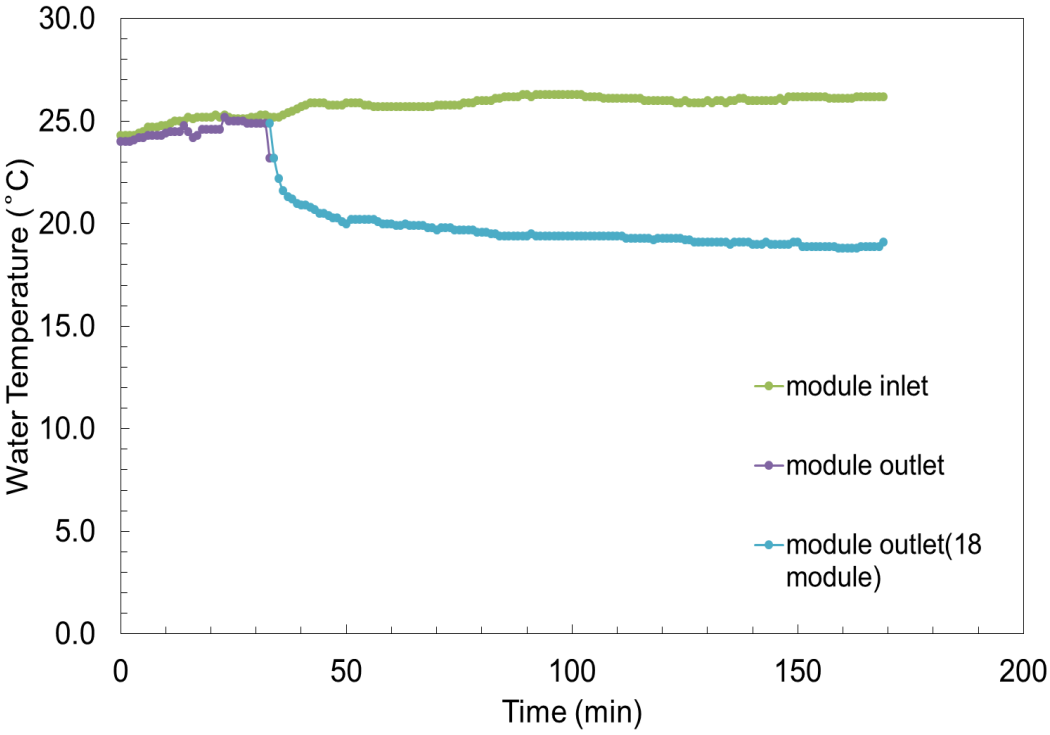

Figure A.27: Plot of water temperature with time for Run 13, 18 pack

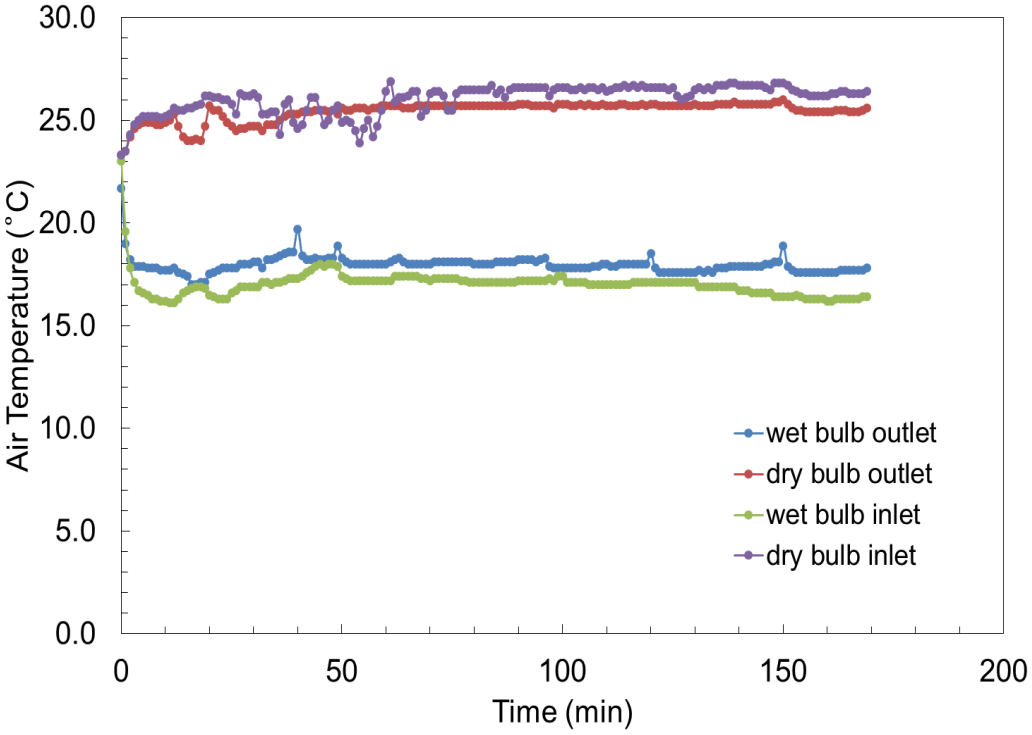

Figure A.28: Plot of air temperature with time for Run 13, 18 pack

Run 14, one pack air and water temperature graphs with time are given in Figure A.29 and A.30:

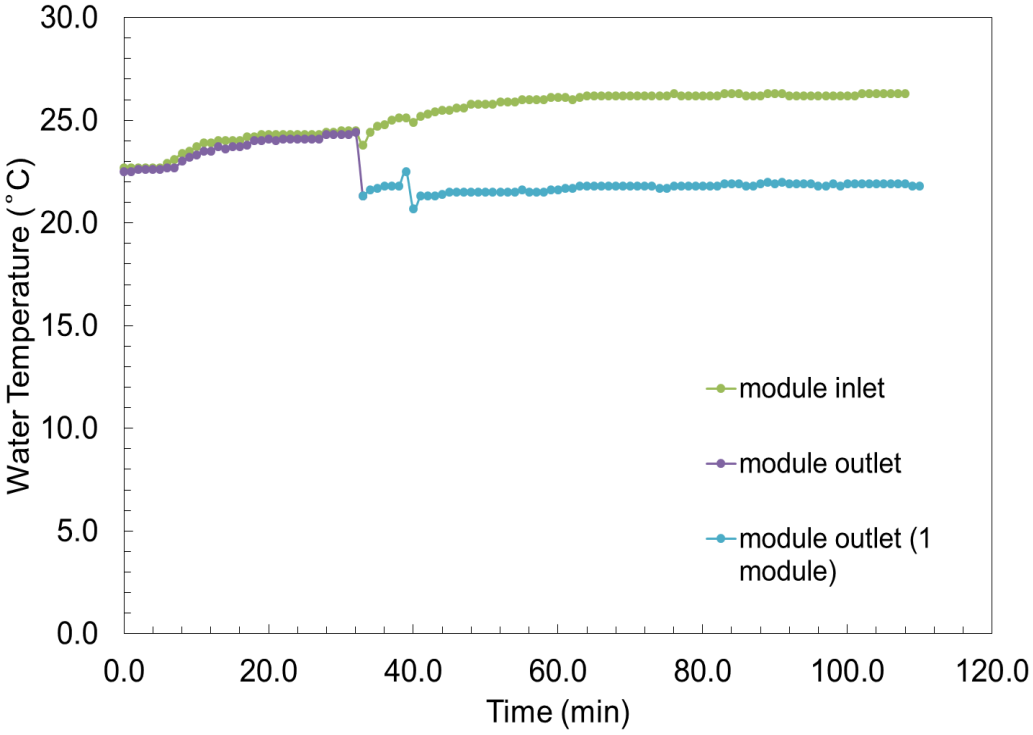

Figure A.29: Plot of water temperature with time for Run 14, 1 pack

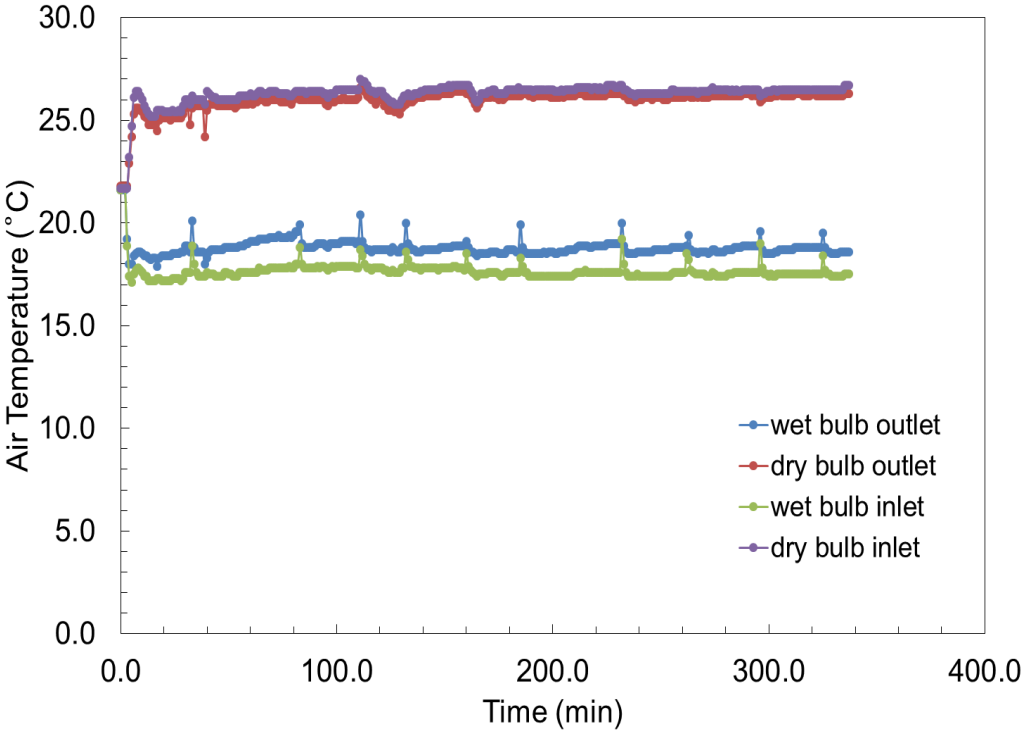

Figure A.30: Plot of air temperature with time for Run 14, 1 pack

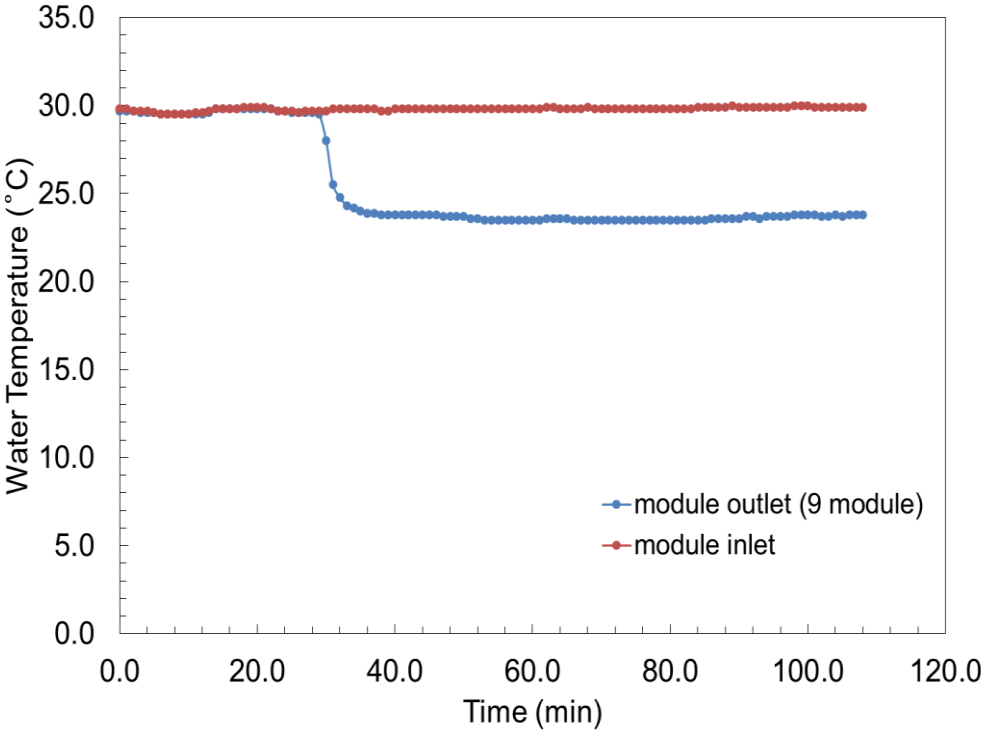

Figure A.31: Plot of water temperature with time for Run 14, 9 pack

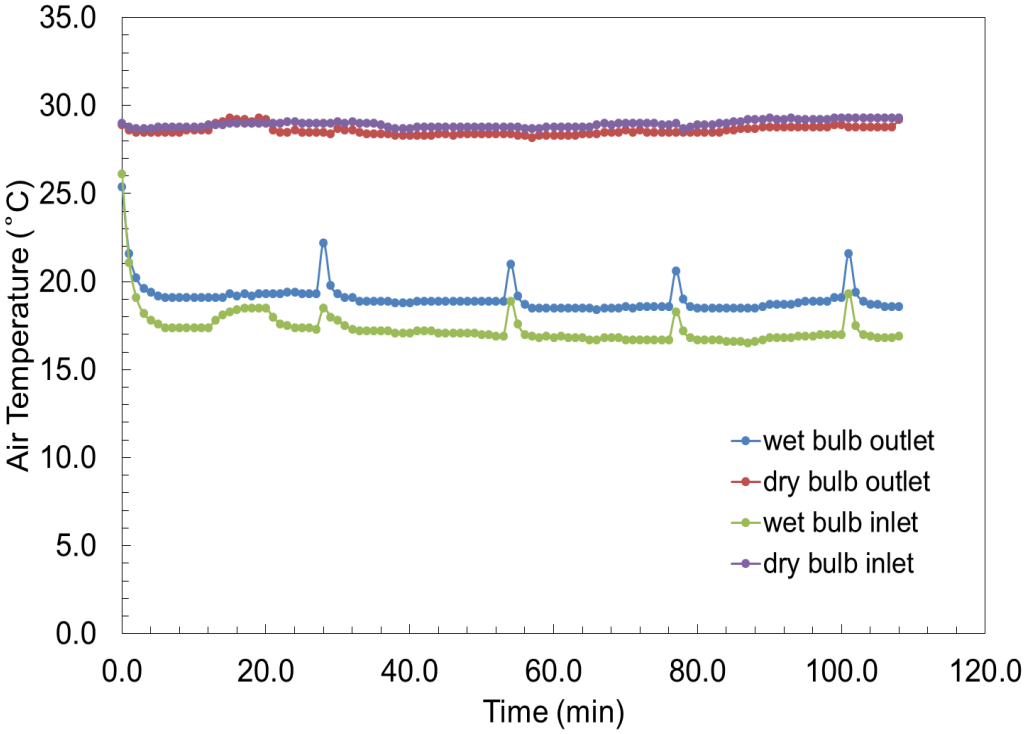

Figure A.32: Plot of air temperature with time for Run 14, 9 pack

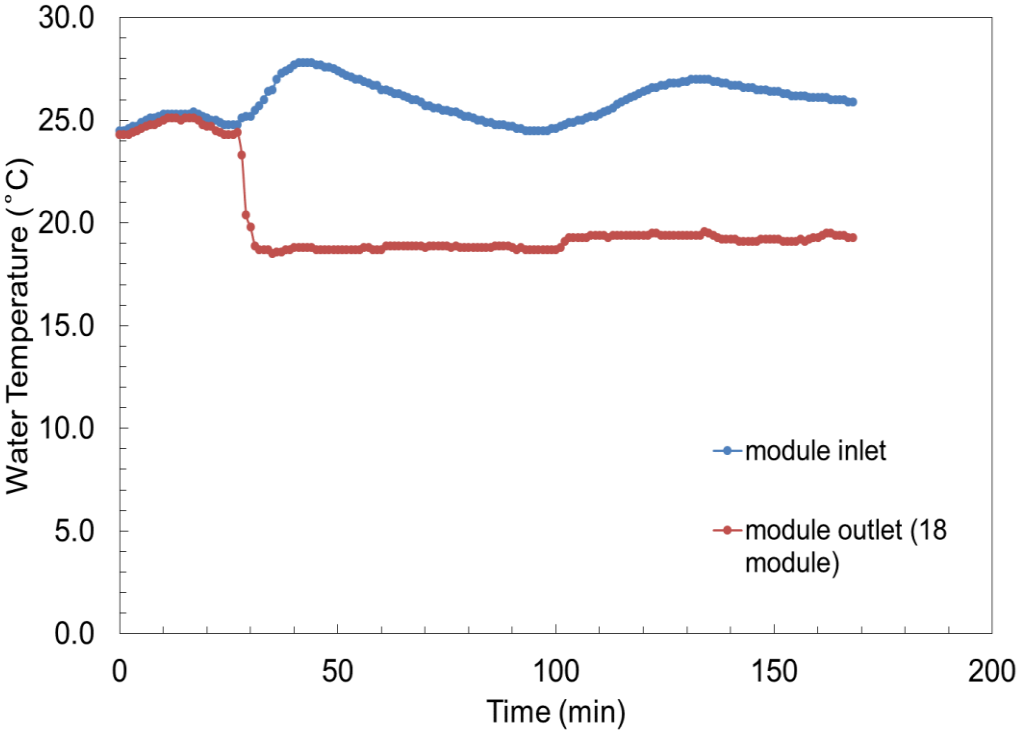

Figure A.33: Plot of water temperature with time for Run 14, 18 pack

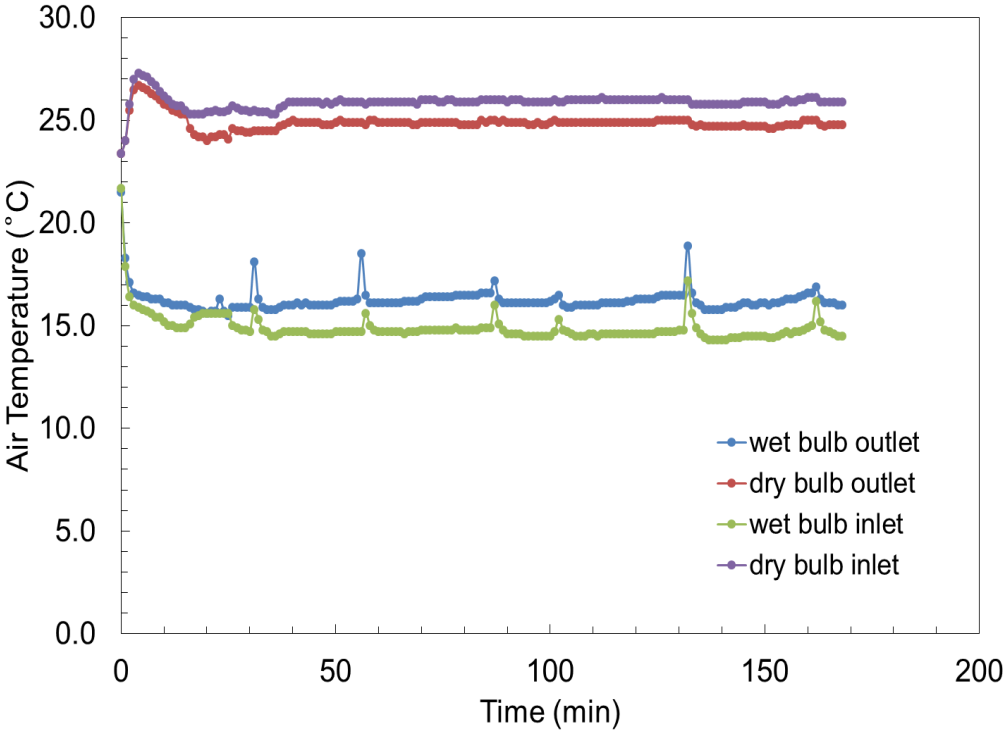

Figure A.34: Plot of air temperature with time for Run 14, 18 pack

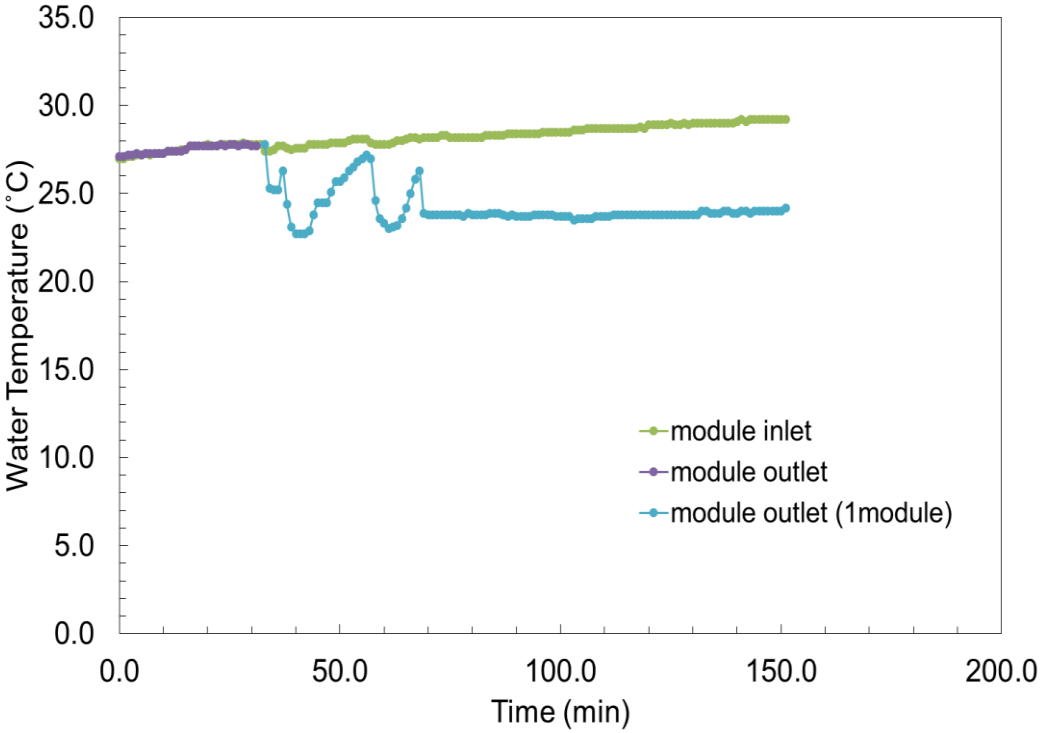

Figure A.35: Plot of water temperature with time for Run 15, 1 pack

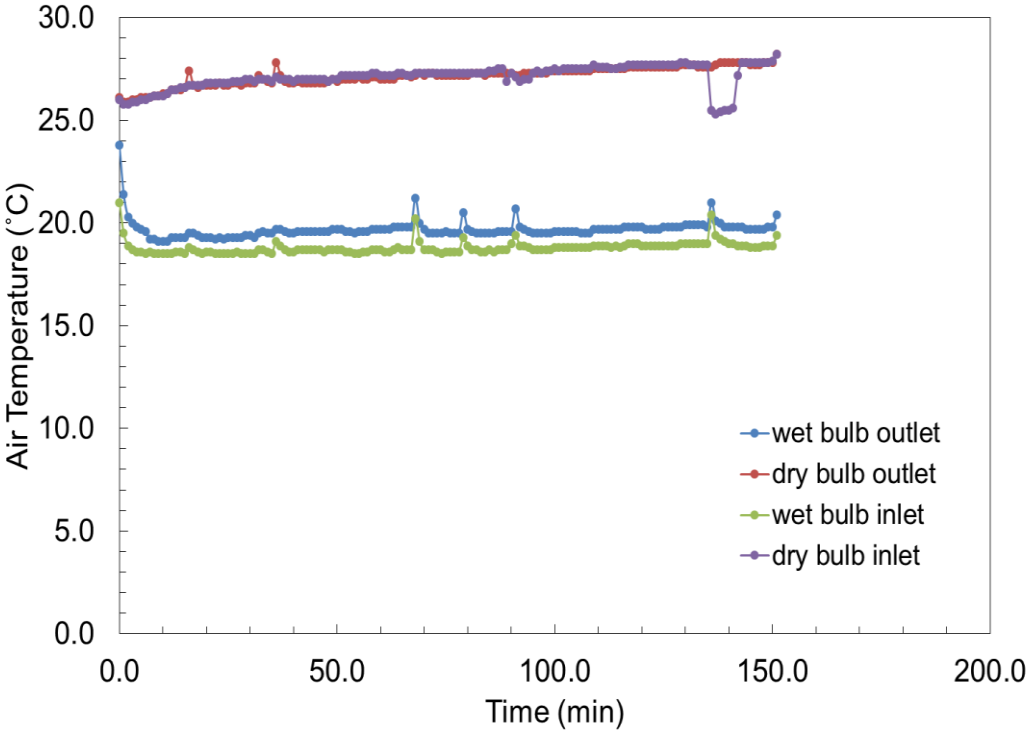

Figure A.36: Plot of air temperature with time for Run 15, 1 pack

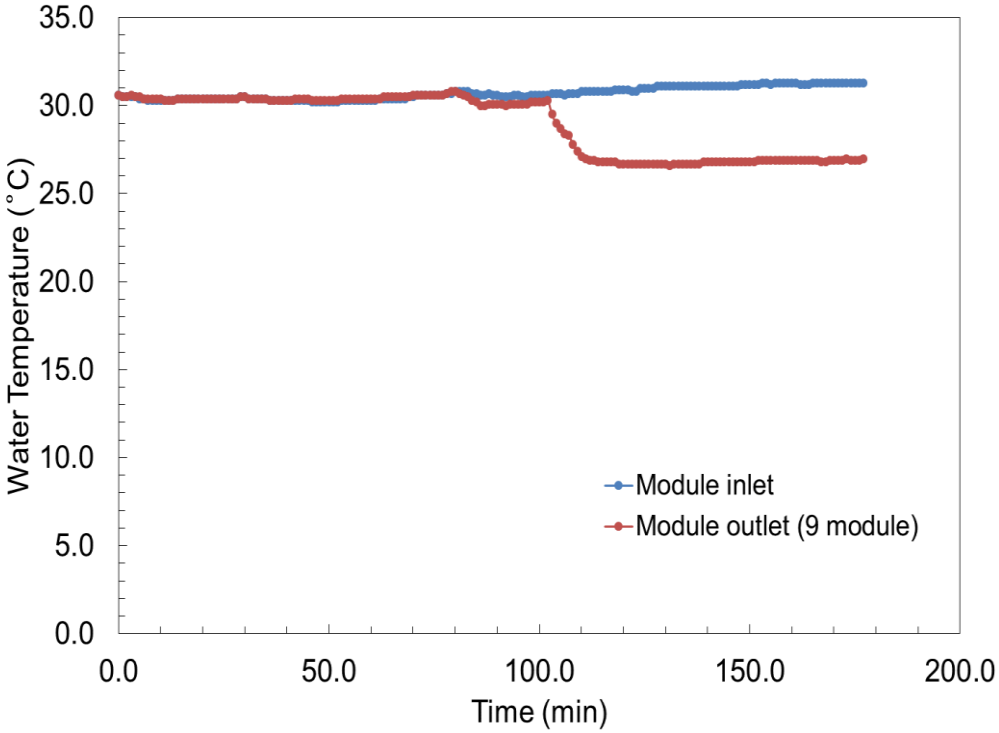

Figure A.37: Plot of water temperature with time for Run 15, 9 pack

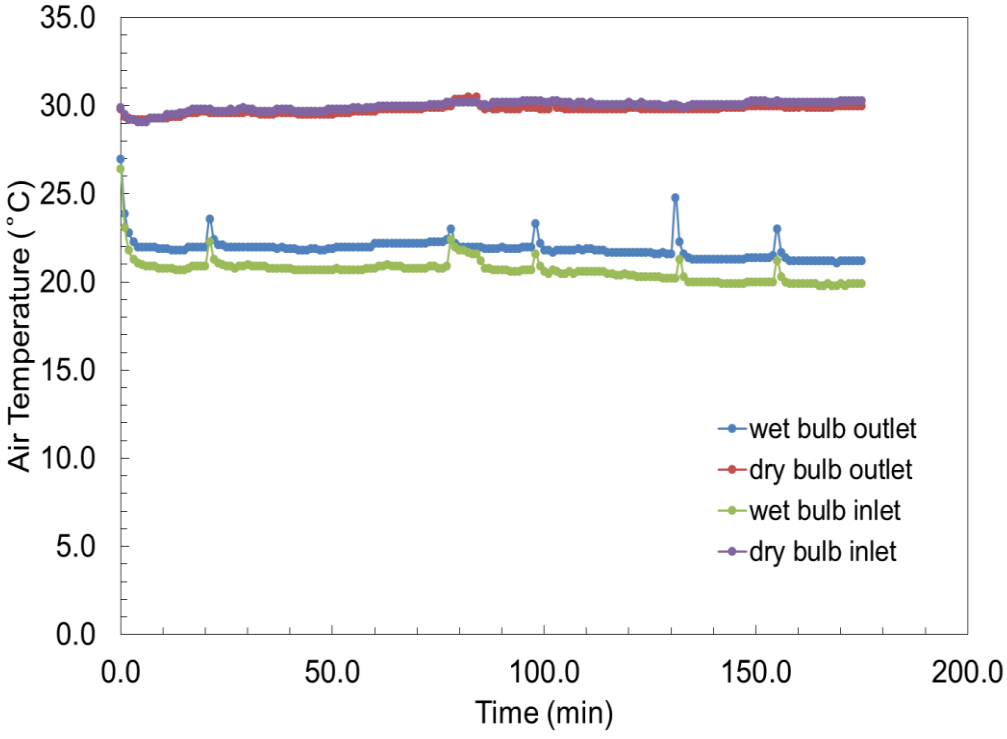

Figure A.38: Plot of air temperature with time for Run 15, 9 pack

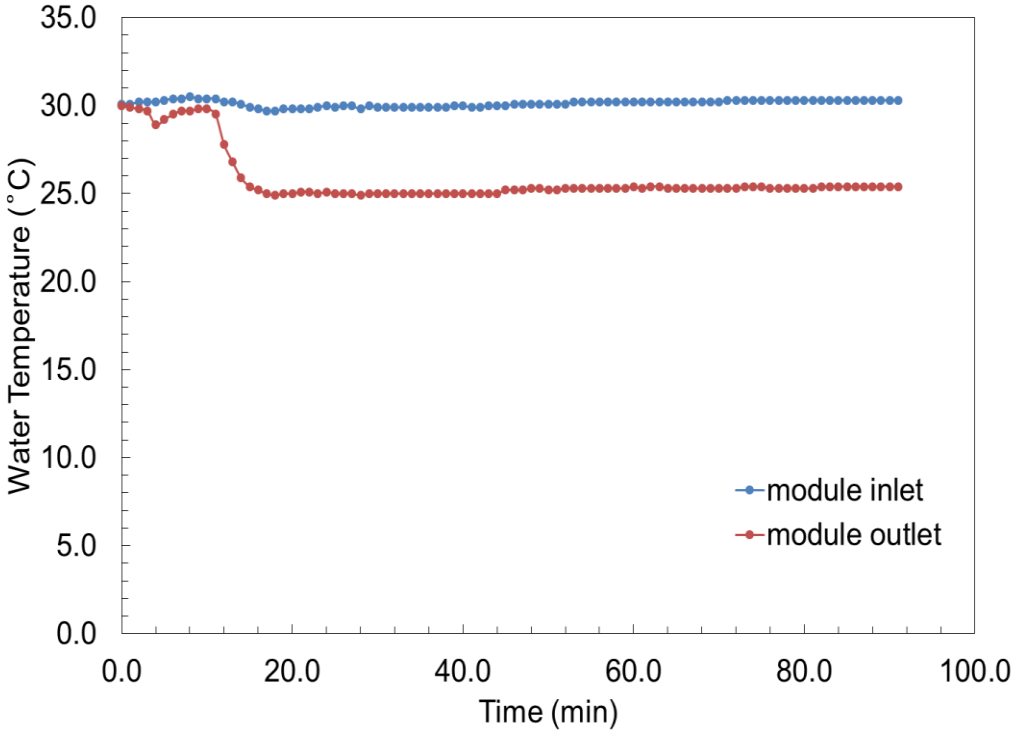

Figure A.39: Plot of water temperature with time for Run 15, 18 pack

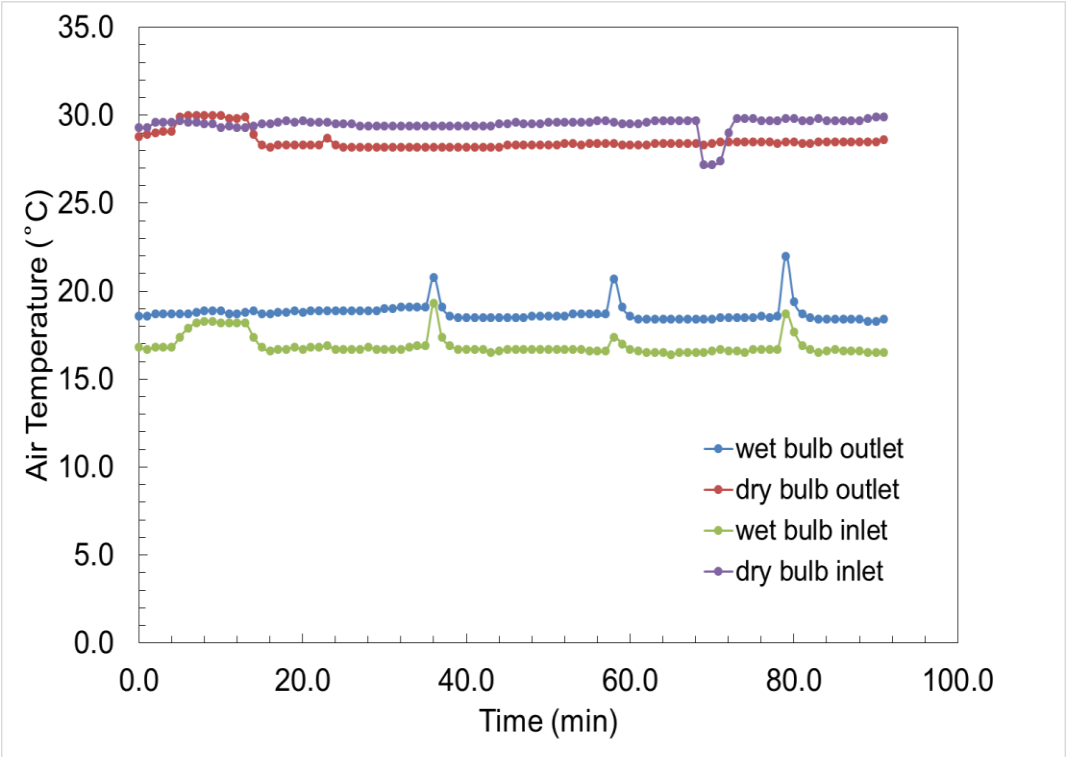

Figure A.40: Plot of air temperature with time for Run 15, 18 pack

Water inlet temperature effect on cooling performance in membrane based system

Table A.9: Experiment parameters and temperature results for module pack effect for 1 pack in parallel connection and 1.84 m/s air velocity

	Run	27.9˚C	31.5˚C	39.7˚C	P(barg)	Water flow rate (mL/min)	L (cm)
Wet bulb inlet temperature (T_1)	19	16.9	16.7	17.1	0	10	30
	20	17.5	18.0	17.9	0	10	30
	21	17.5	17.3	17.6	0	10	30
	Avr.	17.3	17.3	17.5			
	Std.	0.3	0.7	0.4			
Wet bulb outlet temperature (T_2)	19	17.5	17.5	17.6	0	10	30
	20	18.3	18.4	18.6	0	10	30
	21	18.1	18.2	18.4	0	10	30
	Avr.	18.0	18.0	18.2			
	Std.	0.4	0.5	0.5			
Dry bulb inlet temperature (T_3)	19	26.8	27.3	27.5	0	10	30
	20	26.7	27.6	27.9	0	10	30
	21	28.3	29.3	30.0	0	10	30
	Avr.	27.3	28.1	28.5			
	Std.	0.9	1.1	1.3			
Dry bulb outlet temperature (T_4)	19	26.1	26.7	26.8	0	10	30
	20	26.5	27.3	27.4	0	10	30
	21	28.0	28.9	29.5	0	10	30
	Avr.	26.9	27.6	27.9			
	Std.	1.0	1.1	1.4			
	19	26.9	29.5	40.5	0	10	30

Water inlet temperature (T_5)	20	27.2	31.0	38.3	0	10	30
	21	29.6	34.0	40.3	0	10	30
	Avr.	27.9	31.5	39.7			
	Std.	1.5	2.3	1.2			
Water outlet temperature (T_6)	19	23.2	25.0	31.8	0	10	30
	20	23.6	25.7	28.7	0	10	30
	21	24.2	26.5	30.2	0	10	30
	Avr.	23.7	25.7	30.2			
	Std.	0.5	0.8	1.6			

Air and water temperature graphs are given in Figure A.41 and A.42 for Run19:

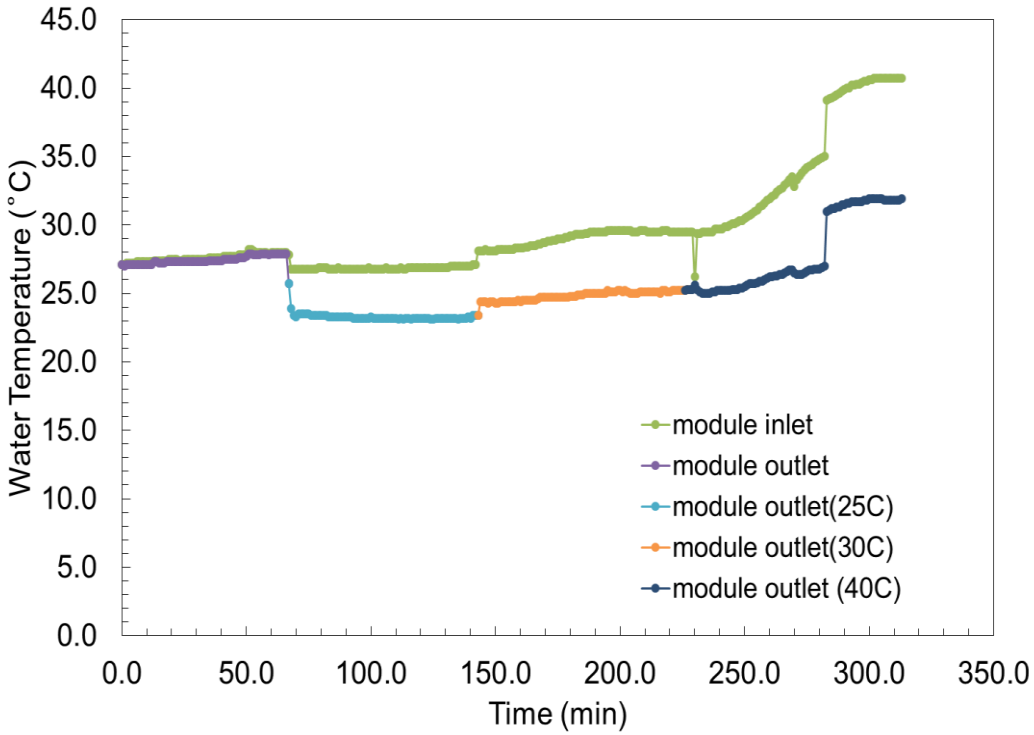

Figure A.41: Plot of water temperature with time for Run 19

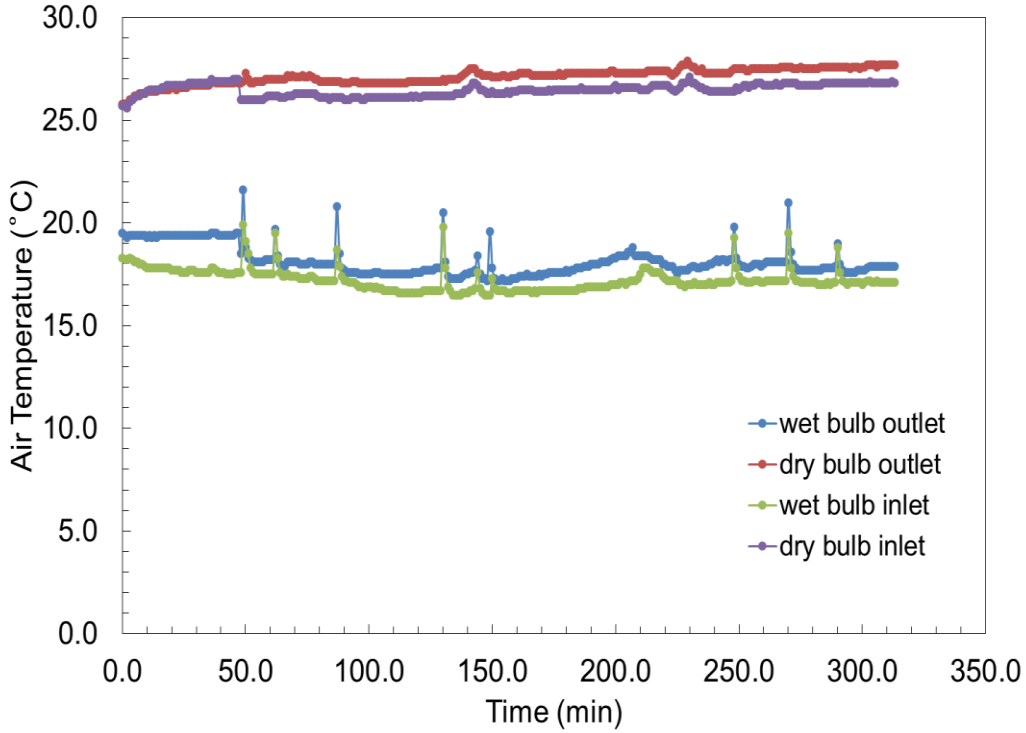

Figure A.42: Plot of air temperature with time for Run 1

Air and water temperature graphs with time are given in Figure A.43 and A.44 for Run 20:

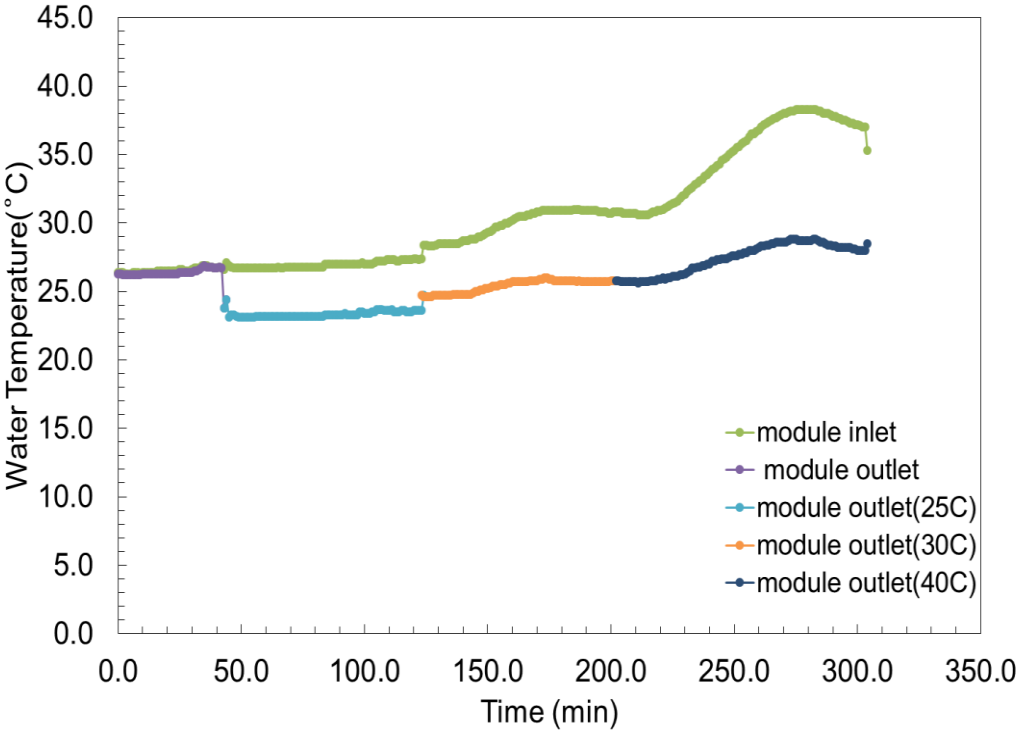

Figure A.43: Plot of water temperature with time for Run 20

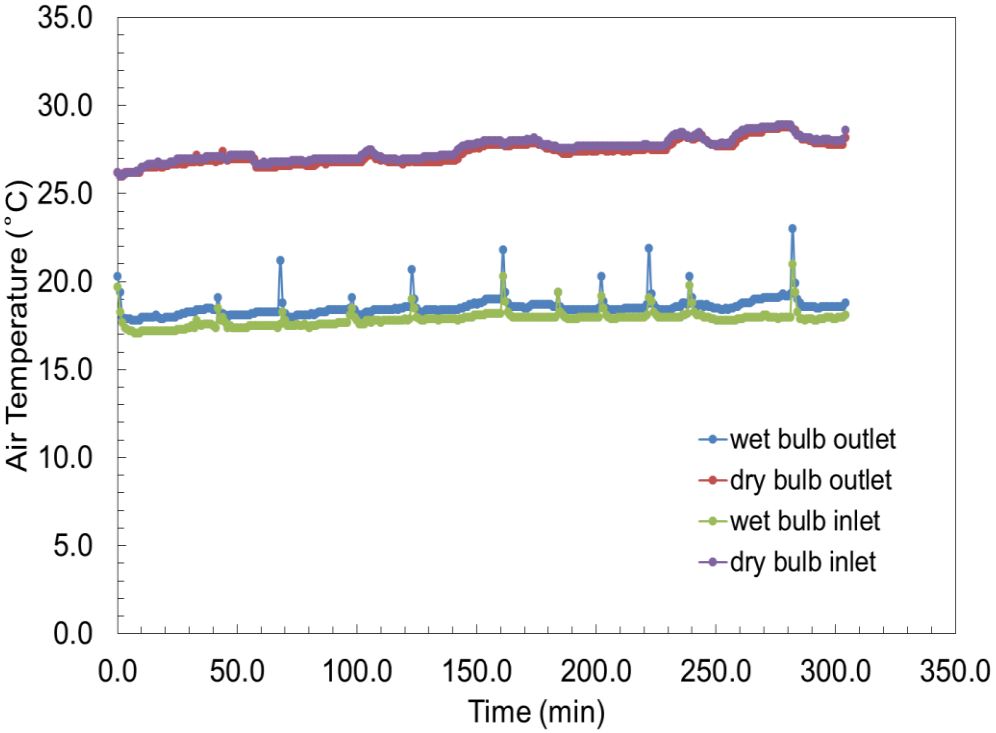

Figure A.44: Plot of air temperature with time for Run 20

Air and water temperature graphs with time are given in Figure A.45 and A.46, for Run 21:

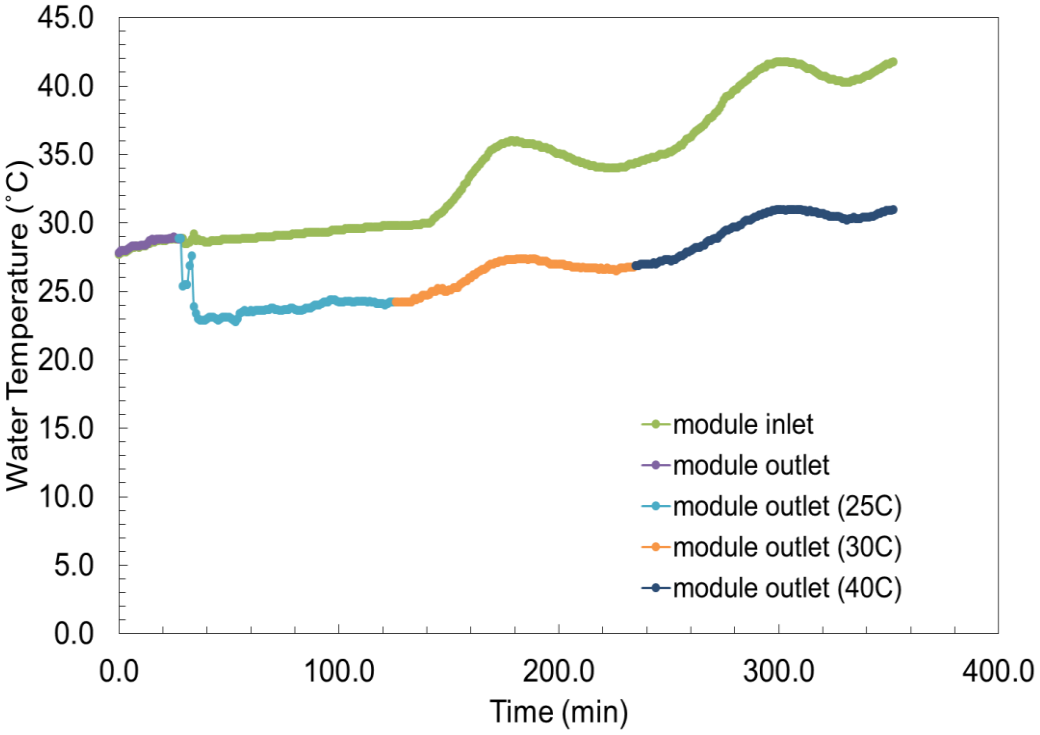

Figure A.45: Plot of water temperature with time for Run 21

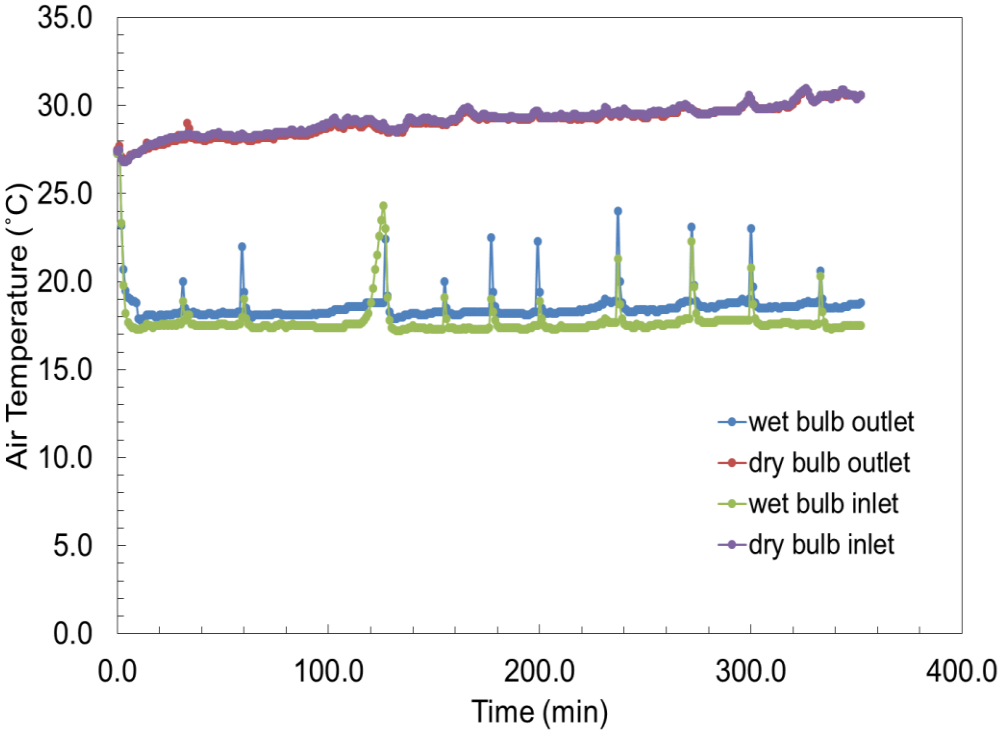

Figure A.46: Plot of air temperature with time for Run 21

Air inlet temperature effect on cooling performance in membrane based system

Table A.10: Experiment parameters and temperature results for air inlet temperature effect for 1.84 m/s air velocity and parallel connection

	Run	27.8˚C	31.7˚C	40.0˚C	P(barg)	Water flow rate (mL/min)	L (cm)
Wet bulb inlet temperature (T_1)	16	15.7	17.9	19.4	0	10	30
	17	17.6	18.7	21.3	0	10	30
	18	16.3	17.4	20.3	0	10	30
	Avr.	16.5	18.0	20.3			
	Std.	1.0	0.7	1.0			
Wet bulb outlet temperature (T_2)	16	16.1	18.8	19.7	0	10	30
	17	18.4	19.0	21.9	0	10	30
	18	16.9	18.0	21.2	0	10	30
	Avr.	17.1	18.6	20.9			
	Std.	1.2	0.5	1.1			
Dry bulb inlet temperature (T_3)	16	27.0	30.7	39.5	0	10	30
	17	28.5	32.6	40.9	0	10	30
	18	28.0	31.7	39.6	0	10	30
	Avr.	27.8	31.7	40.0			
	Std.	0.8	1.0	0.8			
Dry bulb outlet temperature (T_4)	16	26.9	30.5	38.2	0	10	30
	17	28.2	32.4	40.3	0	10	30
	18	27.6	31.1	39.0	0	10	30
	Avr.	27.6	31.3	39.2			
	Std.	0.7	1.0	1.1			
Water inlet temperature (T_5)	16	25.6	25.0	24.7	0	10	30
	17	29.8	28.9	29.0	0	10	30
	18	29.5	30.2	30.3	0	10	30

	Avr.	28.3	28.0	28.0			
	Std.	2.3	2.7	2.9			
Water outlet temperature (T_6)	16	19.1	21.6	22.7	0	10	30
	17	25.2	25.9	27.5	0	10	30
	18	24.2	25.0	26.8	0	10	30
	Avr.	22.8	24.2	25.7			
	Std.	3.3	2.3	2.6			

For Run 16, air and water temperature graphs are given in Figure A.47 and A.48:

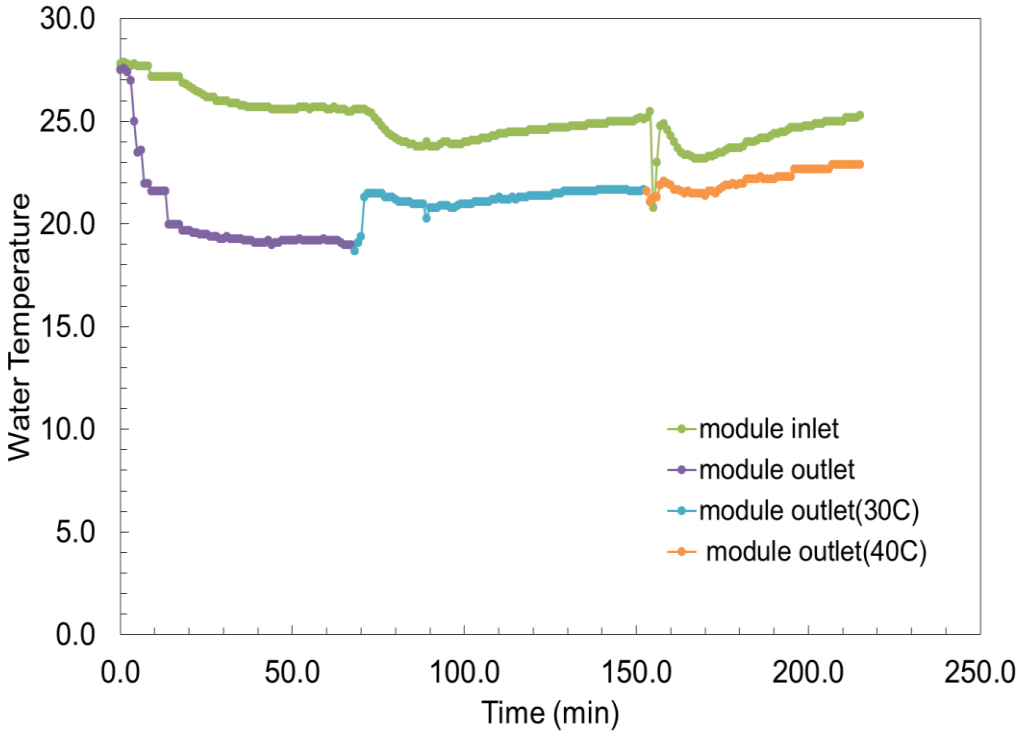

Figure A.47: Plot of water temperature with time for Run 16

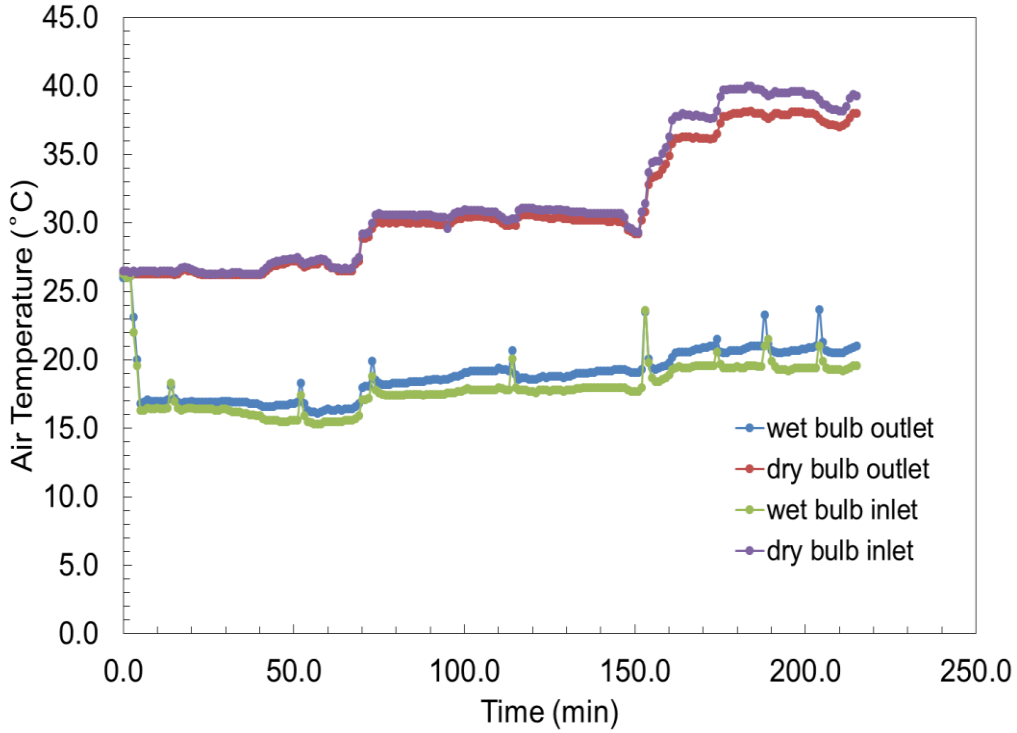

Figure A.48: Plot of air temperature with time for Run 16

For Run 17, air and water temperature graphs are given in Figure A.49 and A.50:

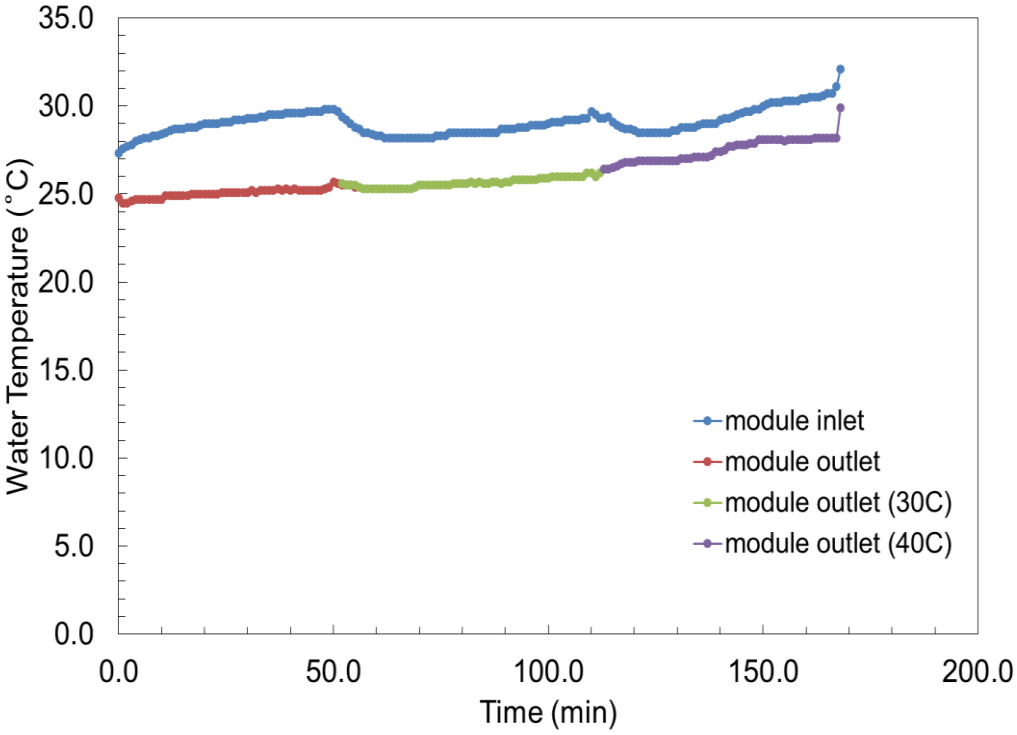

Figure A.49: Plot of water temperature with time for Run 17

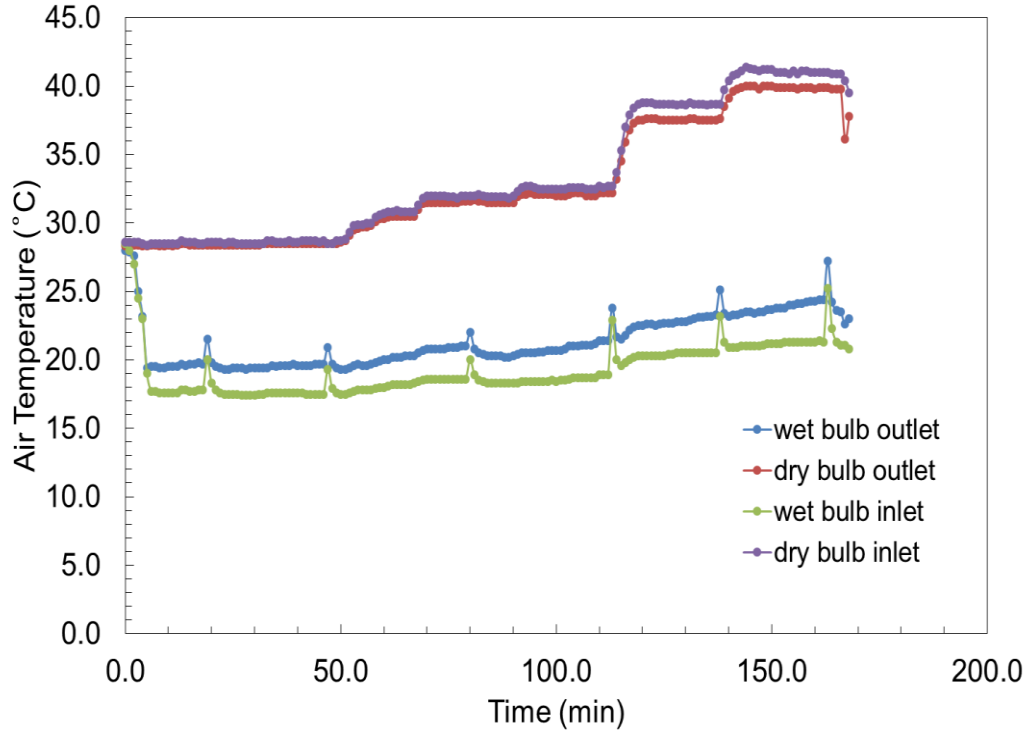

Figure A.50: Plot of air temperature with time for Run 17

For Run 18, air and water temperature graphs are given in Figure A.51 and A.52:

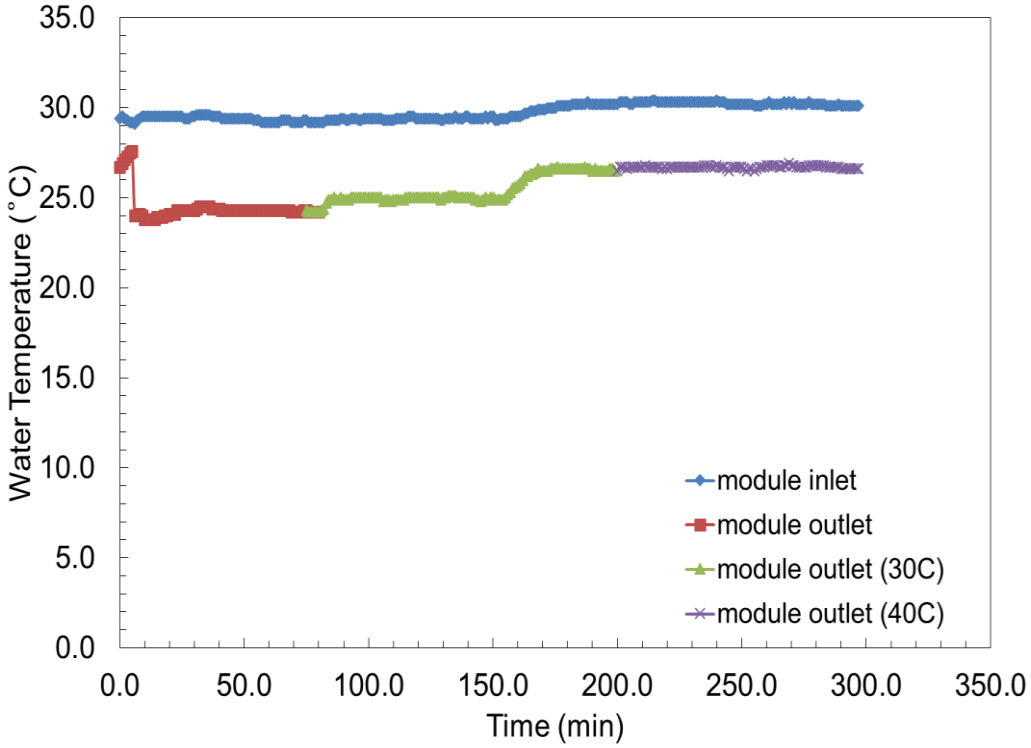

Figure A.51: Plot of water temperature with time for Run 18

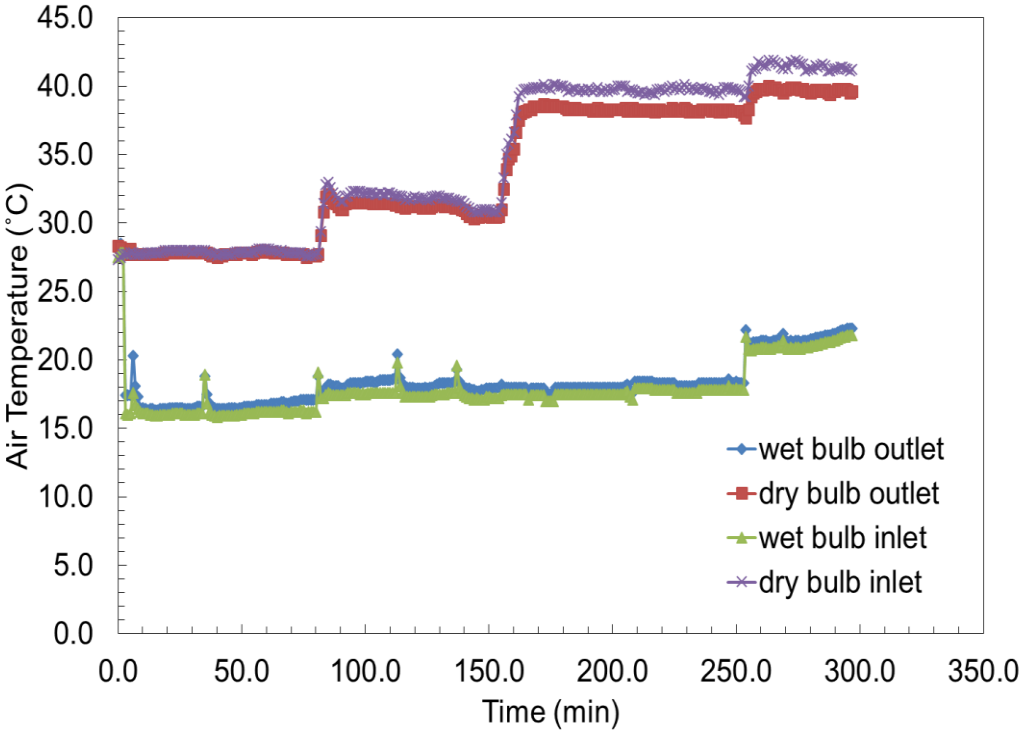

Figure A.52: Plot of air temperature with time for Run 18